INVESTIGATING THE ENTEROVIRUS THEORY OF DISEASE ETIOLOGY IN MYALGIC ENCEPHALOMYELITIS/CHRONIC FATIGUE SYNDROME

A Dissertation

Presented to the Faculty of the Graduate School

of Cornell University

In Partial Fulfillment of the Requirements for the Degree of

Doctor of Philosophy

by

Adam James O'Neal

August 2022

INVESTIGATING THE ENTEROVIRUS THEORY OF DISEASE ETIOLOGY IN MYALGIC ENCEPHALOMYELITIS/CHRONIC FATIGUE SYNDROME

Adam James O'Neal, Ph. D.

Cornell University 2022

Myalgic Encephalomyelitis/Chronic Fatigue Syndrome (ME/CFS) is a complex, multi-system disease whose etiological basis has not been established. Over the years, several pathogenic agents have been implicated with no one pathogen being conclusively identified as responsible for induction of a large number of cases. Enteroviruses (EVs) as a cause of ME/CFS have sometimes been proposed, as they are known agents of acute respiratory and gastrointestinal infections that may persist in chronic infection sites, including the central nervous system, muscle, and heart, potentially resulting in chronic conditions that have symptom constellations like those of ME/CFS.

To gain insight into the association between EVs and ME/CFS, I conducted a comprehensive review of EV studies in ME/CFS and followed this with 1) a broad serological survey of ME/CFS antibody levels to 122 pathogenic antigens and 2) designed and conducted EV-specific targeted RNA sequencing.

A review of prior ME/CFS investigations in ME/CFS revealed a strong prevalence of chronic EV infections across ME/CFS cohorts. The broad survey of anti-pathogen antibody levels in ME/CFS cases did not implicate any one pathogen as a causative factor in ME/CFS, nor do they rule out common pathogens that frequently infect the US population. However, the results did reveal sex-based differences in steady-state humoral immunity, both within the ME/CFS cohort and when compared to trends seen

in the healthy control cohort.

Furthermore, I find that our EV-specific probe set allows efficient viral detection when as few as 10 molecules are present in 1ml of blood. However, whether the technology is employed directly on patient samples or following attempts at *in vitro* biological amplification, EVs were undetected in both ME/CFS and healthy control samples despite all approaches that were pursued.

This work establishes a thorough understanding of the current EV-ME/CFS related literature while simultaneously providing an acutely sensitive and comprehensive approach that will be useful in the future for screening biopsy or cadaver samples from any individuals suspected of having a chronic EV infection.

BIOGRAPHICAL SKETCH

Adam J. O'Neal was born in Fort Riley, Kansas in June of 1988.

Adam spent most of his childhood in Houston, Texas living a classic all-American childhood heavily influenced by sports with involvement in soccer, baseball, football, and swimming. In his early years, Adam was an exuberant personality often described as a "class clown" although he excelled in the classroom. His favorite classes were always science and math with a special love for gym and recess where he could get his energy out.

Throughout his mid to late teens Adam led a life dedicated to becoming a professional soccer player while also dabbling in child acting. With a career in soccer nearly realized, Adam unfortunately sustained a career ending injury that required him to redirect and choose another direction in life. After a time of admittedly struggling, Adam rediscovered his childhood love for science and began to seek resolve in his newly discovered academic identity.

Adam began his journey at Glendale Community College where he developed an academic identity and made a commitment to a future based around science. With many trials and tribulations along the way, Adam eventually arrived at California State University Sacramento where a multitude of influential professors fostered his growing love of science. Most notably, Dr. Thomas Peavy brought Adam into his lab and allowed him to independently tackle ways to detect and monitor the therapeutic effect of stem cells on diabetic chronic wound healing through immunofluorescent techniques. The scholarly products of his work resulted in a publication, first place in an interdisciplinary oral research competition, multiple dean's awards and spotlight in an annual CSU wide publication highlighting top-performing students across the CSU

system.

With his love for science solidified, Adam looked towards grad school to further develop his scientific toolkit and deepen his theoretical understanding of biology. After applying to many cellular and molecular biology-focused graduate programs, Adam found himself attending Cornell University where he was drawn to the lab of Dr. Maureen Hanson, who actively pursues research aimed at investigating the biological basis of Myalgic Encephalomyelitis/Chronic Fatigue Syndrome (ME/CFS). Adam joined the lab in the Fall of 2017 where he focused on developing a targeted RNA sequencing approach aimed at evaluating enteroviruses as disease culprits in ME/CFS. In addition to his thesis research, Adam has also served as a teaching assistant in the MBG department for five semesters, teaching courses on personal genomics and medicine, survey of cell biology, and introductory cell and developmental biology. In addition to the traditional PhD exposure, Adam also served for 2 years as an intern with Cornell's Center for Technology Licensing, where he helped Cornell investigators along the path of technology commercialization. Upon completion of his PhD, Adam will be serving as a Life Science Consultant for ClearView Healthcare Partners in Newton, Massachusetts, where he will apply his expertise in molecular biology and technology commercialization to problems affecting companies involved in the healthcare industry.

This work is dedicated to my family, my loving wife – Hannah O'Neal – and our King Charles Spaniel - Louie – who provided emotional support ad understanding throughout my tenure.

ACKNOWLEDGMENTS

Deserving of upmost thanks is of course, Dr. Maureen Hanson. With an unconventional start to my PhD and serious family health issues along the way, she has served as an incredibly positive, stable and understanding mentor throughout my Cornell tenure. Whenever I am asked about life as a PhD, I never fail to mention that my most cherished aspect is having a PI who has been completely supportive of my career development outside of the traditional continued academic path. I know many of my colleagues were not lucky enough to have their PI's support when applying to intern with Cornell's Center for Technology Licensing.

As to my other committee members, Dr. Andrew Grimson and Dr. Cynthia Leifer have been much appreciated sources of expertise in experimental approaches as well as aligning my PhD timeline and setting annual goals and expectations. They have similarly been completely supportive of my pursuit to becoming a life science consultant to which I am forever grateful.

Thank you to Cornell's Transcriptional Regulation & Expression Facility, most notably Jen Grenier and Ann Tate, for helping to outline and develop our targeted RNAseq experimental design. They have always been willing to share their expertise on all things RNA and continuously accommodate my many questions and requests of their facility. My PhD would have been exponentially more convoluted if it were not for their constant source of clarity.

I also must thank both current and former members of the Hanson lab. Thank you to Ludovic Giloteaux for serving as my primary source of lab support and mentorship along the way. Thanks to Andrew Gipson for career-related talks and for your friendship outside of the lab. Thanks to Carl Franconi for giving organization to my projects and the Hanson lab, your positive attitude and great work ethic is noticed and appreciated by all. I want to thank Alex Mandarano, Jessica Maya, Arnaud

Germain, Vishal Chaudhari, Myat Lin and Katie Glass for your conversations about experiments or life in general.

Thanks to my undergraduate mentors, Thomas Peavy and Thomas Landerholm, who provided the foundation required to achieve in grad school. I am forever grateful for our continued friendship throughout my career.

Anthony Nzessi, Chris Furman, Gael Nicholas, James Chon, and Ed Partlow have been my greatest BMCB friends. They have been great ears when gabbing out experiments and never allowed my time in Ithaca to feel lonely. Memories with these guys are those I will cherish most when looking back on my time in Ithaca.

Of course, many thanks to my Mom and Dad, my wife, my extended family, and all of those who have supported me along my PhD journey.

TABLE OF CONTENTS

LIST OF FIGURES

LIST OF TABLES

CHAPTER 1

The Enterovirus Theory of Disease Etiology in Myalgic Encephalomyelitis/Chronic Fatigue Syndrome: A Critical Review[1]

ABSTRACT

Myalgic Encephalomyelitis/Chronic Fatigue Syndrome (ME/CFS) is a complex, multi-system disease whose etiological basis has not been established. Enteroviruses (EVs) as a cause of ME/CFS have sometimes been proposed, as they are known agents of acute respiratory and gastrointestinal infections that may persist in secondary infection sites, including the central nervous system, muscle, and heart. To date, the body of research that has investigated enterovirus infections in relation to ME/CFS supports an increased prevalence of chronic or persistent enteroviral infections in ME/CFS patient cohorts than in healthy individuals. Nevertheless, inconsistent results have fueled a decline in related studies over the past two decades. This review covers the aspects of ME/CFS pathophysiology that are consistent with a chronic enterovirus infection and critically reviews methodologies and approaches used in past EV-related ME/CFS studies. We describe the prior sample types that were interrogated, the methods used and the limitations to the approaches that were chosen. We conclude that there is considerable evidence that prior outbreaks of ME/CFS were caused by one or more enterovirus groups. Furthermore, we find that the methods used in prior

[1] This work was originally published as "The Enterovirus Theory of Disease Etiology in Myalgic Encephalomyelitis/Chronic Fatigue Syndrome: A Critical Review" by Adam J. O'Neal and Maureen R. Hanson. *Frontiers in Medicine*, 8, 688486. https://doi.org/10.3389/fmed.2021.688486. AO: examined efficacy of published primers in silico. AO and MH: reviewed literature and wrote the paper. Both authors contributed to the article and approved the submitted version.

studies were inadequate to rule out the presence of chronic enteroviral infections in individuals with ME/CFS. Given the possibility that such infections could be contributing to morbidity and preventing recovery, further studies of appropriate biological samples with the latest molecular methods are urgently needed.

INTRODUCTION

Myalgic encephalomyelitis/chronic fatigue syndrome (ME/CFS) is a complex multi-system disease of unknown cause for which there is little insight into the molecular basis of disease progression, persistence and in rare cases - remission. The ME/CFS literature includes findings of patient immune system irregularities, abnormal cellular energy metabolism, and various altered autonomic nervous system manifestations including post-orthostatic tachycardia syndrome, orthostatic intolerance, and dysregulated hypothalamus pituitary adrenal axis. A hallmark symptom, required for many case definitions, is exercise intolerance or post-exertional malaise (PEM) [2, 3]. The name of the illness itself is controversial, with one view holding that Myalgic Encephalomyelitis, a name dating from a series of early outbreaks of the disease [4], defines an illness that is different than Chronic Fatigue Syndrome, a name created in 1988 through a U.S. government committee [5]. A discussion of the case definition and nomenclature is outside of the scope of this article, so we will use “ME/CFS” despite of the possibility that the initial CFS case definition results in inclusion of individuals who would not have met earlier criteria for Myalgic Encephalomyelitis.

ME/CFS case documentation shows evidence of both sporadic events involving singular individuals and regional outbreaks involving significant fractions of affected

communities, especially hospitals, schools, and military bases. Machine learning estimation of ME/CFS prevalence using large-scale medical claims data gives a frequency of diagnosis in the United States that falls somewhere between 1.7 and 3.38 million Americans [6] and world-wide, the prevalence may be as high as 65 million [7]. ME/CFS is not a rare disease and therefore understanding of disease pathophysiology and discovery of standardized biological markers or tests are important to identify appropriate treatments

The pattern of transmissibility, and acute symptom constellation reminiscent of a flu-like illness, led early investigators to hypothesize a viral theory of ME/CFS disease etiology. Indeed, a number of researchers have interrogated a diverse range of microbial pathogens as triggers and/or perpetuators of the ME/CFS disease state. These include but are not limited to Epstein-Barr virus, cytomegalovirus, parvovirus B19, Brucella, Toxoplasma, *Coxiella burnetti*, *Chlamydia pneumoniae*, human herpesviruses, enteroviruses, human T cell leukemia virus II-like virus, spumavirus, hepatitis C virus, and human lentiviruses [8-10].

Between the 1930s and 1960s, a number of globally occurring ME/CFS outbreaks, with a spatiotemporal incidence coinciding with poliovirus epidemics, appeared under the titles of ‘abortive or atypical poliomyelitis’ transitioning to “benign myalgic encephalomyelitis’ or ‘epidemic neuromyasthenia’ as physicians sought a term to describe the symptom profile of affected individuals [11-13]. A ME/CFS outbreak occurred in 1934 California and provides a representative example of clinical features experienced by patients during similar epidemics of the time. Briefly, the 1934 outbreak occurred among roughly 200 hospital employees, primarily female, who fell

ill with what acutely appeared to be poliomyelitis. Epidemiological deviations from what is commonly expected in poliomyelitis epidemics included relatively high attack rates, low mortality rates, low paralytic rates and a high incidence in adults as opposed to young children. Symptoms of sufferers included significant diurnal temperature fluctuations, localized muscular weakness as well as pain and muscle tenderness. Patients further exhibited numbness, paresthesia, exercise intolerance, and recurrent systemic and neurological symptoms. Longitudinal tracking of a subset of these patients showed residual muscle alterations, fatigue, and mental changes. Electromyograms showed generalized, mild, motor neuron changes and observations indicated that recurrences could occur even after many years of relatively normal health [14, 15]. The totality of these findings indicated an infectious agent although tests available at the time could not convincingly implicate a specific culprit.

Subsequent outbreaks displayed the same basic features of the 1934 outbreak with some distinct clinical presentations depending on the region [4, 16, 17]. Overall, most epidemic outbreaks have occurred in mid-spring through early fall indicating a virus with seasonal epidemic trends may be involved. Seasonality is not rare for viruses; many types, including but not limited to echovirus, coxsackievirus and poliovirus-related species, are well known to have strong outbreak seasonality peaking in the month of August or early fall [18, 19]. Outbreaks occurring after 1934 that deserve notable mention based on similar clinical presentations and links to an enteroviral culprit are highlighted below:

- 1949 – 1953 Adelaide, Australia: Dr. R.A. Pellew conducted several animal studies using patient throat washings, feces and cerebrospinal fluid collected from

the 1949-1953 Adelaide outbreak as inoculants into rhesus monkeys, rabbits, mice, and hen eggs. Investigation into two monkeys repeatedly inoculated with patient sample revealed minute red spots along the course of the sciatic nerve, infiltration of lymphocytes and mononuclear cells into nerve roots and nerve fibers showing patchy damage to the myelin sheath with axon swelling. Although similar to poliovirus inoculation outcomes, these monkeys displayed more widespread changes in additional areas of the nervous system with no evidence of damage to nerve cells in the brain and spinal cord. Additionally, severe myocarditis was found in one of the two monkeys studied – myocarditis being most commonly caused by enteroviruses [20, 21].

- 1948 Akureyri, Iceland: Incidence of over 1,000 cases during a 3 month period resulted in the naming of "Icelandic disease," which would later evolve to 'benign myalgic encephalomyelitis' [22]. Those who fell ill with the disease showed classical viral-type illness onset which later developed into a systemic form of the illness with symptoms including low fever and significant muscle tenderness/weakness. Due to the occurrence of concurrent local poliomyelitis epidemics, infectious disease testing was conducted but failed to indicate poliovirus, coxsackievirus or other known encephalitis viruses [4].
- 1956 Thorshofn/Egilsstadir, Iceland: Differential poliovirus vaccination responses between children exposed verses unexposed to the "Icelandic disease" indicated the etiological agent in ME/CFS may be a virus immunologically related to poliovirus. Children in a northeastern village of Iceland, Thorshofn, generated a slight rise in antibody production following vaccine administration whereas

children from Egilsstadir, roughly 200km south, had a much stronger immune response to polio vaccine administration. The difference between the two locations was that children from Eglisstadir were from an area which recently experienced a myalgic encephalomyelitis outbreak whereas children from Thorshofn were not [23]. This indirect evidence of unknown prior immunity was also noted in the aforementioned Adelaide outbreak. This was evidenced by a 43% reduction in polio cases in the south of Australia, where Adelaide is located, compared to regions such as New South Wales and Queensland that reported increased polio cases [24]. Enteroviral cross-immunity is well documented in the enterovirus field and suggests that children in ME/CFS affected areas had been exposed to an agent immunologically similar to poliovirus [25].

Similar epidemic events of ME/CFS have occurred globally over time where patients display acute symptoms are similar to some poliomyelitis-afflicted patients. The later phases of disease progression make evident several differences between ME patients and those with poliomyelitis. The occurrence of considerable symptom constellation overlaps between ME/CFS, poliomyelitis and other non-polio enterovirus-related clinical outcomes as well as similarity in epidemic seasonality is further circumstantial evidence for a relationship between ME/CFS and enteroviruses. One possibility for the co-occurrence of polio and non-polio enteroviral outbreaks may be the environmental source of enteroviruses, which often are contaminated bodies of water. If sewage is contaminating water, consumers may be exposed to multiple types of enteroviruses.

To date, the body of research investigating enterovirus infections in relation to ME/CFS supports an increased prevalence of chronic or persistent infections in several ME/CFS patient cohorts. The majority of early EV-related investigations occurred within the UK from the 1970s to early 2000s, starting with serological tests but advancing to molecular methods including immunohistochemical detection of enterovirus viral capsid protein (VP1) and viral genome detection using RT-PCR [26, 27]. Although a significant number of early papers provided evidence for an association of chronic enteroviral infections with ME/CFS, research into the enteroviral theory of disease etiology largely died out in the early 2000s with a few exceptions [28, 29]. One reason that enteroviral research in ME/CFS has languished is the difficulty of detecting virus after time has passed following an acute infection. Furthermore, because enteroviral infections are frequent and common, a large fraction of the population will have serological evidence of exposures. Another issue is that reports of association of other pathogens and environmental stresses led to the concept that many different types of insults could result in ME/CFS. We are offering a critical evaluation of current literature that may lead to further inquiry into the role of EVs in ME/CFS.

In this review, we will first cover what is known about enteroviruses in relation to tissue tropism and ability to persist in a chronic infectious state. Emphasis will be put on the aspects of ME/CFS patient pathophysiology that are consistent with an active, chronic enterovirus infection. We will provide a critical review of studies that were attempting to identify chronic EV infections. The studies will be categorized based on the research methodology employed and special emphasis will be put on the sample

types used and limitations to the chosen methods. We hope this review may help guide future viral-related studies by highlighting the tissue types and approaches most likely to provide insight into the hypothesis that enterovirus infections are initiating and/or perpetuating the disease state in ME/CFS.

BACKGROUND REGARDING ENTEROVIRUSES

Enterovirus Classification and Basic Molecular Biology

Figure 1.1. Representative enterovirus genome structure with emphasis on 5′UTR Domain I and genome replication. (A) Graphical depiction of EV genome as well as proteolytic processing to produce all structural and non-structural proteins. Number ranges indicate nucleotide positions for domains 1–7 in the 5′UTR of CVB4. (B) 2D illustration of CVB4 Domain I secondary structure. Numbers indicate nucleotide positions. (C) From [1] by license: Creative Commons Attribution 4.0 International. An integrated model for enterovirus replication. Negative-strand synthesis is initiated by circularization of the positive-strand genome via a protein-protein bridge through the interaction of the ternary complex at the 5 ′ -end (3CD and PCBP bound to the cloverleaf structure) and PABP bound to the 3′ -poly(A)tail (I. + II.). CRE-mediated VPg-pUpU acts as primer of the reaction and the polymerase 3D synthesizes the new negative-strand (III.), resulting in a double-stranded intermediate (RF) (IV.). The positive-negative duplex RNA intermediate unwinds, so that the cloverleaf structure at the 5′ -end of the positive-strand can form. 3CD and PCBP bind to the cloverleaf to form a ternary complex, which, in turn, will initiate positive-strand synthesis on the 3′ -end of the negative-strand (V.). The primer, VPg-pUpU, is recruited and binds to the 3′ -terminal AA of the negative strand, and the new positive-strand is synthesized by the polymerase, 3D (VI.).

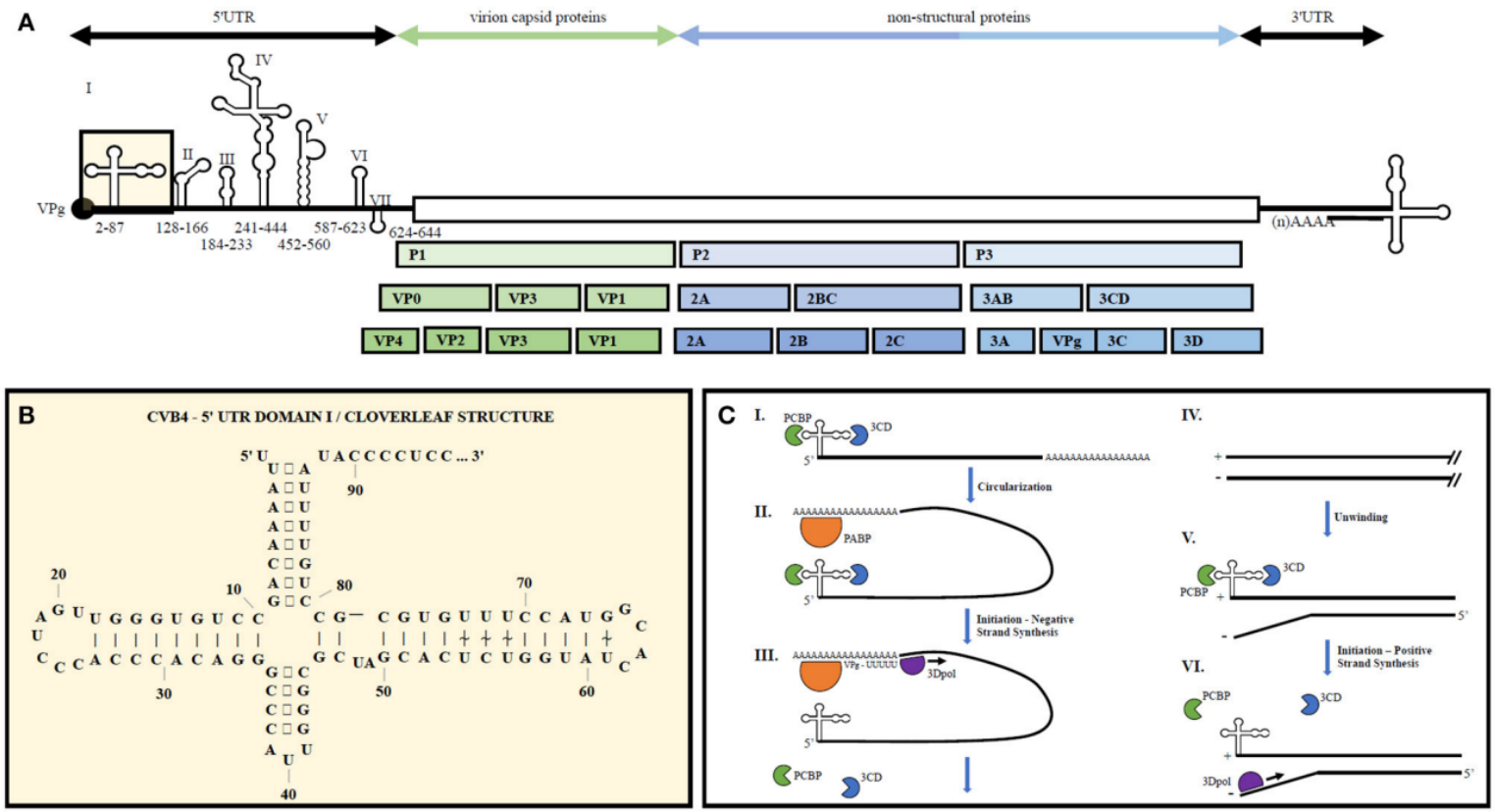
A
5'UTR
virion capsid proteins
non-structural proteins
3'UTR
I
II
III
IV
V
VI
VII
VPg
2-87
128-166
184-233
241-444
452-560
587-623
624-644
(n)AAAA
P1
P2
P3
VP0
VP3
VP1
2A
2BC
3AB
3CD
VP4
VP2
VP3
VP1
2A
2B
2C
3A
VPg
3C
3D
B
CVB4 - 5' UTR DOMAIN I / CLOVERLEAF STRUCTURE
5' U
U A C C C C U C C ... 3'
C
I.
PCBP
3CD
5'
Circularization
II.
PABP
Initiation - Negative Strand Synthesis
III.
VPg - UUUU
3Dpol
IV.
Unwinding
V.
Initiation – Positive Strand Synthesis
VI.

Although poliovirus is the most well-known enterovirus, it belongs to only one of 15 total enterovirus species including enterovirus species A-L and rhinovirus species A-C. Of the true enteroviruses, species A-D are known to have caused a wide spectrum of severe and deadly epidemics in humans [30, 31].

The enterovirus genome consists of a single stranded positive sense RNA molecule roughly 7.5kb in length (**Figure 1.1**). Upon translation via host cell machinery, one full length polypeptide is produced and then proteolytically cleaved into the polyprotein products PI, P2 and P3. P1 encodes four structural proteins, VP1-VP4, forming the non-enveloped virion capsid. P2 and P3 are proteolytically cleaved into 10 nonstructural proteins including 2A to 2C, 3A to 3D as well as precursors 2BC, 3AB and 3CD. Viral genomic RNA is capped on its 5' end with the viral-encoded protein VPg (3B) instead of a methylated nucleotide cap structure.

Enteroviruses gain cellular entry through binding to host cell receptors and undergoing receptor-mediated endocytosis. Cellular receptors vary between EVs and include CD155/poliovirus receptor, integrins αvβ6 and αvβ3, ICAM-1, ICAM-5, CD55/decay accelerating factor, KREMEN1, coxsackievirus and adenovirus receptor (CAR), scavenger receptor B2, P-selectin glycoprotein ligand-1, sialylated glycan, heparan sulfate, neonatal Fc receptor and annexin II [32-34].

Upon cellular entry, translation occurs following ribosome binding onto a type I internal ribosome entry site (IRES) located within the 5'UTR of the viral genome. Replication occurs via the viral encoded RNA-dependent RNA polymerase (3Dpol) which forms the negative sense RNA complement that is used to create additional positive sense RNA genomes [35]. During active infection the ratio of positive to

negative strands is roughly 100:1, whereas chronic infections display a ratio closer to 1:1 [36].

5’ and 3’ UTR secondary structures recruit both viral and host cell proteins to aid in viral translation and replication [37]. The 5’UTR of EVs contains a cloverleaf secondary structure, termed Domain 1, as well as an internal ribosome entry site (IRES) containing six major stem-loop structures (**Figure 1.1**). The 5’UTR is required for initiating both negative and positive strand RNA synthesis. The 3’UTR also contains important secondary structures, two predominant hairpin loops, that are the essential structure of the origin or replication for negative strand synthesis. Proteins bound to the 5’UTR interact with others bound to the genome’s polyadenylation sequence at the 3’ end, thereby promoting viral genome circularization. Circularization allows the 3’UTR secondary structures to act as the initiation site for 3Dpol binding and at the origin of replication [38].

The viral encoded RNA polymerase is error-prone due to lack of a proof-reading mechanism, resulting in high mutation rates throughout enteroviral evolution. Furthermore, intra- and inter-typic genetic recombination may occur between enteroviruses, leading to increased genotypic plasticity. Enterovirus genomes frequently exhibit mosaic genomic sequences leading to a wide variety of genotypic and phenotypic diversity across enterovirus serotypes [39, 40].

Enterovirus Carrier-State vs Steady-State Persistent Infections

Persistent enteroviral infections are generally agreed to occur in two forms, termed carrier-state and steady-state persistence. In carrier-state infections, high levels of infectious virus are produced with infection limited to only a small proportion of cells.

Alternatively, steady-state infections show all cells are simultaneously infected but viral replication is slowed, leading to a non-lytic phenotype with low viral copy numbers per cell. Both types of persistent viral infections are known to occur across human enteroviral species and have been linked to multiple clinical conditions [41-47].

Research on CVB4 infections of pancreatic ductal-like cells (PANC-1) and murine cardiac myocytes (HL-1) shows productive viral replication (10^6 to 10^8 PFU/ml) is restricted to a limited subpopulation of cells in culture and are therefore examples of carrier-state infections *in vitro*. PANC-1 cells exhibiting resistance to lysis via subsequent CVB4 superinfection were determined to be those PANC-1 cells with downregulated coxsackie adenovirus receptor (CAR) expression that became dominant in culture within several passages [44, 46]. These findings together illustrate the host cell's influence in the co-evolutionary balance between host and virus as the host attempts to limit viral infection from spreading via reduction in viral entry receptor expression [47]. CVB1 infection of PANC-1 cells also demonstrates that CVB1 drives downregulation of cellular proteins involved in mitochondrial energy metabolism. Mitochondrial dysfunction, oxidative phosphorylation, fatty acid alpha- and beta-oxidation, citric acid cycle and leucine and valine degradation pathways were significantly enriched among downregulated proteins detected by mass spectrometry. Interestingly, further investigation into the mitochondrial networks of PANC-1 infected cells revealed differential changes in mitochondrial network morphology based on the CVB1 (ATCC vs 10796) strain used to generate carrier-state infections. CVB1 strain 10796 produced fragmented mitochondrial networks whereas uninfected

cells or those infected with CVB1 strain ATCC both showed filamentous mitochondrial networks. Proteomic analysis further supported these findings by revealing a significant downregulation in mitochondrial proteins involved in fusion processes including mitfusion-1, mitofusion-2 and mitochondrial dynamin-like GTPase OPA1 in the strain 10796-induced persistent infection model [48]. In addition to support for carrier-state coxsackievirus-induced infections in the pancreas and heart, in-vitro infection of human astrocyte cells also suggests persistent coxsackievirus infection could occur in the central nervous system (CNS) [49].

Steady-state infections are characterized by all cells in culture having low levels of non-lytic viral replication. Low levels of viral replication lead to decreased viral-induced inhibition of host cell protein synthesis and thus lead to the nonlytic phenotype. To date, multiple studies have shown a subset of enterovirus serotypes, including coxsackieviruses and echoviruses, are able to produce low replicative steady-state infections without cytopathic effect. This phenomenon may be caused by a number of factors including but not limited to 5'UTR terminal deletions that lead to replication deficiencies or reduced type I interferon response elicitation, faulty virion capsid formation due to incomplete capsid polypeptide processing, and alternative EV RNA mutations that lead to abnormalities such as stable and atypical double-stranded RNA complex formation that inhibits further viral positive strand synthesis [35, 36, 50, 51]. In the context of ME/CFS, 5'UTR terminal deletions and/or atypical dsRNA complex formation are notable, as they have been shown to occur in a proportion of ME/CFS patient cohorts in multiple studies [36, 52, 53]. In a number of cases, chronic diseases with some overlap in symptom constellation with ME/CFS show substantial

evidence of disease involvement by persistent infection EV variants. These chronic diseases include idiopathic dilated cardiomyopathy (IDCM) [54], chronic inflammatory myopathy [55], insulin-dependent diabetes mellitus [50, 56, 57], post-polio syndrome [58, 59], and chronic CNS inflammation and lesions [60]. For example, one study of EV positive-IDCM heart tissue detected a positive to negative strand ratio ranging from 2 to 20 [36], while another demonstrated EV-negative to positive strand ratios of 1 to 5 in infected heart tissue [61]. Furthermore, the median viral load in heart tissue was assessed to be 287 EV RNA copies/μg of tissue. Such a low amount presents a significant challenge when trying to detect persistent enteroviral infections in difficult- to-sample/invasive secondary tissue screening sites. Low levels of viral replication result in EV RNA levels so small that they may be past the lower limit of detection [54].

In reviewing the outcomes of persistent in-vitro EV infections, it is clear that EVs with the ability to create carrier-state infections are able to produce cellular outcomes that may be relevant to ME/CFS pathophysiology in an EV variant-dependent manner. As mentioned above, specific CVB1 variants (CVB1 10796) disturb mitochondrial network morphology and lead to a downregulation of proteins relevant to mitochondrial energy metabolism. In regard to EVs that produce steady-state infections, Echovirus 6 and Enterovirus 72 (hepatitis A) are both shown to cause persistent steady-state infections in-vitro [46, 53, 62]. Echovirus 6 is also shown to cause persistent in-vivo infections and is associated with neurological disorders of encephalitis and meningitis [63]. Unfortunately, literature surrounding mitochondrial outcomes relating to these two viruses is bleak at best. Echovirus 6 infection of

cultivated monkey kidney cells shows mitochondria retain their shape but information on mitochondrial enzymology and mitochondrial membrane potential is absent [64]. Although there is a serious lack of literature pertaining to enterovirus steady-state infections and mitochondrial dysfunction, persistent Echovirus 6 infections are associated with nonlytic viral RNA and alterations in capsid protein production including unprocessed capsid polypeptide V0 [62]. Considering the large number of interactions between enteroviral encoded and host proteins, it is reasonable to assume a downregulation and variation in viral encoded protein production during steady-state infections could lead to a mitochondrial dysfunction phenotype different and less extensive than seen in enterovirus carrier-state infections, acute infections, or cells without infection.

Mitochondrial Abnormalities in ME/CFS Cells

There is recent literature that describes differences in immune cell metabolism between ME/CFS patients and controls [46, 64-70]. The relevance of these reports to possible dysfunction of mitochondria in tissues and organs is unclear. Immune cells alter their metabolism while responding to signals indicating a threat is present [71, 72]. It is not known whether the altered mitochondrial metabolism is due to defective signaling or an appropriate immune response that is present in patients rather than healthy individuals, rather than an actual abnormality.

Early studies on 50 ME/CFS patient muscle biopsies found mitochondrial abnormalities described as branching and fusion of mitochondrial cristae upon ultrastructural examination in addition to swelling, vacuolation, myelin figures and secondary lysosomes indicating mitochondrial degeneration. The authors concluded

their work was the first evidence that ME/CFS may be due to a mitochondrial disorder caused by a viral infection [73].

A few years later, right quadricep muscle biopsies from nine ME/CFS patients were assayed via electron microscopy, immunochemistry, mtDNA sequencing (as discussed earlier) and enzyme activity assays. The research group found mitochondrial structure abnormalities, inversion of the cytochrome oxidase/succinate dehydrogenase ratio and a reduction in some mitochondrial enzyme activities. The enzyme activity assay results indicate a reduction of the muscle oxidative property evaluated on multiple mitochondrial matrix enzymes including NADHtr, COX and succinate dehydrogenase. A reduction in mitochondrial enzyme activities was supported for cytochrome c oxidase and citrate synthetase as well [74].

Two recent studies found normal mitochondrial oxidative phosphorylation (oxphos) and normal respiratory chain complex activity compared to healthy controls. However, insight into mitochondrial oxidative phosphorylation was determined using plasma creatine kinase as a surrogate measure of oxphos in muscle [75, 76].

Another recent study used extracellular flux analysis *in vitro* to determine utilization of various substrates by skeletal muscle cells from patients vs. controls. This study found that muscle cells from ME/CFS patients had reduced oxphos in comparison to controls when supplied with glucose as a substrate, while no abnormalities were detected when cells were supplied with galactose or fatty acids [77].

Overall, the literature surrounding mitochondrial dysfunction in ME.CFS patients is suggestive of bioenergetic abnormalities that are within the realm of possible

cellular outcomes based on the nature of the persistent viral infection. Varied findings pertaining to mitochondrial function in ME/CFS muscle biopsies may be due to sampling bias as latent enteroviral infections within secondary infection sites may not be uniform and therefore discovery of a cellular pathophysiology would only be found if the correct tissue location were interrogated.

Enterovirus Cell and Tissue Tropism

Each enterovirus has a distinct cell and tissue level tropism that is governed by both host and viral factors, including cellular virus receptor availability, tissue-specific activity of IRES on viral RNAs, and innate immune antiviral activities such as interferon (IFN) response. Given these conditions, EVs as a whole display a wide spectrum of cell and tissue tropism leading to a wide array of disease outcomes. The diseases may appear as short-duration sicknesses such as the common cold and acute hemorrhagic conjunctivitis or may cause more serious diseases through infiltration into secondary infection sites such as organs, muscle or central nervous system (CNS), causing myocarditis, pericarditis, encephalitis, meningitis, pancreatitis, paralysis and death [77].

CNS regulation of autonomic nervous system output occurs through multi-synaptic connections descending from the hypothalamus and midbrain to preganglionic neurons in the brainstem and spinal cord. The central autonomic system is further comprised of connections between a multitude of limbic system structures, such as the amygdala and hippocampus, to collectively regulate autonomic nervous system (ANS) outflow [78]. The ANS is subdivided into the sympathetic, parasympathetic and enteric nervous systems, which act to control internal body

processes such as blood pressure, heart and breathing rates, body temperature, digestion, metabolism, fluid retention, production of bodily fluids, urination, defecation and sexual response [79].

ME/CFS patients have a number of pathophysiological traits that point to abnormalities in the ANS, including impaired blood pressure variability, orthostatic intolerance, high prevalence and severity of posturalorthostatic tachycardia syndrome (POTS), delayed gastric emptying, impaired thermoregulation in adolescent patients, loss of capacity to recover from acidosis on repeat exercise, abnormal cardiac output and altered brain characteristics in a wide variety of brain regions including the limbic system structures that govern the ANS [1, 27, 80]. These altered brain characteristics include reduced cerebral, brainstem, and cerebral cortex blood flow; impaired reciprocal connectivity between the vasomotor center, midbrain, and hypothalamus regions; increased neuroinflammation across widely distributed brain areas including but not limited to the hippocampus, thalamus, midbrain and pons; reduced cerebral glucose metabolism, and lower brain glutathione [1, 7, 27, 81]. Many of the altered brain characteristics seen in ME/CFS patients are similarly reported in clinical cases associated with neurotropic enteroviruses. For instance, focal enterovirus encephalitis caused by coxsackievirus A3 is associated with focal hypoperfusion in the right frontal lobe that cleared upon patient recovery from the neurotropic enteroviral infection. This example case is largely similar to multiple SPECT studies indicating ME/CFS patients have significant hypo-perfusion in regions of the brain consistent with their patient-specific symptoms [7, 76, 82-84].

There is a diverse spectrum of tropisms for each enterovirus; some EVs are neurotropic in nature while others may be myotropic. Among human enterovirus families A-D, there exists a subset of EVs that are known to be neurotropic; these include EV71, multiple coxsackievirus group A members, all coxsackievirus group B members, poliovirus and EVD68, among many others. Not surprisingly, different neurotropic enteroviruses gain CNS access via alternative strategies and thus display distinct CNS tissue tropism. For example, poliovirus mainly infects and replicates in motor neurons in the anterior horn of the spinal cord, while EV71 primarily targets neuronal progenitor cells (NPSCs) and astrocytes [1]. NPSC infection is particularly advantageous for viral dissemination, transmission, replication, and persistence. For instance, NPSC infection may expand CNS presence as the infected NPSCs differentiate into neuronal, astrocyte and oligodendrocyte lineages. Furthermore, NPSC migration following differentiation allows access into new CNS locations, and lastly, EV infection of NPSCs may trigger EV-specific genomic changes that allow the virus to persist in a latent state due to the quiescent cellular environment of nonactivated NPSCs or NPSCs that have moved to a neuronal cell fate [3].

EVs gain access to the CNS through a diverse set of entry mechanisms including direct infection of brain microvascular endothelial cells, retrograde axonal transport following muscle infection, exosomal transport across the blood-brain barrier (BBB), and hitchhiking inside of migratory infected immune cells with BBB privilege [75]. Infection outcomes can follow expected changes such as halting of host cell cap-dependent translational events and production of cytopathic effects causing tissue

lesions. However, EVs may also establish a persistent/chronic infection producing atypical clinical outcomes, as may be the case in ME/CFS [83].

Several known EV-CNS infections display autonomic dysfunction symptoms reminiscent of those described in ME/CFS patients. Damage to the ANS is well documented following poliovirus infection; postmortem histopathology routinely demonstrates damage to the reticular formation region of the brainstem whether or not the patient displayed spinal cord damage or paralysis [76]. The reticular formation, a network of neurons located in the brainstem that project into the hypothalamus, thalamus, and cortex, plays a role as a cardiodepressor that lowers cardiovascular output. Post-polio syndrome (PPS) patients exhibit a high prevalence of hypertension and tachycardia while ME/CFS patients display high rates of POTS, which is accompanied by drop in blood pressure. The difference in autonomic dysfunction outcomes between ME/CFS and PPS patients may possibly be due to infection with genetically distinct EV serotypes with different neurotropism and thus different clinical manifestations. However, white matter brain lesions upon MRI, slowing of electroencephalography outputs, clinical impairment of attention, and abnormal hypothalamic pituitary adrenal axis function are shared between patients with PPS and those with ME/CFS [84]. Nevertheless, there is a controversy about whether the reports of excess white matter lesions in ME/CFS patients are instead related to age, a misdiagnosis of neurological disorder, or due to major depression. A quantitative summary of rigorous data pertaining to white matter lesions in ME/CFS reported no significant increase in the lesions [3], but studies that use more advanced neuroimaging methods are needed.

Three ME/CFS post-mortem brain autopsy studies found enteroviral genomic RNA and VP1capsid protein in the hypothalamus, brainstem, cerebral cortex, medial temporal lobe, lateral frontal cortex, occipital lobe, and cerebellum [1, 75, 85]. These findings provide additional support that a persistent EV infection within patient limbic and extra-limbic tissues is possible and could be driving the ANS dysfunction observed in ME/CFS patients.

CNS infections by other EVs such as EV71 and the group B coxsackieviruses result in ANS dysfunctions reminiscent of ME/CFS pathophysiology. EV71 brainstem encephalitis occasionally induces symptoms of ANS involvement including fluctuating blood pressure, tachycardia or bradycardia, hypertension or hypotension and respiratory distress. EV71 CNS-specific clinical manifestations include myoclonic jerk, polio-like syndrome, lethargy, limb weakness, altered mental status, encephalomyelitis, encephalitis, aseptic meningitis, and rhombencephalitis [86, 87]. Of these EV71-related ANS/CNS clinical manifestations, altered blood pressure regulation, altered heart rate regulation, myoclonic jerk, lethargy, limb weakness and altered mental status are reported in ME/CFS patients, indicating a large overlap in symptom constellations between ME/CFS patients and neurotropic EV infections[88, 89].

To summarize, some serotypes of EVs exhibit CNS tropism and have the ability to produce persistent viral infections that result in atypical and distinct chronic clinical outcomes. Another complicating factor is the production of EV quasispecies, a population of EVs with subpopulations that consist of specific genotypic variants, each with genotypically-dependent functional characteristics. The proportion of the

different quasispecies in the overall population dictates infection initiation, progression and dynamics of clinical presentation [12].

DETECTION OF ENTEROVIRUSES

World Health Organization EV Surveillance Guidelines

The World Health Organization, in conjunction with the U.S. Centers for Disease Control, have published guidelines for enterovirus surveillance that details recommended procedures for specimen preservation as well as optimal methods for enterovirus detection and characterization. Although not all human enteroviruses can be propagated in cell culture, the guidelines state that multiple attempts should be made across a variety of cell lines including: primary African green, cynomolgus or rhesus monkey kidney cells (AGMK, CMK, RMK), rhesus monkey kidney (LLC-MK2), African green monkey kidney (Vero, BGMK, GMK), Madin Darby canine kidney (MDCK), human diploid cells lines (MRC-5, WI-38, SF), human embryonic kidney (HEK), human embryonic fibroblast (HEF), human epithelial carcinoma (HEp-2), and human rhabdomyosarcoma (RD) cells [90].

The guidelines further state the preferred and alternative sample types to use in cell culture inoculation depending on the clinical syndrome noted in patients. Based on the occurrence of encephalitis and respiratory clinical syndromes in a large proportion of ME/CFS cohorts, preferred sample types include brain tissue and broncho-alveolar lavage, with alternatively approved sample types, including cerebrospinal fluid (CSF), feces, throat swab, oropharyngeal swab, nasopharyngeal swab, and rectal swab [1].

Approaches and Limitation of EV Detection Strategies Employed in ME/CFS Studies

Across the enterovirus and virus literature at large, a number of methodologies are used to detect the presence of enteroviral infection in patients. In the early years of virus detection, biological approaches such as serological testing and cell culture methods were employed. Isolation via cell culture requires patient samples to be inoculated into enterovirus-susceptible cell lines and then examined periodically for the presence of viral-induced changes such as cytopathic effect (CPE), which is described as cells becoming rounded, refractile and shrinking before detaching from the cell surface. The identity of the isolated virus was then confirmed/typed via tests such as neutralization of infectivity with serotype-specific antisera or immunochemistry using fluorescent antibodies. The main disadvantages to cell culture are that inoculation depends on quality of the patient sample and requires variable and sometimes extended time periods to allow detection [5, 75]. Some enteroviruses, especially persistent enterovirus variants, do not produce CPE in cell culture. Without CPE, screening for viral nucleic acid or protein would be necessary.

Serological testing is confounded by several factors. First, enteroviruses often produce clinical disease before the appearance of antibodies, making their detection retrospective. Furthermore, enteroviruses and rhinoviruses have extensive antigenic heterogeneity and lack cross-reacting antigens, so that many different antigens would be needed to detect anti-EV antibodies [3, 5, 7]. Virus antigen detection can be achieved both by immunohistochemical detection and ELISA. Viral antigens such as VP1 exhibit sequence similarity between serotypes, which is an advantage in detection of enteroviruses, but also means that serotype identification is not feasible solely from reaction with a VP1 antigen. Commercial labs with serological tests for EVs are far

from comprehensive. For instance, the Enterovirus IgG/IgA/IgM ELISA kits sold via Virotech Diagnostics detects 14 (CVA9, CVA16, CVB2, CVB4, CVB5 and Echo 5, 11, 15, 17, 22, 23, 25, 33) of the roughly 120 known EV serotypes [6]. The Enterovirus Antibody Panel lab test provided by ARUP Laboratories similarly detects 14 EV serotypes (CVA9, CVB1-6, Echo 6, 7, 9, 11 and 30, poliovirus types 1 and 3) although the serotypes differ slightly [91]. Negative detection of EVs via these commercially available serological tests does not conclusively eliminate the possibility of an EV infection. Other companies, such as SERION Diagnostics and Immuno-Biological Laboratories also sell enterovirus-specific ELISA kits but with the added benefit of using recombinant antigens. The recombinant antigens are made from conserved and subtype specific domains across a subset of human enteroviruses and are therefore likely to demonstrate antigens for all known human enteroviruses. These kits have an increased comprehensive nature, but a positive detection cannot reveal exactly which EV serotype is the culprit in question.

A serological method for detection of antibodies to enteroviruses that has not yet been employed in ME/CFS is the peptide array, which is comprised of tiled peptides corresponding to a virus family. Such an array designed to probe human herpesviruses has been used to compare ME/CFS patients to healthy controls and individuals with other diseases [3]. An enterovirus peptide array was successfully used to detect antibodies against EV-68 in some samples of cerebrospinal fluid and serum from patients with acute flaccid myelitis [1].

The most popular detection method for identification of enteroviruses is RT-PCR, with amplification directed at conserved regions of the enterovirus genome, including

those encoding the 5'UTR, 3Dpol and VP1. VP1 is the region of choice to conduct enterovirus typing. However, low sequence similarity amidst the approximately 120 enterovirus serotypes means that no one primer set is robustly comprehensive so that RT-PCR methods would have a lower chance of identifying novel EV serotypes than unbiased sequencing. RT-PCR experiments that use primers directed at the 5'UTR of enteroviruses can be problematic if the enterovirus contains mutations within the primer binding region, as is known to happen during persistent infection. Traditional RT-PCR approaches have reduced ability to identify novel enteroviruses that could be etiological agents in new diseases.

Northern blots using sequences complementary to EV genomic regions to detect viral RNA in a gel are similarly confounded by a lack of comprehensiveness, as the probe sequence might fail to hybridize to EV serotypes that have sufficient variation in targeted sequences. For greater sensitivity and breadth, many researchers have instead used an unbiased RNAseq approach to detect enterovirus nucleic acids in patient samples. In terms of disadvantages, RNAseq is expensive and requires significant read depth in sequencing to identify low copy transcripts among the sea of nucleic acids that are being sequenced. Capture approaches have been developed to enhance sensitivity and increase breadth of viral detection [75, 85, 86] (**Table 1.1**).

Critical Review of EV Detection in ME/CFS by Method Used

Tissue Culture Reports

To date, ME/CFS studies reporting the use of tissue culture for EV detection have used CSF and feces in 1 and 4 studies, respectively [82, 87-89]. The singular CSF study reported two EV infections in a cohort of 4 patients, while the 4 fecal

studies reported an increased EV infection prevalence in 2 of 4 studies, with cohorts ranging from a 22-25% prevalence across patient cohorts (**Table 1.1**).

Table 1.1. Compilation of enterovirus-specific ME/CFS studies listed by tissue type and sub-grouped based on EV detection methodology. Many studies utilize multiple detection methods resulting in the total number of studies not equaling the number of studies based on each method.

	Positive Studies	Total Studies	Prevalence in Positive Cohorts
Blood	20	24	8-100%
Serological Test	16	20	8-90%
PCR	4	5	18-100%
RNAseq	0	2	N/A
Muscle	8	11	13-53%
PCR	6	9	13-100%
Northern Blot	4	4	21-50%
VP1 Immunochemistry	0	1	N/A
Throat Swab	1	1	17%
PCR	1	1	17%
Gastrointestinal Tissue	2	2	82%
PCR	1	1	37%
VP1 Immunochemistry	2	2	82%
dsRNA Immunochemistry	1	1	64%
Heart Tissue	1	1	N/A
PCR	1	1	N/A
Cerebrospinal Fluid	1	2	N/A
Tissue Culture	1	1	50%
EV IgG ELISA	0	1	N/A
Brain Tissue	3	3	N/A
PCR	2	2	N/A
VP1 Immunochemistry	2	2	N/A
Feces	2	4	22-25%
PCR	0	1	N/A
Tissue Culture	2	4	22-25%
Electron Microscopy	0	1	N/A

Although the prevalence of EV infections in these studies was generally shown to be significantly increased compared to healthy control cohorts, limitations in patient sample types and cell culture models may have led to findings that underrepresent the prevalence of EV infections in patient cohorts. Of the five cell culture studies, one study used only one cell type [12], 3 studies used two cell types [5, 90, 92] and one study used three cell types [7].

The most comprehensive study, which utilized three cell culture types, included green monkey kidney cells, RD cells and HeLa cells, which together supply a diversity of enterovirus receptors including CAR, CD155 and DAF. These cultures therefore detect a wide diversity of enteroviruses although the system is still not totally comprehensive. No enterovirus-positive fecal samples were found within a cohort of 12 ME/CFS patients [6] when the triple-cell culture method was used. EVs may be absent in these patients, but lack of detection might also be attributed to the presence of an enterovirus that uses an alternative receptor as well as the low likelihood of detecting EV infections in the stool samples of chronically ill patients with persistent infections in secondary sites such as muscle and brain tissue. Furthermore, the investigators were searching for CPE, and EVs present in chronic infections commonly undergo genetic changes which reduce CPE. An example of the inadequacy of CPE is a report that inoculated cell cultures were negative for CPE production in human fetal lung fibroblast and tertiary monkey kidney cell cultures but were nevertheless positive upon RT-PCR [5].

Two studies utilized Hep-2, VERO, and monkey kidney tissue cultures for identification of enterovirus from CSF and feces from 4 and 76 patients, respectively. Innes et al. [91] identified enterovirus in 2 of 4 CSF samples and one of 4 feces samples [75]. Yousef et al. [51] found that 17/76 patients tested positive for enterovirus infection while only 2/30 controls tested positive [93]

Studies reporting the absence of enterovirus infections in ME/CFS patient cohorts using tissue culture approaches had small sample sizes and incomprehensive cell culture systems. Small sample sizes along with the fact that EVs harboring 5'UTR

deletions do not produce CPE means that no definitive conclusion can be made about the absence of EVs from the data in these studies. Furthermore, fecal samples usually identify only acute enterovirus infections and not chronic ones that might be in secondary infection sites. Nevertheless, some studies that screened suboptimal sample types with culture methods did find an increased prevalence of EV infections, which might have been due to inclusion of patients who were still in the acute phase of illness.

Serological Testing for EVs

A wide variety of serological tests for detection of EVs have been developed. Studies between the 1970s and late 1990s that screened for EV infections in ME/CFS patients largely focused on serological testing. The diversity of testing employed in a total of 20 serological based ME/CFS studies included neutralization, complement fixation, micro-metabolic inhibition, ELISA, indirect immunofluorescence, and VP1 antigen detection tests. In total, 16 of the 20 studies found an increased prevalence of CVB signals in ME/CFS cohorts with positive findings ranging from 8-90% compared to the positive findings in healthy control cohorts that ranged from 0-65% (**Table 1.1**) [94].

The vast majority of studies evaluated the presence of antibodies directed only against CVB enteroviruses, with a few exceptions in which echo30- and echo9-directed IgG antibodies were screened via ELISA [95]. A notable study was performed in 1997, in which neutralization tests for 11 enteroviruses (CVB1-6 and echo6,7,9,11,30) found that 100 out of 200 tested patients had elevated enteroviral titers [53].

Although serological testing in ME/CFS cohorts generally shows an increase in the prevalence of EV antibodies, the findings often lack clinical specificity as a high prevalence of EV antibodies are found in the general population from previous exposure. In a retrospective study, it cannot be known whether the enterovirus infection occurred before or after ME/CFS disease onset without having paired sera from both time periods.

Immunochemistry to Detect EV Capsid Proteins and dsRNA

The enteroviral capsid protein VP1 is commonly used for identification of enteroviral virions in ME/CFS patient tissues. In total, 5 studies have used this technique on a variety of patient sample types, including muscle, gastrointestinal, and brain tissue (**Table 1.1, Table Apx1.1**) [9, 32, 92, 96-98]. Of these, 4 out of 5 studies identified the presence of VP1 capsid proteins in patient tissue. The fourth study did not detect VP1 staining in samples of a cohort of 30 ME/CFS patients, despite RT-PCR signals that indicated the presence of EV-RNA in 13 of the same 30 patients. The authors suggested that the difference in PCR and VPI immunochemistry resulted from persistent but latent enteroviral infection in patient muscle tissues, in which no detectable amount of virion particles were being produced [99].

The remaining 3 studies showed positive VP1 staining in both gastrointestinal and brain tissues [38, 60, 100]. Gastrointestinal samples exhibited positive staining rate of 82% in two patient cohorts (n=165, n=416). Comparative cohorts for these two studies were healthy controls (n=34) and patients with functional dyspepsia (FD) (n=66), which displayed a positive VP1 staining rate of 20% and 83%, respectively [101, 102]. Both the ME/CFS and FD patient cohorts showed dsRNA staining for 64% and 63%

of patients, respectively [103]. Because persistent/chronic EV infections with reduced CPE and viral replication typically have a 1:1 ratio between enteroviral positive and negative RNA strands, finding a high rate of dsRNA in patient tissues indicates the likely presence of persistent enteroviral infections. One study found VP1 in fibroblasts of small blood vessels in the cerebral cortex and in a small fraction of glial cells in brain [104], while another detected VP1 instead in the pontomedullary junction, medial temporal lobe, lateral frontal cortex, occipital lobe, cerebellum and midbrain [47].

Molecular Approaches to Detect EV Infections

We identified 24 reports of the use of either Northern Blot (n=4) [35, 44, 105], RT-PCR (n=18) [2, 3, 46, 57, 63, 84, 106-113] or RNAseq (n=2) [114, 115] across multiple sample types including blood, feces, muscle, brain, heart, gastrointestinal tissue and throat swabs. In a few cases, a single publication used RT-PCR on multiple sample types; thus, there are 20 independent studies amongst the 24 reports. Seventeen of the twenty publications report detection of EVs in patient samples or indicate an increased prevalence of EV infections compared to control cohorts (**Table 1.1, Table Apx1.1)**.

Table 1.2. In-silico PCR amplification results using primers reported throughout enterovirus-specific ME/CFS publications. Nested-PCR studies (methods 3, 5, 7, and 8) are reported as PCR amplification results for both of PCR (1st round), (2nd round). Values indicate number of EVs with a positive PCR amplification out of 117 total EVs tested for amplification. In-silico PCR was performed using Geneious Prime v2019.1.1. Primer design uses a modified version of Primer3 v2.3.7. Primers could bind anywhere on sequence (1 mismatch): in-silico PCR testing allowed 1 mismatch to be tolerated between the primer and its complementary site on the EV transcript. The 1 allowed mismatch was not allowed to occur within 2 base pairs of 3′ end. The 1 mismatch PCR parameter therefore indicates an in-silico PCR amplification with low forgiveness for incomplete complementarity and reduces the likelihood of off target amplification events (4 mismatches): in-silico PCR testing allowed 4 mismatches to be tolerated between the primer and its complementarity site on the EV transcript. All 4 mismatches could occur at any site within the primer and EV transcript complementarity region. The 4 mismatch PCR parameter therefore indicates an in-silico PCR amplification with high forgiveness for incomplete complementarity and increases the likelihood of both on and off target amplification events.

Publications	PCR primers and probes	No. Amplified EVs: 1 mismatch	No. Amplified EVs: 4 mismatches
(131, 140)	1: EP1, EP4 and EP2 (probe)	52/117	92/117
(141)	2: EP1, EP4	85/117	112/117
(52, 133, 143, 144)	3: 1(EP1, EP4), 2(P6, P9)	(85/117), (50/117)	(112/117), (112/117)
(96)	4: Primer 2, Primer 3 and Probe	102/117	112/117
(142)	5: 1(OL252, OL68), 2(OL24, OL253)	(21/117), (0/117)	(111/117), (3/117)
(20, 98, 136)	6: RNC2, NC1, E2 and Probe	89/117	108/117
(116)	7: 1(Primer 1, Primer 4), 2(Primer 2, Primer 3 and Probe)	(77/117), (39/117)	(103/117), (75/117)
(117)	8: 1(Primer 1, Primer 2), 2(Primer 3, Primer 4)	(65/117), (65/117)	(110/117), (110/117)

The 4 Northern blot studies used muscle tissue biopsies and were all positive for viral RNA, indicating an EV prevalence between 21-50% in ME/CFS with control cohorts showing a prevalence between 0-1% [40, 44, 116, 117]. The two RNAseq studies were negative for the presence of EV in blood, whether or not blood was taken before or after an exercise stress that exacerbated subject symptoms [118, 119]. While RNAseq is a more comprehensive approach to enterovirus detection than Northern blots, these studies cannot be directly compared since one used muscle tissue and the other assayed blood samples.

With regard to EV studies that applied RT-PCR methods, 5 of the 17 reports indicated no significant difference in EV prevalence between ME/CFS and control cohorts. The 5 reports were performed on peripheral blood leukocytes [36], muscle tissue [51, 62, 120], and feces [121]. A list of all 8 PCR approaches/methods, indicating the primer sets employed in RT-PCR experiments, was first compiled, and then each PCR set was examined for its effectiveness for detection of all 117 known EV serotypes (**Table 1.2, Table Apx1.2 and Table Apx1.3**). In-silico PCR was run with conservative allowances (1 mismatch and no mismatches within 2 base pairs of the 3'end) as well as less conservative allowances (4 mismatches with mismatches being allowed on the 3'end) to give a range of possible experimental results, given that one in-silico PCR experiment does not likely represent the true in-vitro PCR outcomes. The less conservative in-silico experiments resulted in predicted binding to multiple locations, sometimes over 15 locations along an EV genome, and thus were not likely to represent results that would be gained from an actual experiment. Examining the conservative in-silico PCR experiments that used 1 mismatch and 0

allowed mismatches within the 3'end of the primer (**Table Apx1.2**) indicated methods 1, 3, 5, 7 and 8 are low in their comprehensive nature with 52, 50, 21/0, 39 and 65 EVs being amplified out of 117 respectively. Interestingly, four [55, 63, 122] of the five [7, 84, 123-125] studies indicating a lack of EV presence by RT-PCR used primer sets from methods 1, 7 and 8, which amplify 44%, 33% and 56% of known human enteroviruses, respectively. Therefore, an EV infection could have been present and simply escaped detection due to the primer sets employed. One study reported 20.8% (n=48) of the ME/CFS cohort to have detectable EVs compared to 0% (n=29) of controls even though method 5 was used, in which round 2 PCR primers amplify 0% of EVs under conservative PCR parameters and 3% of EVs under less conservative parameters. Either that reported primer sequence does not function as expected in the in-silico PCR or the particular EV that was detected in these patients is one of the few able to be observed with method 5 primers. Poor in-silico PCR amplification using method 5 was caused by the primer OL253 (5'-GATACTYTGAGCNCCCAT-3') used in the second round PCR. First round primers, OL252 and OL68, as well as second round primer OL24 had binding rates to the EV serotypes with only OL253 lacking in-silico hybridization. Overall, RT-PCR experiments with low rates of positive in-silico PCR amplification are strongly correlated with publications indicating insignificant differences in EV prevalence between controls and patients (**Table 1.2, Table Apx1.2 and Table Apx1.3**).

As mentioned earlier, EVs are known to exhibit mutations in the 5'UTR that result in replication deficiencies. Interestingly, all 8 PCR methodologies used primer pairs targeting the 5'UTR with the exception of method 5 whose reverse primers target the

VP4 and VP2 genomic regions (**Figure 1.2**). This is an important consideration as patients infected with EV variants exhibiting 5'UTR deletions may not be successfully targeted by the primer sets employed across these PCR methodologies. In conclusion, PCR studies aimed at identifying EVs in ME/CFS have been crippled by the use of incomprehensive primer sets that target potentially deleted portions of the viral genome.

Figure 1.2. Schematic showing primer binding sites across an enteroviral genome. 5'UTR domains are indicated by roman numerals. Numbers on top of the representative genome indicate nucleotide position. Forward and reverse primers as well as probes (if applicable) are indicated across all 8 PCR methodologies used across enterovirus-related ME/CFS studies. Dark blue arrows indicate forward primers, dark green arrows indicated reverse primers, second round primers used in nested PCR approaches are indicated by light blue (forward) and light green (reverse) arrows. Red bars indicate probes, and the one grey arrow indicates a primer used in the primary reverse transcription step.

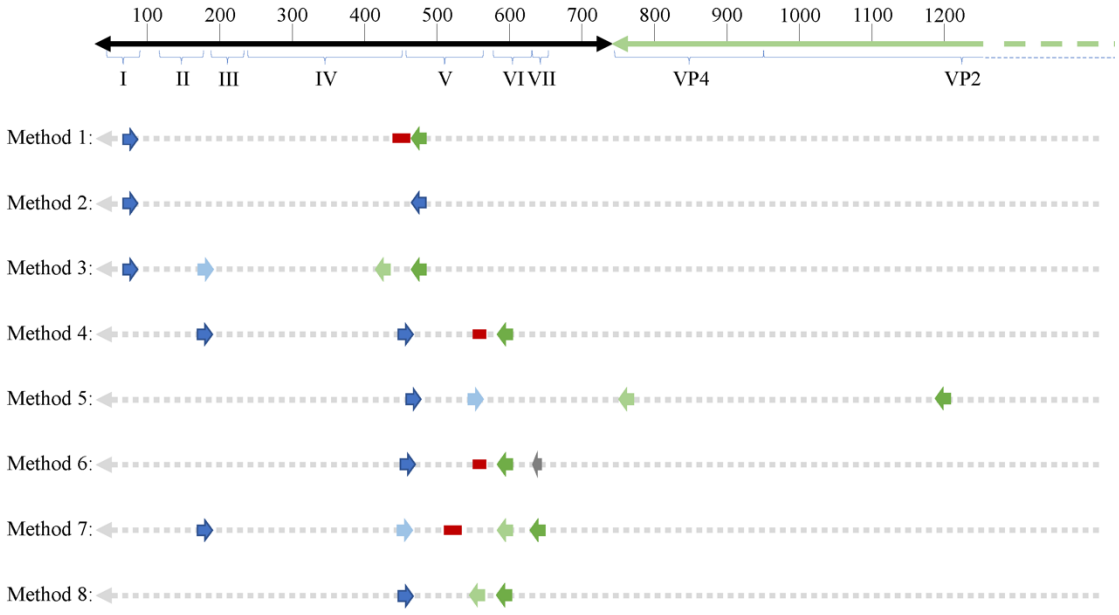

DISCUSSION

Multiple aspects of the ME/CFS pathophysiology, especially related to autonomic dysfunction, are reminiscent of chronic neurotropic enterovirus-related diseases and

clinical outcomes. This fact, in conjunction with the enterovirus-like seasonality of ME/CFS epidemics, often occurring in spatiotemporal incidence with known poliomyelitis epidemics of the time, gives strong justification for the conclusion that enteroviruses have been etiological agents in ME/CFS outbreaks.

Many ME/CFS patients in a variety of studies indicate a viral-like illness immediately preceded their ME/CFS symptoms. However, surveys also indicate that patients ascribe their onset to a variety of other reasons, including emotional stress, life events, recent travel, accidents, toxic substances, or mold [126, 127]. However, some of these events and exposures could merely be coincidental and actually be due to an enteroviral infection that was unnoticed or very mild, given that many enteroviral infections are asymptomatic [128]. The COVID19 pandemic has made it obvious that persistent symptoms can arise from mild or asymptomatic infections [129]. Were the existence of SARS CoV-2 not known, many of the individuals with long-lasting symptoms of COVID 19 might readily have ascribed their mysterious illness to some other factor than viral infection.

Post-acute viral syndromes may not all fit the diagnostic criteria recommended by the U.S. Institute of Medicine (IOM) for ME/CFS [91], as the victims of a number of viral infections have not been thoroughly investigated over long time periods. Further, even the definition of ME/CFS or SEID itself may be lumping together disparate phenomena [130]. The last report on the 2003 SARS outbreak patients exhibiting long-term symptoms followed them up to only three years later [131]. At this writing, individuals who contracted SARS-CoV-2 and did not recover completely have been ill no more than 14 months, and many are displaying not only symptoms required for the

IOM definition of ME/CFS, but additional ones, suggesting that further study may differentiate them at the molecular/biochemical level from individuals with pre-2020 ME/CFS. New information from ongoing studies of the consequences of COVID19 may indicate that the definition of ME/CFS will need to be refined to distinguish it from post-acute SARS-CoV-2 syndrome, even though a number of symptoms overlap. Notably, Gulf War Illness victims have symptoms that overlap with ME/CFS, but a number of studies are able to distinguish them from individuals with ME/CFS who did not participate in Gulf War era military activities [17, 27, 132, 133].

A relatively small number of viruses have been identified as possible triggers for ME/CFS, making the concept held by some, that "any virus" can lead to ME/CFS, unsupported by evidence. One of the few studies of viral triggers of fatiguing syndromes is being carried out in Australia, namely the Dubbo study of post-infective fatigue syndromes, which follows individuals with diagnosed Ross River virus, Epstein-Barr Virus (EBV), as well as Q fever (a bacterial rather than viral infection) [39, 134, 135]. Given the geographic limitation to Ross River virus exposure, it is not likely that it is a major cause of ME/CFS worldwide.

There appears to be a special relationship between herpesvirus infection and ME/CFS, as recently reviewed [64, 136]. Whether this is actually a relationship between enteroviral and herpesviral infection is not known. Several studies have documented that a certain percentage of people who contract mononucleosis from Epstein-Barr virus infection will still be ill 6 months or more, exhibiting symptoms diagnostic of ME/CFS [36]. Surveys often indicate that a proportion of patients believe their ME/CFS followed an acute case of mononucleosis or other type of

herpesvirus infection [45, 121, 122]. However, given that enteroviruses are known often to cause mild or asymptomatic infections, it is possible that individuals who report ME/CFS after mononucleosis or other herpesviral infections may have also had an inciting enterovirus infection before or after the herpesvirus infection. In fact, one may speculate that an undetected enteroviral infection could make an individual more susceptible to symptomatic cases of EBV infection, for example. Most individuals are infected with EBV as children, yet a number of patients have reported an adult-onset EBV infection as triggering their ME/CFS. Perhaps these adult cases are actually mis-diagnosed reactivated infections. Indeed, there are several reports of reactivated herpesvirus infections in ME/CFS patients [55, 120]. Furthermore, a few studies have discovered impaired immunological response to EBV in ME/CFS patients [64, 137]. Is this impaired response due to a prior or ongoing enteroviral infection? Whether or not herpesviruses may incite ME/CFS or merely take advantage of immune disruptions caused by enteroviral infections, they may contribute to the symptoms of the illness, and may prevent recovery, as illustrated by a subset that improves upon anti-herpesvirus drug treatment [138-140].

Our review emphasizes that EV-related ME/CFS literature indicates that some patients exhibit chronic enteroviral infection. Furthermore, our review highlights a number of experimental weaknesses (cohort size, tissue type interrogated, methodological approach, etc.) that exist across the EV-ME/CFS literature for studies both supporting or opposing increased EV infection prevalence in ME/CFS patients vs. healthy controls. Those studies that do not support an increased prevalence of EV infections in ME/CFS patient cohorts using RT-PCR are especially confounded with

issues related to incomprehensive RT-PCR primer design. Considering that the majority of patient samples interrogated have been collected from patients in the chronic stage of illness, too few studies have been directed at more appropriate secondary infection tissue sites that would give insight into the possibility of persistent myotropic or neurotropic enteroviruses. Indeed, the majority of studies interrogating muscle tissue and all studies we have identified interrogating brain tissue or cerebrospinal fluid via PCR or tissue culture have found detectable signs of EV infection. It is evident that more research must be conducted in order to determine whether or not the majority of pre-2020 ME/CFS cases have arisen from EV infection. At the time of this writing, there have been a number of anecdotal reports of individuals experiencing remission of long-term COVID19 symptoms after receiving anti-SARS COV2 vaccines. Such a therapy will not be possible for any ME/CFS patients whose illness is due to chronic infection unless the persistent virus is identified.

Moving forward, studies aimed at identifying chronic EV infections in ME/CFS patients need to consider quality and types of samples to interrogate as well as methodological approaches to employ. The key samples suggested to interrogate further would include brain tissue, cerebrospinal fluid, and muscle biopsy samples. As of now, we could identify only 5 studies reporting on the assessment of either brain (n=3) or cerebrospinal fluid (n=2) and these studies are either on individual patients or cohorts of up to 7. Muscle biopsies have been chosen as the source of patient tissue sample in a total of 11 identified studies, but problems in RT-PCR primer design, small cohorts and few biological tissue replicates means the conclusions of the 8

studies reporting an increased EV prevalence in ME/CFS cohorts may be underrepresenting the true prevalence. Furthermore, the 3 studies indicating a lack of increased prevalence may have been unable to identify the EV serotype in question.

In terms of methodological approaches, RT-PCR with optimal primer sets and or RNAseq with target capture enrichment should be utilized as the methodology of choice for EV detection specifically. Both experimental approaches may be modified to allow detection of both positive and negative strand viral transcripts and are also advantageous in their ability to detect low copy number transcripts. Targeted RNAseq has the increased benefit of being completely comprehensive for the enteroviral family, allowing complete genomic sequencing as well as an increased likelihood of identifying novel EV serotypes possibly at play in an illness such as ME/CFS whose inciting pathogen remains unidentified.

REFERENCES

1. Vogt D, Andino R. An RNA Element at the 5′-End of the Poliovirus Genome Functions as a General Promoter for RNA Synthesis. PLoS pathogens. 2010;6:e1000936.

2. Julien J, Leparc-Goffart I, Lina B, Fuchs F, Foray S, Janatova I, et al. Postpolio syndrome: poliovirus persistence is involved in the pathogenesis. J Neurol. 1999;246(6):472-6.

3. Lim EJ, Son CG. Review of case definitions for myalgic encephalomyelitis/chronic fatigue syndrome (ME/CFS). J Transl Med. 2020;18(1):289.

4. Lévêque N, Renois F, Talmud D, Nguyen Y, Lesaffre F, Boulagnon C, et al. Quantitative genomic and antigenomic enterovirus RNA detection in explanted heart tissue samples from patients with end-stage idiopathic dilated cardiomyopathy. J Clin Microbiol. 2012;50(10):3378-80.

5. Hyde BM, Goldstein J, Levine P, editors. The Clinical and Scientific Basis of Myalgic Encephalomyelitis/Chronic Fatigue Syndrome. Ottawa, Canada: Nightingale Research Foundation; 1992.

6. Fisman D. Seasonality of viral infections: mechanisms and unknowns. Clin Microbiol Infect. 2012;18(10):946-54.

7. Hyde B. Understanding Myalgic Encephalomyelitis. Ottawa Canada: Nightingale Press; 2020. 315 p.

8. Kim KS, Chapman NM, Tracy S. Replication of coxsackievirus B3 in primary cell cultures generates novel viral genome deletions. J Virol. 2008;82(4):2033-7.

9. Glenet M, N'Guyen Y, Mirand A, Henquell C, Lebreil AL, Berri F, et al. Major 5′terminally deleted enterovirus populations modulate type I IFN response in acute myocarditis patients and in human cultured cardiomyocytes. Sci Rep. 2020;10(1):11947.

10. Gibson JP, Righthand VF. Persistence of echovirus 6 in cloned human cells. J Virol. 1985;54(1):219-23.

11. Chia J, Chia A, Wang D, El-Habbal R. Functional Dyspepsia and Chronic Gastritis Associated with Enteroviruses. Open J Gastroenterol. 2015;05:21-7.

12. Tam PE, Messner RP. Molecular mechanisms of coxsackievirus persistence in chronic inflammatory myopathy: viral RNA persists through formation of a double-stranded complex without associated genomic mutations or evolution. J Virol. 1999;73(12):10113-21.

13. Tomas C, Brown AE, Newton JL, Elson JL. Mitochondrial complex activity in permeabilised cells of chronic fatigue syndrome patients using two cell types. PeerJ. 2019;7:e6500.

14. Muir P, Nicholson F, Sharief MK, Thompson EJ, Cairns NJ, Lantos P, et al. Evidence for persistent enterovirus infection of the central nervous system in patients with previous paralytic poliomyelitis. Ann N Y Acad Sci. 1995;753:219-32.

15. Pearce EL, Poffenberger MC, Chang CH, Jones RG. Fueling immunity: insights into metabolism and lymphocyte function. Science. 2013;342(6155):1242454.

16. Pinkert S, Klingel K, Lindig V, Dörner A, Zeichhardt H, Spiller OB, et al. Virus-host coevolution in a persistently coxsackievirus B3-infected cardiomyocyte cell line. J Virol. 2011;85(24):13409-19.

17. Righthand VF, Blackburn RV. Steady-state infection by echovirus 6 associated with nonlytic viral RNA and an unprocessed capsid polypeptide. J Virol. 1989;63(12):5268-75.

18. Missailidis D, Sanislav O, Allan CY, Smith PK, Annesley SJ, Fisher PR. Dysregulated provision of oxidisable substrates to the mitochondria in ME/CFS lymphoblasts. Int J Mol Sci. 2021;22(4).

19. Mandarano AH, Maya J, Giloteaux L, Peterson DL, Maynard M, Gottschalk CG, et al. Myalgic encephalomyelitis/chronic fatigue syndrome patients exhibit altered T cell metabolism and cytokine associations. J Clin Invest. 2020;130(3):1491-505.

20. Tomas C, Brown A, Strassheim V, Elson JL, Newton J, Manning P. Cellular bioenergetics is impaired in patients with chronic fatigue syndrome. PLoS One. 2017;12(10):e0186802.

21. Tomas C, Newton J. Metabolic abnormalities in chronic fatigue syndrome/myalgic encephalomyelitis: a mini-review. Biochem Soc Trans. 2018;46(3):547-53.

22. Geltink RIK, Kyle RL, Pearce EL. Unraveling the complex interplay between T cell metabolism and function. Annu Rev Immunol. 2018;36:461-88.

23. Van Cauwenbergh D, Nijs J, Kos D, Van Weijnen L, Struyf F, Meeus M. Malfunctioning of the autonomic nervous system in patients with chronic fatigue syndrome: a systematic literature review. Eur J Clin Invest. 2014;44(5):516-26.

24. Wyller VB, Godang K, Mørkrid L, Saul JP, Thaulow E, Walløe L. Abnormal thermoregulatory responses in adolescents with chronic fatigue syndrome: relation to clinical symptoms. Pediatrics. 2007;120(1):e129-37.

25. Burnet RB, Chatterton BE. Gastric emptying is slow in chronic fatigue syndrome. BMC Gastroenterol. 2004;4(1):32.

26. Jones DEJ, Hollingsworth KG, Jakovljevic DG, Fattakhova G, Pairman J, Blamire AM, et al. Loss of capacity to recover from acidosis on repeat exercise in chronic fatigue syndrome: a case–control study. Eur J Clin Invest. 2012;42(2):186-94.

27. Barnden LR, Kwiatek R, Crouch B, Burnet R, Del Fante P. Autonomic correlations with MRI are abnormal in the brainstem vasomotor centre in Chronic Fatigue Syndrome. NeuroImage Clin. 2016;11:530-7.

28. Mueller C, Lin JC, Sheriff S, Maudsley AA, Younger JW. Evidence of widespread metabolite abnormalities in Myalgic encephalomyelitis/chronic fatigue syndrome: assessment with whole-brain magnetic resonance spectroscopy. Brain Imaging Behav. 2020;14(2):562-72.

29. Nakatomi Y, Mizuno K, Ishii A, Wada Y, Tanaka M, Tazawa S, et al. Neuroinflammation in Patients with Chronic Fatigue Syndrome/Myalgic Encephalomyelitis: An ^{11}C-(R)-PK11195 PET Study. J Nucl Med. 2014;55(6):945-50.

30. Peterson PK, Sirr SA, Grammith FC, Schenck CH, Pheley AM, Hu S, et al. Effects of mild exercise on cytokines and cerebral blood flow in chronic fatigue syndrome patients. Clin Diagn Lab Immunol. 1994;1(2):222-6.

31. Costa DC, Tannock C, Brostoff J. Brainstem perfusion is impaired in chronic fatigue syndrome. Qjm. 1995;88(11):767-73.

32. Chen B-S, Lee H-C, Lee K-M, Gong Y-N, Shih S-R. Enterovirus and Encephalitis. Front Microbiol. 2020;11.

33. Bodian D. Histopathologic basis of clinical findings in poliomyelitis. Am J Med. 1949;6(5):563-78.

34. Bruno RL. Chronic Fatigue, Fainting and Autonomie Dysfunction. J Chroic Fatigue Syndr. 1997;3(3):109-16.

35. Richardson J. Viral isolation from brain in Myalgic Encephalomyelitis. J Chroic Fatigue Syndr. 2001;9(3-4):15-9.

36. John Chia DW, Andrew Chia, Rabiha El-Habbal. Chronic enterovirus (EV) infection in a patient with myalgic encephalomyelitis / chronic fatigue syndrome (ME/CFS) – Clinical, Virologic and Pathological Analysis. 2015.

37. Nigel S. Severe ME in Children. Healthc. 2020;8(211):211-.

38. Rhoades RE, Tabor-Godwin JM, Tsueng G, Feuer R. Enterovirus infections of the central nervous system. Virology. 2011;411(2):288-305.

39. Europe WHOROf. Enterovirus Surveillance Guidelines: Guidelines for Enterovirus Surveillance in Support of the Polio Eradication Initiative: World Health Organization, Regional Office for Europe.

40. Chiang P-S, Huang M-L, Luo S-T, Lin T-Y, Tsao K-C, Lee M-S. Comparing molecular methods for early detection and serotyping of enteroviruses in throat swabs of pediatric patients. PloS one. 2012;7(10):e48269-e.

41. Muir P, Kämmerer U, Korn K, Mulders MN, Pöyry T, Weissbrich B, et al. Molecular typing of enteroviruses: current status and future requirements. The European Union Concerted Action on Virus Meningitis and Encephalitis. Clin Microbiol Rev. 1998;11(1):202-27.

42. Laboratories A. Enterovirus Antibodies Panel: ARUP Laboratories; 2021 [Product Description]. Available from: https://ltd.aruplab.com/Tests/Pub/2014108.

43. Metsky HC, Siddle KJ, Gladden-Young A, Qu J, Yang DK, Brehio P, et al. Capturing sequence diversity in metagenomes with comprehensive and scalable probe design. Nat Biotechnol. 2019;37(2):160-8.

44. Innes SGB. Encephalomyelitis resembling benign myalgic encephalomyelitis. Lancet. 1970;295(7654):969-71.

45. Caroline MAS, Willem JGM, Jos WMvdM, Jan HMMV, Gijs B, Jan FMF, et al. Enteroviruses and the Chronic Fatigue Syndrome. Clin Infect Dis. 1994;19(5):860.

46. Lindh G, Evengård B, Lindquist L, Samuelson A, Hedlund KO, Ehrnst A. No findings of enteroviruses in Swedish patients with chronic fatigue syndrome. Scand J Infect Dis. 1996;28(3):305-7.

47. Yousef GE, Mann GF, Smith DG, Bell EJ, Murugesan V, McCartney RA, et al. Chronic enterovirus infection in patients with postviral fatigue syndrome. Lancet. 1988;331(8578):146-50.

48. Keighley BD, Bell EJ. Sporadic myalgic encephalomyelitis in a rural practice. J R Coll Gen Pract. 1983;33(251):339-41.

49. Calder BD, Warnock PJ, McCartney RA, Bell EJ. Coxsackie B viruses and the post-viral syndrome: a prospective study in general practice. J R Coll Gen Pract. 1987;37(294):11-4.

50. Douche-Aourik F, Berlier W, Feasson L, Bourlet T, Harrath R, Omar S, et al. Detection of enterovirus in human skeletal muscle from patients with chronic inflammatory muscle disease or fibromyalgia and healthy subjects. 2003. p. 540-7.

51. Chia JKS, Chia AY. Chronic fatigue syndrome is associated with chronic enterovirus infection of the stomach. J Clin Pathol. 2008(1):43.

52. Archard LC, Bowles NE, Behan PO, Bell EJ, Doyle D. Postviral Fatigue Syndrome: Persistence of Enterovirus RNA in Muscle and Elevated Creatine Kinase. J R Soc Med. 1988;81(6):326-9.

53. Cunningham L, Bowles NE, Lane RJM, Dubowitz V, Archard LC. Persistence of enteroviral RNA in chronic fatigue syndrome is associated with the abnormal production of equal amounts of positive and negative strands of enteroviral RNA. J Gen Virol. 1990;71(6):1399-402.

54. Bowles NE, Bayston TA, Zhang HY, Doyle D, Lane RJ, Cunningham L, et al. Persistence of enterovirus RNA in muscle biopsy samples suggests that some cases of chronic fatigue syndrome result from a previous, inflammatory viral myopathy. J Med. 1993;24(2-3):145-60.

55. McArdle A, McArdle F, Jackson MJ, Page SF, Fahal I, Edwards RH. Investigation by polymerase chain reaction of enteroviral infection in patients with chronic fatigue syndrome. Clinl Sci. 1996;90(4):295-300.

56. Lane RJM, Soteriou BA, Zhang H, Archard LC. Enterovirus related metabolic myopathy: a postviral fatigue syndrome. J Neurol Neurosurg Psychiatry. 2003(10):1382.

57. Galbraith DN, Nairn C, Clements GB. Phylogenetic analysis of short enteroviral sequences from patients with chronic fatigue syndrome. J Gen Virol. 1995;76 (Pt 7):1701-7.

58. Galbraith DN, Nairn C, Clements GB. Evidence for enteroviral persistence in humans. J Gen Virol. 1997;78 (Pt 2):307-12.

59. Clements GB, McGarry F, Nairn C, Galbraith DN. Detection of enterovirus-specific RNA in serum: the relationship to chronic fatigue. J Med Virol. 1995;45(2):156-61.

60. McGarry F, Gow J, Behan PO. Enterovirus in the Chronic Fatigue Syndrome. Ann Intern Med. 1994;120(11):972-3.

61. Nairn C, Galbraith DN, Clements GB. Comparison of coxsackie B neutralisation and enteroviral PCR in chronic fatigue patients. J Med Virol. 1995;46(4):310-3.

62. Gow JW, Behan WM, Clements GB, Woodall C, Riding M, Behan PO. Enteroviral RNA sequences detected by polymerase chain reaction in muscle of

patients with postviral fatigue syndrome. BMJ (Clinical research ed). 1991;302(6778):692-6.

63. Gow JW, Behan WM, Simpson K, McGarry F, Keir S, Behan PO. Studies on enterovirus in patients with chronic fatigue syndrome. Clin Infect Dis. 1994;18 Suppl 1:S126-9.

64. Swanink CM, Vercoulen JH, Bazelmans E, Fennis JF, Bleijenberg G, van der Meer JW, et al. Viral antibodies in chronic fatigue syndrome. Clin Infect Dis. 1995;21(3):708-9.

65. Chu L, Valencia IJ, Garvert DW, Montoya JG. Onset patterns and course of Myalgic Encephalomyelitis/Chronic Fatigue Syndrome. Front Pediatr. 2019;7:12.

66. Johnston SC, Staines DR, Marshall-Gradisnik SM. Epidemiological characteristics of chronic fatigue syndrome/myalgic encephalomyelitis in Australian patients. Clin Epidemiol. 2016;8:97-107.

67. Morens DM, Pallansch MA. Epidemiology. In: Rotbart HA, editor. Human Enterovirus Infections. Washington, D.C.: ASM Press; 1995. p. 3-23.

68. Committee IoM. Beyond myalgic encephalomyelitis/chronic fatigue syndrome: redefining an illness Washington, D.C.: National Academies Press; 2015.

69. Twisk FN. A critical analysis of the proposal of the Institute of Medicine to replace myalgic encephalomyelitis and chronic fatigue syndrome by a new diagnostic entity called systemic exertion intolerance disease. Curr Med Res Opin. 2015;31(7):1333-47.

70. Moldofsky H, Patcai J. Chronic widespread musculoskeletal pain, fatigue, depression and disordered sleep in chronic post-SARS syndrome; a case-controlled study. BMC Neurol. 2011;11:37.

71. Baraniuk JN, Shivapurkar N. Exercise - induced changes in cerebrospinal fluid miRNAs in Gulf War Illness, Chronic Fatigue Syndrome and sedentary control subjects. Sci Rep. 2017;7(1):15338.

72. Fletcher MA, Rosenthal M, Antoni M, Ironson G, Zeng XR, Barnes Z, et al. Plasma neuropeptide Y: a biomarker for symptom severity in chronic fatigue syndrome. Behav Brain Funct. 2010;6:76.

73. Smylie AL, Broderick G, Fernandes H, Razdan S, Barnes Z, Collado F, et al. A comparison of sex-specific immune signatures in Gulf War illness and chronic fatigue syndrome. BMC Immunol. 2013;14:29.

74. Cvejic E, Li H, Hickie IB, Wakefield D, Lloyd AR, Vollmer-Conna U. Contribution of individual psychological and psychosocial factors to symptom severity and time-to-recovery after naturally-occurring acute infective illness: The Dubbo Infection Outcomes Study (DIOS). Brain Behav Immun. 2019;82:76-83.

75. Hickie I, Davenport T, Wakefield D, Vollmer-Conna U, Cameron B, Vernon SD, et al. Post-infective and chronic fatigue syndromes precipitated by viral and non-viral pathogens: prospective cohort study. BMJ. 2006;333(7568):575.

76. Rasa S, Nora-Krukle Z, Henning N, Eliassen E, Shikova E, Harrer T, et al. Chronic viral infections in myalgic encephalomyelitis/chronic fatigue syndrome (ME/CFS). J Transl Med. 2018;16(1):268.

77. Katz BZ, Jason LA. Chronic fatigue syndrome following infections in adolescents. Curr Opin Pediatr. 2013;25(1):95-102.

78. Ablashi DV, Eastman HB, Owen CB, Roman MM, Friedman J, Zabriskie JB, et al. Frequent HHV-6 reactivation in multiple sclerosis (MS) and chronic fatigue syndrome (CFS) patients. J Clin Virol. 2000;16(3):179-91.

79. Montoya JG, Kogelnik AM, Bhangoo M, Lunn MR, Flamand L, Merrihew LE, et al. Randomized clinical trial to evaluate the efficacy and safety of valganciclovir in a subset of patients with chronic fatigue syndrome. J Med Virol. 2013;85(12):2101-9.

80. Watt T, Oberfoell S, Balise R, Lunn MR, Kar AK, Merrihew L, et al. Response to valganciclovir in chronic fatigue syndrome patients with human herpesvirus 6 and Epstein-Barr virus IgG antibody titers. J Med Virol. 2012;84(12):1967-74.

81. Valdez AR, Hancock EE, Adebayo S, Kiernicki DJ, Proskauer D, Attewell JR, et al. Estimating Prevalence, Demographics, and Costs of ME/CFS Using Large Scale Medical Claims Data and Machine Learning. Front Pediatr. 2019;6:412-.

82. Chia JKS. The role of enterovirus in chronic fatigue syndrome. J Clin Pathol. 2005(11):1126.

83. Carruthers BM, van de Sande MI, De Meirleir KL, Klimas NG, Broderick G, Mitchell T, et al. Myalgic encephalomyelitis: International Consensus Criteria. J Intern Med. 2011;270(4):327-38.

84. Parish JG. Early outbreaks of 'epidemic neuromyasthenia'. Postgrad Med J. 1978;54(637):711-7.

85. Gilliam AG. Epidemiological study of an epidemic, diagnosed as poliomyelitis, occurring among the personnel of the los angeles county general hospital durring the summer of 1934.: Washington, Public Health Service, for sale by the Supt. of Docs., U.S. Govt. Print. Off.; 1938.

86. Pellew RA. Further Investigations on a Disease Resembling Poliomyelitis Seen in Adelaide. Med J Aust. 1955;2.

87. Sigurdsson B, Gudnadottir M, Petursson G. Response to poliomyelitis vaccination. Lancet. 1958;1(7016):370-1.

88. Baggen J, Thibaut HJ, Strating JRPM, van Kuppeveld FJM. The life cycle of non-polio enteroviruses and how to target it. Nat Rev Microbiol. 2018;16(6):368-81.

89. Anand SK, Tikoo SK. Viruses as modulators of mitochondrial functions. Adv Virol. 2013;2013:738794-.

90. Sane F, Caloone D, Gmyr V, Engelmann I, Belaich S, Kerr-Conte J, et al. Coxsackievirus B4 can infect human pancreas ductal cells and persist in ductal-like cell cultures which results in inhibition of Pdx1 expression and disturbed formation of islet-like cell aggregates. Cell Mol Life Sci. 2013;70(21):4169-80.

91. Blattner RJ. Benign myalgic encephalomyelitis (Akureyri disease, Iceland disease). J Pediatr. 1956;49(4):504-6.

92. Krogvold L, Edwin B, Buanes T, Frisk G, Skog O, Anagandula M, et al. Detection of a Low-Grade Enteroviral Infection in the Islets of Langerhans of Living Patients Newly Diagnosed With Type 1 Diabetes. Diabetes. 2015;64(5):1682.

93. Wang H, Li Y. Recent Progress on Functional Genomics Research of Enterovirus 71. Virol Sin. 2019;34(1):9-21.

94. Feuer R, Ruller CM, An N, Tabor-Godwin JM, Rhoades RE, Maciejewski S, et al. Viral persistence and chronic immunopathology in the adult central nervous system following Coxsackievirus infection during the neonatal period. J Virol. 2009;83(18):9356-69.

95. Lietzén N, Hirvonen K, Honkimaa A, Buchacher T, Laiho JE, Oikarinen S, et al. Coxsackievirus B Persistence Modifies the Proteome and the Secretome of Pancreatic Ductal Cells. iScience. 2019;19:340-57.

96. Simmonds RS, Szücs G, Metcalf TG, Melnick JL. Persistently infected cultures as a source of hepatitis A virus. Appl Environ Microbiol. 1985;49(4):749-55.

97. Wilfert CM, Buckley RH, Mohanakumar T, Griffith JF, Katz SL, Whisnant JK, et al. Persistent and Fatal Central-Nervous-System ECHOvirus Infections in Patients with Agammaglobulinemia. N Engl J Med. 1977;296(26):1485-9.

98. Smits B, van den Heuvel L, Knoop H, Küsters B, Janssen A, Borm G, et al. Mitochondrial enzymes discriminate between mitochondrial disorders and chronic fatigue syndrome. Mitochondrion. 2011;11(5):735-8.

99. Byrne JHe. Neuroscience Online: An Electronic Textbook for the Neurosciences. Department of Neurobiology and Anatomy: McGovern Medical School at The University of Texas Health Science Center at Houston (UTHealth); 1997.

100. Schmaling KB, Lewis DH, Fiedelak JI, Mahurin R, Buchwald DS. Single-photon emission computerized tomography and neurocognitive function in patients with chronic fatigue syndrome. Psychosom Med. 2003;65(1):129-36.

101. Yang SD, Li PQ, Zhu CP, Tao JP, Deng L, Liu HS, et al. Clinical manifestations of severe enterovirus 71 infection and early assessment in a Southern China population. BMC Infect Dis. 2017;17(1).

102. Diagnostics V. Enterovirus ELISA: ViroTech Diagnostics; 2021 [Detailed Product Description]. Available from: http://www.virotechdiagnostics.com/fileadmin/user_upload/Doc/FL/FL_EC116G00_116A00_116M00e.pdf.

103. Loebel M, Eckey M, Sotzny F, Hahn E, Bauer S, Grabowski P, et al. Serological profiling of the EBV immune response in Chronic Fatigue Syndrome using a peptide microarray. PLoS One. 2017;12(6):e0179124.

104. No JS, Kim W-K, Cho S, Lee S-H, Kim J-A, Lee D, et al. Comparison of targeted next-generation sequencing for whole-genome sequencing of Hantaan orthohantavirus in Apodemus agrarius lung tissues. Sci Rep. 2019;9(1):16631.

105. Fegan KG, Behan PO, Bell EJ. Myalgic encephalomyelitis--report of an epidemic. J R Coll Gen Pract. 1983;33(251):335-7.

106. Richardson J. Enteroviral and toxin mediated myalgic encephalomyelitis/chronic fatigue syndrome and other organ pathologies. New York, London, Oxford: Haworth Press; 2001. 247 p.

107. Williams CH, Kajander T, Hyypia T, Jackson T, Sheppard D, Stanway G. Integrin alpha v beta 6 is an RGD-dependent receptor for coxsackievirus A9. J Virol. 2004;78(13):6967-73.

108. Yamayoshi S, Fujii K, Koike S. Receptors for enterovirus 71. Emerg Microbes Infect. 2014;3(7):e53-e.

109. Alidjinou EK, Engelmann I, Bossu J, Villenet C, Figeac M, Romond MB, et al. Persistence of Coxsackievirus B4 in pancreatic ductal-like cells results in cellular and viral changes. Virulence. 2017;8(7):1229-44.

110. Zhang X, Zheng Z, Shu B, Liu X, Zhang Z, Liu Y, et al. Human astrocytic cells support persistent coxsackievirus B3 infection. J Virol. 2013;87(22):12407-21.

111. Vallbracht A, Hofmann L, Wurster KG, Flehmig B. Persistent infection of human fibroblasts by hepatitis A virus. J Gen Virol. 1984;65 (Pt 3):609-15.

112. Booth NE, Myhill S, McLaren-Howard J. Mitochondrial dysfunction and the pathophysiology of Myalgic Encephalomyelitis/Chronic Fatigue Syndrome (ME/CFS). Int J Clin Exp Med. 2012;5(3):208-20.

113. Tomas C, Elson JL, Newton JL, Walker M. Substrate utilisation of cultured skeletal muscle cells in patients with CFS. Sci Rep. 2020;10(1):18232.

114. Ichise M, Salit IE, Abbey SE, Chung DG, Gray B, Kirsh JC, et al. Assessment of regional cerebral perfusion by 99Tcm-HMPAO SPECT in chronic fatigue syndrome. Nucl Med Commun. 1992;13(10):767-72.

115. Hyde B. The Nightingale Research FOundation Definition of Myalgic Encephalomyelitis: The Nightingale Research Foundation 2007.

116. Lee KY. Enterovirus 71 infection and neurological complications. Korean J Pediatr. 2016;59(10):395-401.

117. Mishra N, Ng TFF, Marine RL, Jain K, Ng J, Thakkar R, et al. Antibodies to enteroviruses in cerebrospinal fluid of patients with Acute Flaccid Myelitis. mBio. 2019;10(4).

118. Calder BD, Warnock PJ. Coxsackie B infection in a Scottish general practice. J R Coll Gen Pract. 1984;34(258):15-9.

119. O'Neal AJ, Hanson MR. The enterovirus theory of disease etiology in Myalgic Encephalomyelitis/Chronic Fatigue Syndrome: a critical review. Front Med. 2021;8:688486.

120. Bouquet J, Gardy JL, Brown S, Pfeil J, Miller RR, Morshed M, et al. RNA-Seq Analysis of Gene Expression, Viral Pathogen, and B-Cell/T-Cell Receptor Signatures in Complex Chronic Disease. Clin Infect Dis. 2017;64(4):476-81.

121. Cunningham L, Bowles NE, Archard LC. Persistent virus infection of muscle in postviral fatigue syndrome. Br Med Bull. 1991;47(4):852-71.

122. Bouquet J, Li T, Gardy JL, Kang X, Stevens S, Stevens J, et al. Whole blood human transcriptome and virome analysis of ME/CFS patients experiencing post-exertional malaise following cardiopulmonary exercise testing. PloS one. 2019;14(3):e0212193-e.

123. Kronbichler A, Kresse D, Yoon S, Lee KH, Effenberger M, Shin JI. Asymptomatic patients as a source of COVID-19 infections: A systematic review and meta-analysis. Int J Infect Dis. 2020;98:180-6.

124. Cameron B, Flamand L, Juwana H, Middeldorp J, Naing Z, Rawlinson W, et al. Serological and virological investigation of the role of the herpesviruses EBV, CMV and HHV-6 in post-infective fatigue syndrome. J Med Virol. 2010;82(10):1684-8.

125. Freyche MJ, Payne AM, Lederrey C. Poliomyelitis in 1953. Bull World Health Organ. 1955;12(4):595-649.

126. Rotbard HA, ed. Human Enterovirus Infection. Washington, D.C.: ASM Press; 1995. 445 p.

127. Zoll J, Heus HA, van Kuppeveld FJ, Melchers WJ. The structure-function relationship of the enterovirus 3'-UTR. Virus Res. 2009;139(2):209-16.

128. Alnaji FG, Bentley K, Pearson A, Woodman A, Moore JD, Fox H, et al. Recombination in enteroviruses is a ubiquitous event independent of sequence homology and RNA structure. bioRxiv. 2020:2020.09.29.319285.

129. Tracy S, Smithee S, Alhazmi A, Chapman N. Coxsackievirus can persist in murine pancreas by deletion of 5' terminal genomic sequences. J Med Virol. 2015;87(2):240-7.

130. Oikarinen M, Tauriainen S, Oikarinen S, Honkanen T, Collin P, Rantala I, et al. Type 1 Diabetes Is Associated With Enterovirus Infection in Gut Mucosa. Diabetes. 2012;61(3):687.

131. Goldstein JA, Mena I, Jouanne E, Lesser I. The Assessment of Vascular Abnormalities in Late Life Chronic Fatigue Syndrome by Brain SPECT. J Chronic Fatigue Syndr. 1995;1(1):55-79.

132. Zhang C, Baumer A, Mackay IR, Linnane AW, Nagley P. Unusual pattern of mitochondrial DNA deletions in skeletal muscle of an adult human with chronic fatigue syndrome. Hum Mol Genet. 1995;4(4):751-4.

133. Zeineh MM, Kang J, Atlas SW, Raman MM, Reiss AL, Norris JL, et al. Right Arcuate Fasciculus Abnormality in Chronic Fatigue Syndrome. Radiology. 2014;274(2):517-26.

134. Siessmeier T, Nix WA, Hardt J, Schreckenberger M, Egle UT, Bartenstein P. Observer independent analysis of cerebral glucose metabolism in patients with chronic fatigue syndrome. J Neurol Neurosurg Psychiatry. 2003;74(7):922.

135. Storch GA. Diagnostic Virology. Clin Infect Dis. 2000;31(3):739-51.

136. Briese T, Kapoor A, Mishra N, Jain K, Kumar A, Jabado OJ, et al. Virome Capture Sequencing Enables Sensitive Viral Diagnosis and Comprehensive Virome Analysis. mBio. 2015;6(5):e01491-15.

137. Ariza ME. Myalgic Encephalomyelitis/Chronic Fatigue Syndrome: The Human Herpesviruses Are Back! Biomolecules. 2021;11(2).

138. Jason LA, Cotler J, Islam MF, Sunnquist M, Katz BZ. Risks for Developing ME/CFS in College Students Following Infectious Mononucleosis: A Prospective Cohort Study. Clin Infect Dis. 2020.

139. Chu L, Valencia IJ, Garvert DW, Montoya JG. Deconstructing post-exertional malaise in myalgic encephalomyelitis/ chronic fatigue syndrome: A patient-centered, cross-sectional survey. PLoS One. 2018;13(6):e0197811.

140. Buchwald D, Cheney PR, Peterson DL, Henry B, Wormsley SB, Geiger A, et al. A chronic illness characterized by fatigue, neurologic and immunologic disorders, and active human herpesvirus type 6 infection. Ann Intern Med. 1992;116(2):103-13.

CHAPTER 2

Survey of Anti-Pathogen Antibody Levels in Myalgic Encephalomyelitis/Chronic Fatigue Syndrome[2]

ABSTRACT

Infectious pathogens are implicated in the etiology of myalgic encephalomyelitis/chronic fatigue syndrome (ME/CFS) because of the occurrence of outbreaks of the disease. While a number of different infectious agents have been associated with the onset of ME/CFS, the identity of a specific organism has been difficult to determine in individual cases. The aim of our study is to survey ME/CFS subjects for evidence of an infectious trigger and/or evidence of immune dysregulation via serological testing of plasma samples for antibodies to 122 different pathogen antigens. Immune profiles were compared to age-, sex-, and BMI-matched controls to provide a basis for comparison. Antibody levels to individual antigens surveyed in this study do not implicate any one of the pathogens in ME/CFS, nor do they rule out common pathogens that frequently infect the US population. However, our results

[2] This work was originally published as "Survey of Anti-Pathogen Antibody Levels in Myalgic Encephalomyelitis/Chronic Fatigue Syndrome" by Adam J. O'Neal Katherine A. Glass, Christopher J. Emig, Adela A. Vitug, Steven J. Henry, Dikoma C. Shungu, Xiangling Mao, Susan M. Levine, and Maureen R. Hanson. *Proteomes* 10, no. 2: 21. https://doi.org/10.3390/proteomes10020021. Conceptualization, A.J.O., M.R.H. and C.J.E.; subject recruitment, D.C.S., X.M. and S.M.L.; provision of some plasma samples, D.C.S. and X.M.; antibody assays, A.A.V., S.J.H. and C.J.E.; data analysis, A.J.O., M.R.H., K.A.G. and C.J.E.; original draft preparation, A.J.O., K.A.G. and M.R.H.; writing—review and editing, C.J.E., S.J.H. and S.M.L. All authors have read and agreed to the published version of the manuscript

revealed sex-based differences in steady-state humoral immunity, both within the ME/CFS cohort and when compared to trends seen in the healthy control cohort.

INTRODUCTION

Myalgic encephalomyelitis/chronic fatigue syndrome (ME/CFS) is a complex, multi-system disease; its diagnosis requires the occurrence of profound fatigue, post-exertional malaise, sleep dysfunction, pain, two or more cognitive/neurological manifestations, and at least one symptom related to autonomic dysfunction, neuroendocrine dysfunction, or immune dysfunction, according to the Canadian Consensus Criteria (CCC) [1]. In the acute phase of illness, many ME/CFS sufferers complain of a flu-like illness characterized by fever, chills, sore throat, headache, and muscle aches. Acute illnesses prior to long-term chronic illness have been observed in both sporadic, isolated cases of ME/CFS as well as in clusters and outbreaks, where tens or hundreds of individuals are affected over a short period of time in the same general geographic location [2].

Reports of epidemic events with symptom constellations reminiscent of ME/CFS have been recorded as early as the late 1600s to the mid-1700s [2-4]. Since these initial outbreaks, an infectious culprit in ME/CFS disease onset has been suspected. Early investigations following the 1934 Los Angeles County Hospital outbreak [5] focused on enteroviruses (EVs) as disease initiators due to: (1) the spatiotemporal overlap between ME/CFS outbreaks and known poliomyelitis epidemics of the time; (2) the seasonality of ME/CFS outbreaks matching those of enteroviral outbreaks; and (3) the ME/CFS symptom constellation overlapping with symptoms described across known chronic enteroviral clinical outcomes [6-8]. Although many clues point to

enteroviruses as etiologic agents of this disease, other research groups have put forward additional causal agents as potential disease initiators in ME/CFS—including, but not limited to, Brucella, *Chlamydia pneumoniae*, *Coxiella burnetti*, cytomegalovirus, Epstein-Barr virus, other human herpesviruses, hepatitis C virus, human lentiviruses, human T-cell leukemia virus II-like virus, parvovirus B19, Borna virus, spumavirus, and *Toxoplasma gondii* [6, 9-13].

Evidence for immune dysfunction in some ME/CFS sufferers includes reduced natural killer cell toxicity, altered inflammatory cytokine and immunoglobulin profiles, inconsistent reports on altered T- and B-cell function, and an increased incidence and family history of other immune disorders and autoimmune disorders such as fibromyalgia and Hashimoto's thyroiditis [14, 15]. To explore whether evidence exists for an infectious trigger and/or immune dysregulation in ME/CFS, we surveyed plasma samples from ME/CFS subjects and matched controls for antibodies to 122 different pathogenic antigens. The aim of our study is to determine whether individuals with ME/CFS exhibit higher levels of antibodies to a pathogen in comparison to controls and/or evidence of an altered immune system based on anti-pathogen antibody profiles. While absence of historical exposure and antibodies to a rare pathogen would provide evidence against that pathogen as causal in ME/CFS, our assays provide no information regarding the possibility that a pathogen family that frequently circulates amidst the general population might result in ME/CFS in a subset of those infected.

RESULTS

Subject Characteristics

In total, the study population consisted of 105 subjects, including 44 healthy control subjects and 59 ME/CFS subjects (**Table 2.3**). The healthy control cohort consisted of 29 females and 15 males, while the ME/CFS cohort consisted of 47 females and 12 males (**Table 2.3**). All individuals who were selected met the Canadian Consensus Criteria for ME/CFS. The average age was similar between groups at 46.2 ± 10.8 years in ME/CFS subjects and 42.1 ± 14.2 years in controls ($p = 0.11$, **Table 2.3**). Average body mass index (BMI) was also similar between groups at 26.5 ± 5.8 in ME/CFS and 27.5 ± 5.0 in controls ($p = 0.30$, **Table 2.3**); 43% of ME/CFS subjects indicated a gradual onset of disease, while 57% described a sudden onset of disease (**Table 2.3**). ME/CFS illness duration varied, with a range of 1 to 38 years and an average of 12.1 ± 9.6 years (**Table 2.3**). ME/CFS onset occurred in all subjects before SARS-COV2 emerged. Bell Scale ratings were significantly different between groups, with scores averaging 34.0 ± 12.4 and 95.5 ± 8.4 for ME/CFS subjects and controls, respectively ($p < 0.001$, **Table 2.3**). Both the physical and mental component scores (PCS and MCS, respectively) derived from the SF-36 short survey were, as expected, higher in the control group ($p < 0.001$, **Table 2.3**), indicating better health. No subjects were reported to be taking immune-modulating drugs.

Anti-Pathogen Antibody Profiles between ME/CFS Cases and Controls

To determine whether differences in anti-pathogen antibody levels exist between the ME/CFS and control cohorts, we (1) used PCA to see if broad trends or differences could be identified when comparing serological responses to all 122 antigens collectively and (2) compared the serological responses to each antigen. Individual antigen differences between ME/CFS and control subjects were explored to determine

whether they might implicate an etiological agent or ME/CFS disease perpetuator. We first compared all ME/CFS cases and controls and then looked at each sex independently.

Dataset Amendment for Outlier Influence Does Not Significantly Alter Findings Related to Antibody Profile Differences

Figure 2.1. Comparison of ME/CFS and control antibody profiles with and without outlier replacement. (A) PCA of ME/CFS vs. control subjects using log2 dataset. (B) PCA of ME/CFS vs. control using log2 BPCA-estimated outlier replacement dataset. H = Hopkins statistic. PCA legend indicates patients (blue) vs. controls (red). (C) Violin plot depicting fold-change relationship between case and control subjects within each dataset.

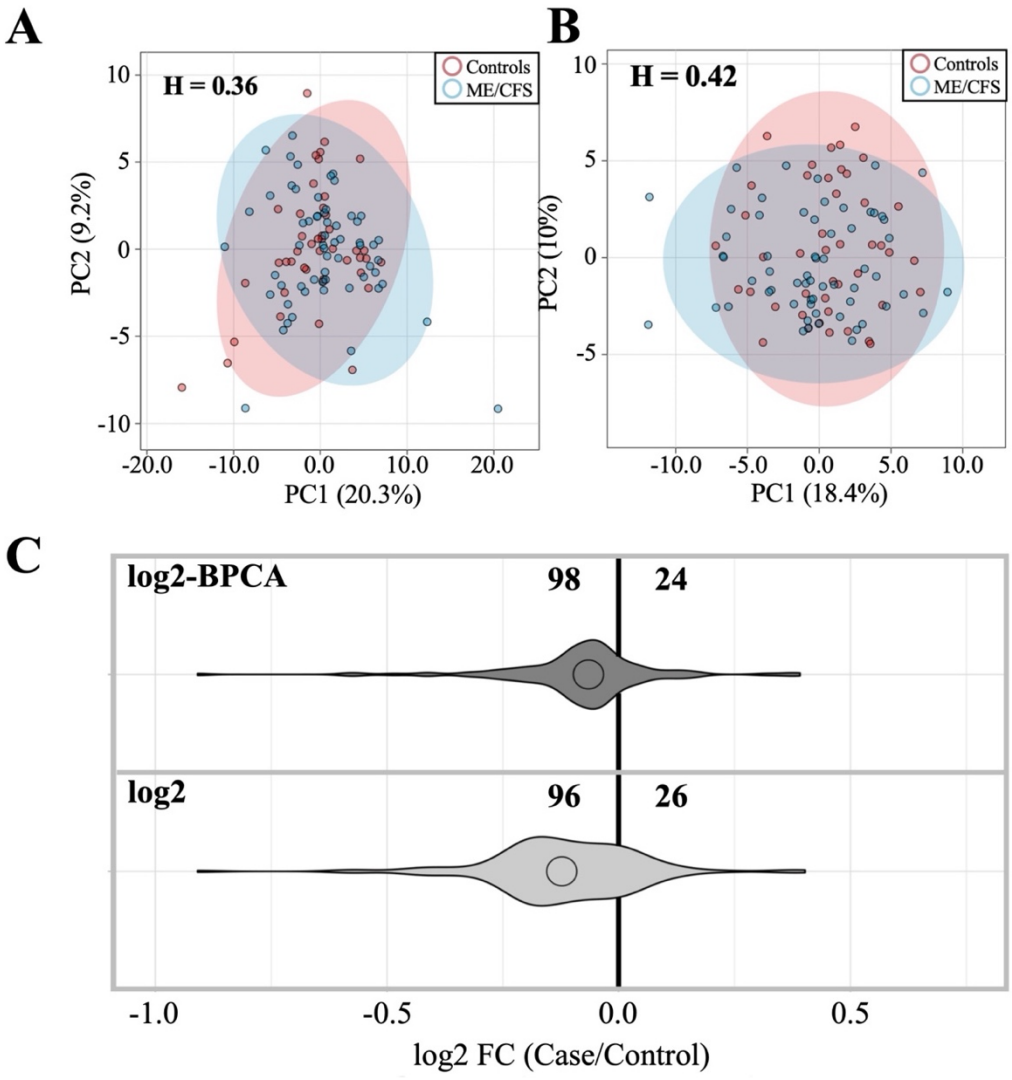

Extensive overlap in case (n = 59) and control (n = 44) ellipses, proximity of case and control population means, as well as Hopkins statistic scores less than 0.5 indicate that ME/CFS and healthy control cohorts are indistinguishable in terms of antibody levels to the 122 antigens surveyed when the antigens are considered collectively via PCA (**Figure 2.1A-B**).

Roughly 80% of the antigens (96–98/122) trend toward decreased mean antibody levels in cases relative to controls, and this trend is maintained when effects of outlier influence are attenuated (**Figure 2.1C, Tables Apx2.2, Apx2.3**). Outlier influence attenuation was carried out to ensure trends in the data were representative of the entire cohort instead of artifactual trends influenced by one or a few subjects with dramatic differences in log2MFI values, possibly due to recent infection or an unusual absence of exposure to a common pathogen.

Table Apx2.1 explains antigen nomenclature. In total, seven antigens (Astrovirus, Coxsackievirus A9, Norovirus GII.4 capsid protein (VP1), Rhinovirus A15, *Streptococcus pyogenes* 1, and *Streptococcus pyogenes* 2, and *Streptococcus dysgalactiae*) are shown to have significantly different antibody levels between cases and controls ($p < 0.05$, $q > 0.05$), with the significance of RhinoA15-lysate being limited to the non-outlier amended dataset (**Table 2.1, Figure 2.2, Tables Apx2.2, Apx2.3**). However, for the total population, none of these seven antigens remained significant after FDR correction. Of the six significant antigens following BPCA replacement, Norovirus GII.4-VP1 was the only antigen with increased antibody levels in cases relative to controls (**Table 2.1, Figure 2.2, Tables Apx2.2, Apx2.3**). The remaining analyses presented herein were conducted on the outlier amended

dataset unless otherwise stated.

log2 Dataset					log2-BPCA Dataset				
Pathogen	**ME/CFS**	**Control**	***p***	**q**	**Pathogen**	**ME/CFS**	**Control**	***p***	**q**
Streptococcus dysgalactiae-lysate	2.7 ± 0.9	3.1 ± 0.9	0.003	0.39	*Streptococcus dysgalactiae*-lysate	2.6 ± 0.7	3.1 ± 0.7	0.001	0.18
Streptococcus pyogenes-lysate2	5.3 ± 1.8	6.2 ± 1.9	0.008	0.49	Astrovirus-Lysate	1.7 ± 0.3	2.0 ± 0.5	0.003	0.18
Streptococcus pyogenes-lysate	2.8 ± 0.8	3.1 ± 0.9	0.016	0.59	CoxA9	4.0 ± 0.8	4.4 ± 0.8	0.007	0.20
CoxA9	4.1 ± 1.1	4.4 ± 0.8	0.019	0.59	*Streptococcus pyogenes*-lysate2	5.3 ± 1.8	6.2 ± 1.9	0.008	0.20
RhinoA15-Lysate	2.6 ± 0.6	2.9 ± 0.8	0.040	0.76	*Streptococcus pyogenes*-lysate	2.8 ± 0.8	3.2 ± 0.7	0.008	0.20
Astrovirus-Lysate	2.0 ± 0.9	2.1 ± 0.7	0.042	0.76	NoroGII.4-Capsid	9.9 ± 1.0	9.6 ± 1.1	0.027	0.55
NoroGII.4-Capsid	9.4 ± 2.1	9.0 ± 1.9	0.044	0.76					

Table 2.1. Antigens with significantly different antibody levels between case and control with and without outlier replacement. Log2 MFI mean ± standard deviation and Mann–Whitney *p*-value are indicated for each pathogen. Data are shown for the original dataset as well as the outlier amended dataset. Blue indicates a lower antibody level in patients relative to controls, and red indicates a lower antibody level in controls relative to patients. *p* = *p*-value, q = q-value.

Figure 2.2. Boxplots-6 antigens with significantly different antibody levels from controls following outlier replacement ($p < 0.05, q > 0.05$). Antigens are listed from left to right and top to bottom based on *p*-value (**Table 2.1**). Y-axis = log2MFI values. Yellow diamond indicates sample mean. Black line running horizontal through the boxplot indicates sample median.

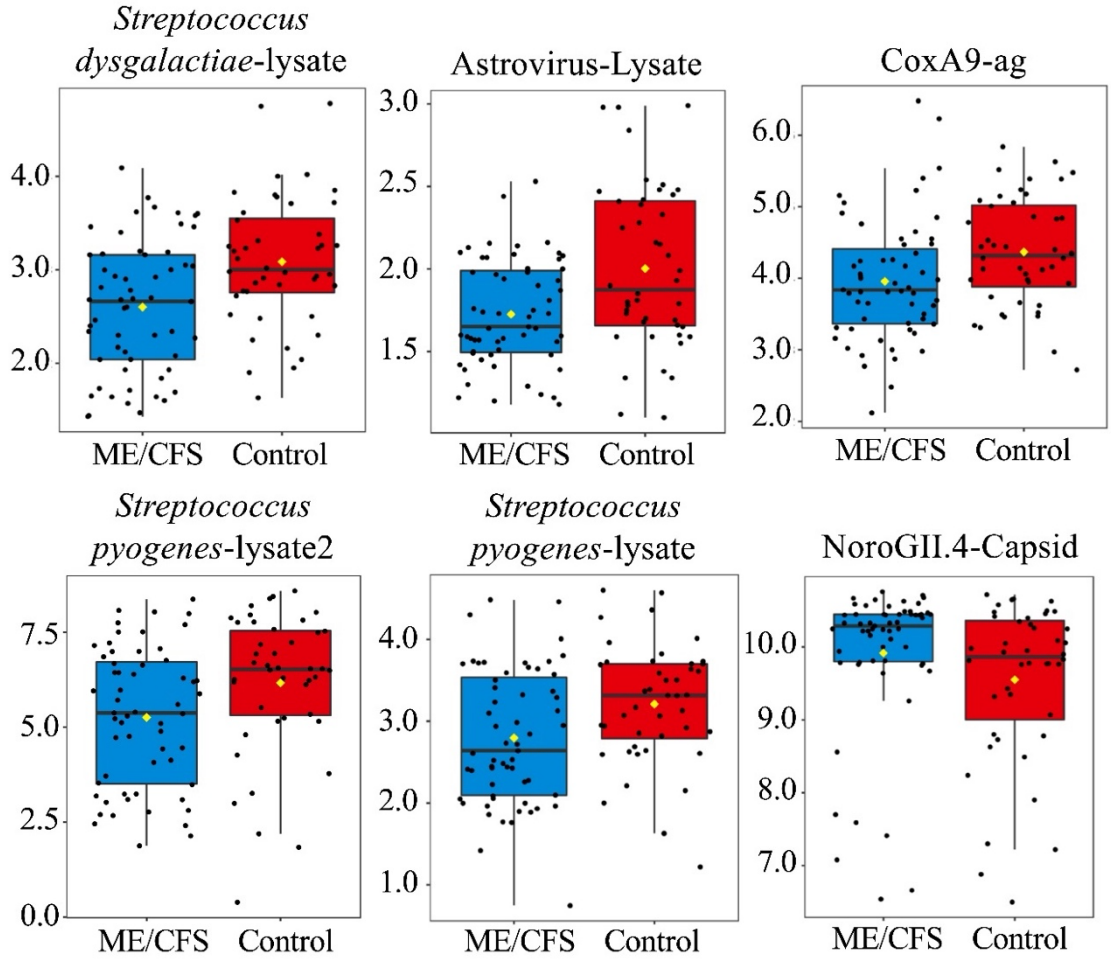

Sex-Based Sub grouping Reveals Differences between Male and Female Antibody Profiles

When the dataset is subgrouped according to male ($n = 27$) and female ($n = 76$) within both case and control cohorts, we discover that sex-specific antibody profile differences occur both within and between cohorts (**Figure 2.3, Tables Apx2.3, Apx2.4**). Intra-cohort analysis within the ME/CFS cohort (**Figure 2.3A**) revealed that males show a trend toward lower mean antibody levels compared to females for most

Figure 2.3. Inter- and intra-cohort sex-specific antibody profile trends. (A,B) Intra-cohort comparisons (female/male). (A) ME/CFS male vs. ME/CFS female. (B) Control male vs. control female. (C,D) Inter-cohort comparisons (case/control). (C) ME/CFS male vs. control male. (D) ME/CFS female vs. control female. (Purple) antigens with average antibody levels higher in females. (Orange) antigens with average antibody levels higher in males. (Blue) antigens with average antibody levels lower in cases than controls. (Red) antigens with average antibody levels lower in controls than in cases. Horizontal line in volcano plot indicates $p = 0.05$. (E,F) Violin plots depicting fold change. All, male, and female subgroup antigen fold changes between case and control are shown. Less than zero indicates lower in case vs. control. (E) Log2 dataset without outlier replacement; (F) log2 dataset with BPCA-estimated outlier replacement.

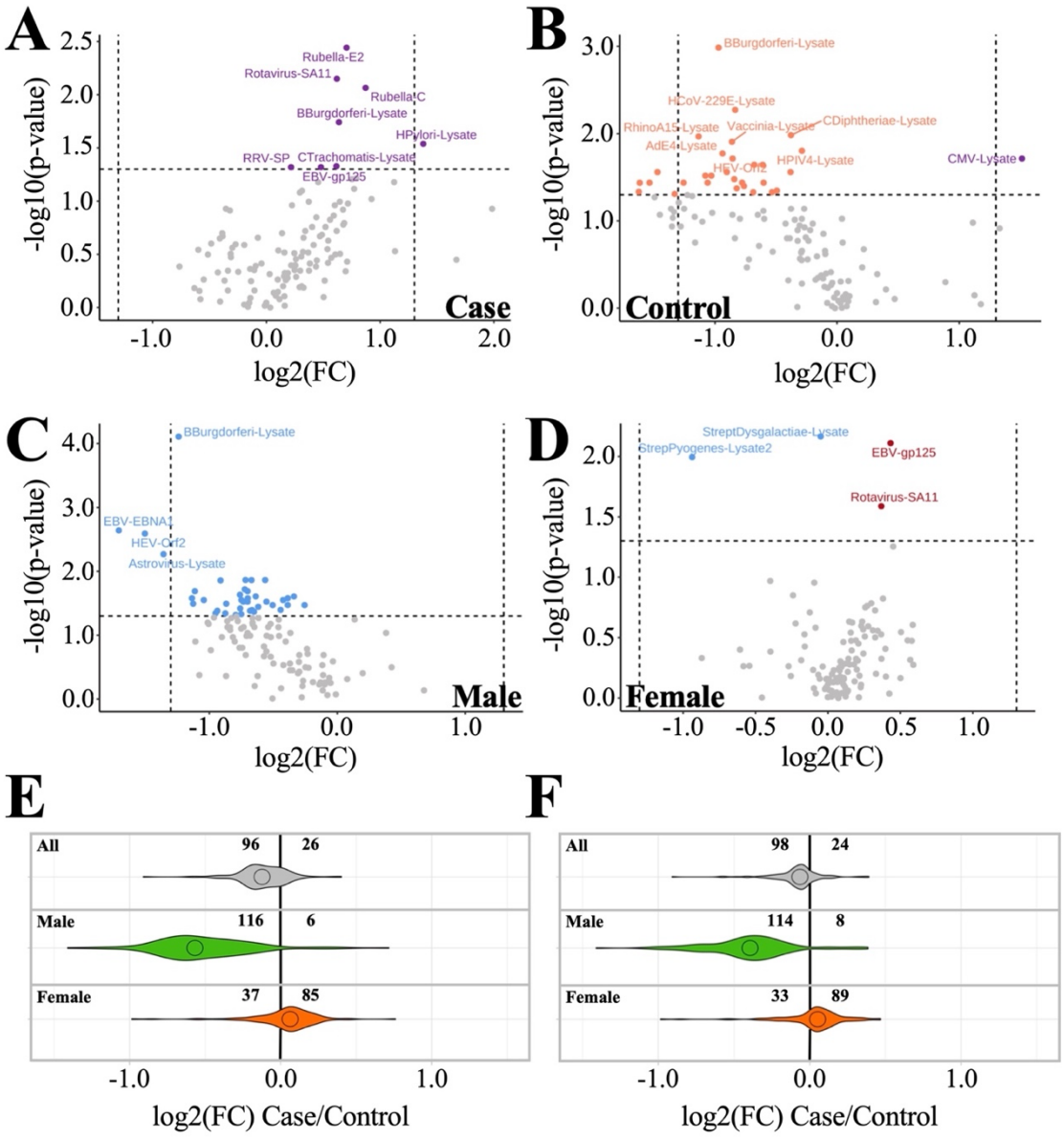

antigens tested. Of these antigens, eight antibody levels were shown to be significantly

different ($p < 0.05$) between ME/CFS male and female subjects (Rubella-E2, Rotavirus-SA11, Rubella-C, *B. burgdorferi*-lysate, H. pylori-lysate, RRV-SP, *C. Trachomatis*, and EBV-gp125) (**Figure 2.3A**). Conversely, the control cohort showed males as having higher mean antibody levels than females for most antigens tested, with most antigens having log2 fold changes (female/male) less than zero (**Figure 2.3B**). Of these 13 antigens, CMV-lysate was the only one with an average antibody level higher in control females rather than lower (**Figure 2.3B**).

When looking at inter-cohort analyses (**Figure 2.3C–F**), we see male subjects (n = 27) follow the same general trends as the total subject dataset (**Figure 2.3A,C,E**) but with even greater contrast between patients and controls, as indicated by (1) an increase in the number of antigens (114/116, up from 96/98 out of 122), showing a trend toward decreased antibody levels in cases vs. controls, and (2) an increase in the number of antigen levels found to be significantly different ($p < 0.05$) between patient and control (42, up from 6/7 out of 122) (**Figure 2.3C,E,F, Tables Apx2.3 and Apx2.4**). Of these, *B. burgdorferi*-lysate is the only antigen with antibody levels found to be significantly different following false discovery rate (FDR) correction ($q < 0.05$) (**Figure 2.3C**). Females (n = 76) show an opposite trend when compared to the total and male subject datasets (**Figure 2.3A,E,F, Table 2.2**). ME/CFS females have only 33–37/122 antigens with antibody levels trending lower than control females, while most antigens (85–89/122) exhibit increased antibody levels in ME/CFS cases relative to control (**Figure 3D–F**). Four antigens show significant differences at $p < 0.05$, but zero antigens are identified as significant following FDR correction. In short, males

Male (n = 42: Top 9 Ranked by p-value + Rotavirus-SA11)					Female (n = 4)				
Pathogen	**ME/CFS**	**Control**	p	**q**	**Pathogen**	**ME/CFS**	**Control**	p	**q**
B.burgdorferi-lysate	1.0 ± 0.6	2.0 ± 0.7	0.000	0.01	*Streptococcus dysgalactiae*-lysate	2.6 ± 0.7	3.2 ± 0.6	0.003	0.39
EBV-EBNA1	3.0 ± 0.9	4.4 ± 1.2	0.002	0.12	*Streptococcus pyogenes*-lysate2	5.2 ± 1.7	6.2 ± 1.9	0.010	0.47
RhinoA15-lysate	2.3 ± 0.5	2.9 ± 0.5	0.005	0.12	*EBV-gp125*	7.1 ± 0.8	6.7 ± 0.9	0.012	0.47
Astrovirus-lysate	1.6 ± 0.3	2.2 ± 0.6	0.005	0.12	Rotavirus-SA11	2.9 ± 0.6	2.6 ± 0.5	0.033	0.98
HEV-Orf2	3.2 ± 0.8	4.1 ± 0.8	0.007	0.12					
RhinoB14-lysate	2.1 ± 0.4	2.5 ± 0.3	0.010	0.12					
SARS2-lysate	1.3 ± 0.4	1.9 ± 0.5	0.010	0.12					
CoxB2-lysate	0.9 ± 0.2	1.4 ± 0.5	0.012	0.12					
C. trachomatis-lysate	0.8 ± 0.3	1.3 ± 0.6	0.014	0.12					
Rotavirus-SA11	2.4 ± 0.5	2.9 ± 0.7	0.025	0.12					

Table 2.2. List of antigens for which antibody levels are significantly different between ME/CFS and healthy controls by sex. Values are given as log2 MFI averages ± standard deviations. Blue indicates lower antibody levels in cases than in controls. Red indicates lower levels in controls than in cases. n = number of antigens with significant differences ($p <$ 0.05) in antibody levels between case and control. $p = p$-value, q = q-value.

and females show opposing relationships of antibody levels when comparing ME/CFS and control subjects.

Of the anti-pathogen antibody levels found to have $p < 0.05$ differences between patients and controls in the male and female cohorts, Rotavirus-SA11 is the only antigen with significantly different antibody levels in both cohorts. The two cohorts have opposing Rotavirus SA-11 findings, with ME/CFS males having lower antibody levels than control males and ME/CFS females having higher antibody levels than control females (**Tables Apx2.3 and Apx2.4**).

Age and Illness Duration Subgroup Analyses Reveals Additional Insights into Antibody Profiles

ME/CFS and control cohorts were organized by subgroups of under 50 ($n = 62$) vs. over 50 ($n = 41$) and compared both within and between groups (**Figure 2.4A–E**). Hopkins statistics scores for all five comparisons fall below 0.5 and, therefore, suggest we are unable to distinguish between the subgroups compared. In addition, we compared sex-based age differences, including comparing females under 50 to females over 50 (Figure 4F) as well as males under 50 to males over 50 (**Figure 2.4G**). Once again, Hopkins statistics scores indicate the two populations are not distinguishable based on antibody responses to the 122 pathogen antigens surveyed. Finally, subjects were stratified based on short- (less than or equal to 5 years) vs. long-term (greater than 5 years) illness duration, and PCA again indicated there were no significant differences (**Figure 2.4H**).

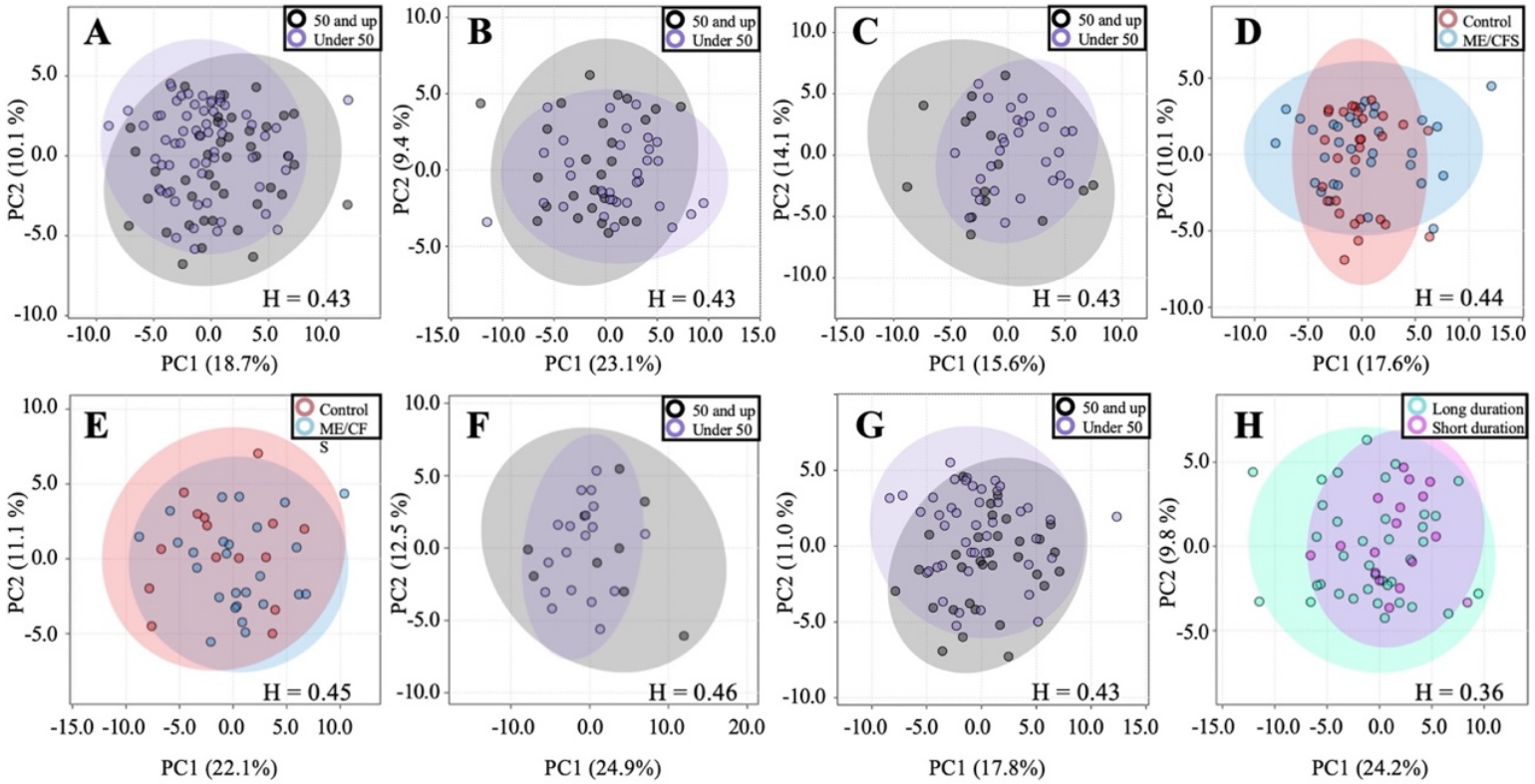

Figure 2.4. Age- and illness-duration-based antibody profile comparisons. (A) All subjects under 50 vs. all subjects 50 and up. (B) ME/CFS under 50 vs. ME/CFS 50 and up. (C) Control under 50 vs. control over 50. (D) ME/CFS vs. control under 50. (E) ME/CFS vs. control over 50. (F) Male under 50 vs. male over 50. (G) Female under 50 vs. female over 50. (H) ME/CFS short (≤5 years) vs. long (>5 years) illness duration. H = Hopkins statistic. Hopkins statistic is individually given for each PCA. (Black) 50 and up. (Purple) under 50. (Red) control. (Blue) ME/CFS. (Turquoise) long duration. (Fuchsia) short duration. (I–L) Volcano plot highlighting antigens with significantly different levels between age groups overall and within experimental subgroups (Over 50/Under 50). (I) All subjects under 50 vs. all subjects over 50. (J) ME/CFS under 50 vs. ME/CFS over 50. (K) Control under 50 vs. control over 50. (L) Female under 50 vs. female over 50. (Light purple) antigen level is lower in the over 50 age group. (Black) antigens higher in the over 50 age group.

Figure 2.4. cont.

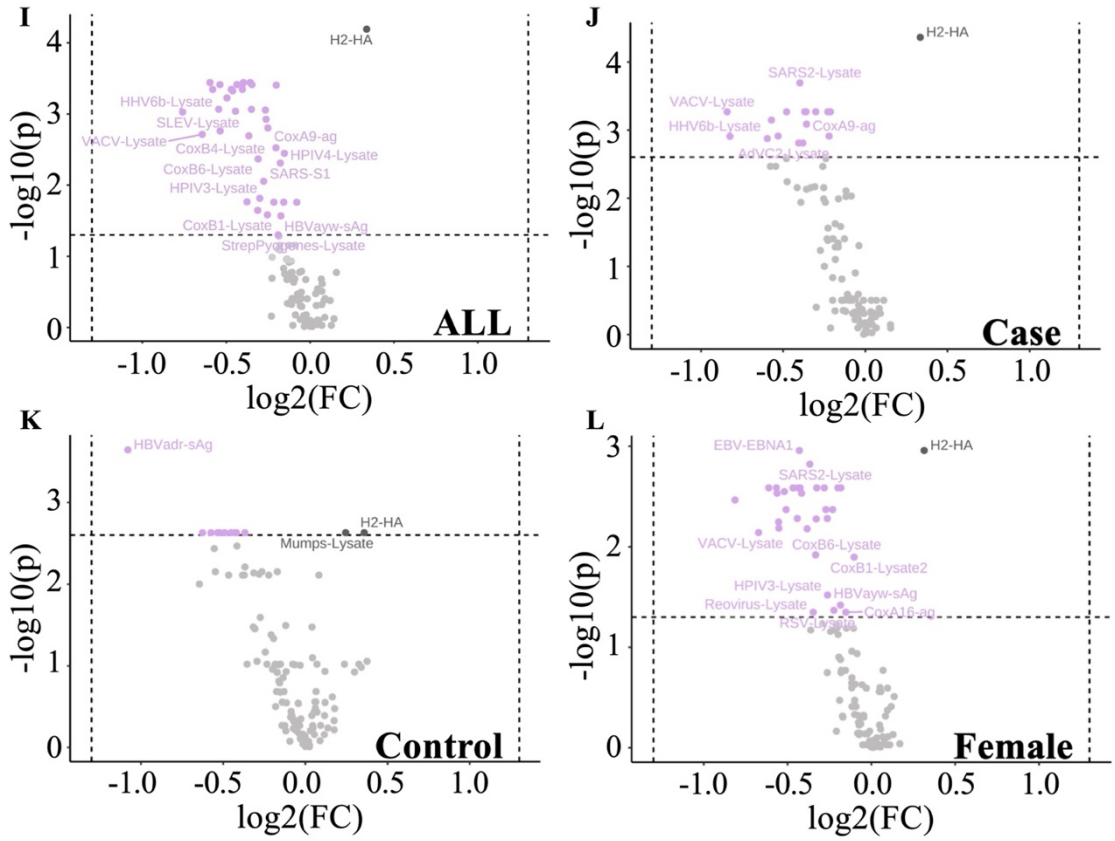

Statistical analysis of individual antigens shows a subset of antibody responses to specific antigens significantly differ ($p < 0.05$, $q < 0.05$) between under 50 and over 50 age groups when considering all subjects (**Figure 2.4I**), ME/CFS subjects alone (**Figure 2.4J**), control subjects alone (**Figure 2.4K**), and female subjects alone (**Figure 2.4L**). A complete list of identified pathogens within each grouping is presented in **Table Apx2.5**.

DISCUSSION

Pathogens have been continuously put forward as potential ME/CFS disease initiators and/or exacerbating agents. The occurrence of clustered outbreaks, the often

sudden onset of disease, and reports of "flu-like" symptoms during acute phases of disease progression suggest an infectious pathogenic agent. Survey data obtained from ME/CFS subjects enrolled in this study is consistent with this theory, as 33 of 58 survey respondents with ME/CFS reported a sudden disease onset, with 17 of the 33 respondents reporting a viral or viral-like disease at onset, characterized by sore throat, low-grade fever, etc.

Our study population consisted of ME/CFS and healthy control subjects matched for age, sex, and BMI (**Table 2.3**). In total, we surveyed the antibody profile of 59 ME/CFS and 44 healthy control subjects to 122 pathogenic antigens. Antigens surveyed were chosen to represent common human pathogens across all seven Baltimore classification viral types as well as subsets of bacterial and protozoan clades (**Table Apx2.1**). The antibody detection method employed in our study is unable to discriminate between antibody classes because the secondary antibody that was used detects a combination of IgG, IgA, and IgM. Because this assay has not been cross-validated with established diagnostic ELISAs that are usually Ig class-specific, our knowledge of the connection between the statistical significance of the antibody levels measured here and clinical significance is limited. However, the Luminex platform is a well-established epidemiological and basic science research tool for multiplex serology, and antibody responses measured via Luminex typically correlate well with diagnostic ELISAs [16-18]. Insight into ME/CFS anti-pathogen immune profiles reveals support for sex- and age-based immune differences that may exist across ME/CFS disease demographics.

Sex-based subgrouping shows that male and female cases differ in their anti-

pathogen immune profiles. Female subjects had 85–89/122 antigens with log2 fold changes greater than zero in cases relative to controls, whereas 114–116/122 antigens in males showed log2 fold changes below zero (**Figure 2.3C–F**). While most of the differences were not significant, the opposite trends between male and female antibody levels indicate it is inappropriate to combine data from the two sexes. Immunological differences between sexes are well known; for example, susceptibility to various autoimmune diseases varies between sexes [19]. Sex differences exist in ME/CFS, given that more women than men are diagnosed with the disease [20]. Furthermore, plasma metabolites differ between male and female ME/CFS cases and controls [21]. The contrast between males and females is even further magnified when we realize the only shared significantly different antibody level between sexes is Rotavirus-SA11 ($p < 0.05$, $q > 0.05$), whose correlation with controls is opposite between males and females.

Rotaviruses typically infect infants and children with no significant sex-specific difference in burden between males and females. Adult infections are rare but still occur. Typically, adult infection is derived from endemic disease, epidemic outbreaks, travel-related gastroenteritis, and infections transmitted from children to adults [22]. Of the adult outbreaks, no preference is seen between male or female adults [23]. Lack of congruency between the epidemiology of ME/CFS and rotavirus suggests that the finding of rotavirus significance is not related to ME/CFS disease initiation or progression. Factors leading to this conclusion include contrasting epidemic seasonality between ME/CFS and rotavirus epidemics, small symptom overlap, and deviations when comparing expected incidence, distribution, and demographics of

afflicted individuals.

Overall, females exhibit levels of antibodies to four antigens that are significantly different ($p < 0.05$, $q > 0.05$) between case and control, with antibody levels to two antigens (*Streptococcus dysgalactiae*-lysate and *Streptococcus pyogenes*-lysate) being decreased in case vs. control and two antigens (EBV-gp125 and Rotavirus SA11) being increased in case vs. control (**Figure 2.3D**). The finding of increased EBV antibodies to viral capsid antigen (VCA) glycoprotein 125 (EBV-gp125, encoded by the BALF4 gene) in our female cohort suggests a possible link to EBV (**Table Apx2.2**). However, the difference was not significant after FDR correction. Additionally, we found that, altogether, females had higher antibody responses to EBV-gp125 than males ($p < 0.05$, $q > 0.05$), which supports the conclusion that this result is specific to females and not a statistical artifact of the smaller sample size for males in this study. We also measured antibody levels to one other EBV antigen, Epstein-Barr nuclear antigen 1 (EBNA-1), and did not find any difference between case and control females. This is not surprising, as approximately 90% of adults worldwide have been infected with EBV and anti-EBNA-1 IgG may persist for life, simply indicating a past infection [24]. Differences in EBV humoral immunity between ME/CFS patients and healthy controls have been found in other studies, including several that also used the Canadian Consensus Criteria to select ME/CFS subjects [22,29,30]. Enhanced IgG levels against EBNA-6 were found using a peptide microarray platform [25], but the same result was not significant via Luminex [18].

Clinical diagnostic assays for EBV for either recent or past infection use a different viral capsid antigen, p18 [26], so EBV-gp125 antibody responses have not

been as widely studied. EBV-gp125 has been examined in one other serology study with ME/CFS patients, but that study did not find differences between patients and controls when measuring IgG and IgM separately and looking at both sexes collectively [18]. In our assay, IgM and IgA against EBV-gp125 are also contributing to the signal. These isotypes are associated with recent infection or reactivation [24]. Unfortunately, we cannot conclude whether or not our result is clinically significant without confirming the result via ELISA and assaying additional EBV antigens, including those present in already developed diagnostic ELISAs for EBV. Additionally, the assessment of EBV reactivation is outside the scope of our assay. Although they did not subset their study population into males and females, Domingues et al. found a negative association between controls and patients that did not self-identify as having an infectious disease trigger for seropositivity to the EBV antigens VCA (p18) and EBNA-1 [27]. The result was similar when adjusting for sex as a confounding factor. In the same group of subjects, but without evaluating any subsets, the levels of anti-VCA IgG and seropositivity status were not different between ME/CFS subjects and controls [28]. While our broad survey of a variety of pathogens did not thoroughly investigate the EBV antibody response, this finding of higher antibody responses to EBV-gp125 in female patients warrants further investigation and confirmation with a larger sample size.

Males have a surprising set of 42 antibody levels that are significantly lower ($p < 0.05$) compared to controls, with *B. burgderfori*-lysate being the only antigen significant after FDR correction ($q < 0.05$) (**Figure 2.3C, Table 2.2**). *B. burgdorferi*-lysate is derived from the Lyme disease spirochete, a tick-borne pathogen that, in

some individuals, is thought to cause chronic Lyme disease, which has symptoms that overlap with ME/CFS. Results obtained from our male cohort do not implicate Lyme disease as a possible disease culprit because the average case antibody level for this antigen is lower than control. One caveat to this result is that this antigen is derived from whole lysate, which has a higher incidence of nonspecific binding than recombinant antigens. Follow-up studies focused on antibody responses in ME/CFS and/or chronic Lyme disease using recombinant protein antigens would help confirm or refute this finding. Despite a relatively small male sample size, we found more differences in antibody levels between ME/CFS subjects and controls in males than in females. One hypothesis, put forward by Domingues et al. to explain immunological findings regarding human herpesviruses in ME/CFS, is that CD4+ regulatory T-cells are hyperactive, resulting in the suppression of humoral immune responses [29]. Dysregulation of immune cells in males may thus result in the observed lower levels of antibodies not only to *B. burgdorferi* but also to a large number of pathogens (**Figure 2.3**).

Age-based cohort stratification provides additional insight into humoral immune biology, with a large number of antigens identified with significantly different antibody levels between subjects under 50 and those over 50 (**Figure 2.4A–C,G,I–L**). Age 50 is a common age for menopause in females. Although PCA does not separate the general subgroups, comparing all subjects under 50 to all subjects over 50 (**Figure 2.4I**), as well as females under 50 to females over 50 (**Figure 2.4L**), we see that roughly 1/3 of antigens are significantly lower in the 50-and-over age group following FDR correction. This trend is maintained when stratifying by age within the case-only

cohort (**Figure 4J**), but to a lesser degree, with fewer identified antigens.

Of the 122 antigens for which antibodies were assayed, 49 represent positive sense single-stranded RNA viruses. Of these 49, the majority are members of the Picornaviridae, which includes enteroviruses. Non-polio enteroviruses have been implicated in outbreaks of ME/CFS. In our study, antibodies to 15 coxsackievirus antigens, 1 EV71 antigen, 1 EV68 antigen, 6 poliovirus antigens, and 3 rhinovirus antigens—representing five groups of enteroviruses—were assayed (**Table Apx2.1**). Of these, only the levels of Coxsackie virus A9 were significantly different ($p < 0.05$, $q > 0.05$) between male cases and male controls, with lower levels in cases (**Figure 2.2, Table Apx2.3**). The current study is not able to determine whether or not an enterovirus might have incited a large proportion of ME/CFS cases because enteroviral infections occur in the general population worldwide so often each year [30]. In the US alone, there are 30–50 million enteroviral infections each year, of which 10–15 million are symptomatic [31]. As a result, even if enteroviruses were inciting agents of most ME/CFS cases, both cases and controls would be expected to have largely overlapping levels of antibodies. Our dataset shows antibodies to the enterovirus antigens surveyed exhibit very small fold-change differences between cohorts, which is expected due to the aforementioned frequency of infections. Our assays cannot determine whether some subjects have been exposed to particular variants of certain enteroviruses that have not infected other subjects. The possibility remains that ME/CFS cases arise from an uncommon variant of one or more enteroviruses or another type of virus and/or an uncommon reaction to a common endemic virus.

One limitation of this study is that the antibody response we measured is a combination of IgG, IgA, and IgM antibodies. We recommend that future studies in this area investigate multiple Ig classes and subclasses independently. If a pathogen that commonly infects a large percentage of the population (such as an enterovirus or a herpesvirus) is involved in ME/CFS etiology, it is likely that the differential humoral immune response to that pathogen could be highly nuanced and is simply not detected in our assay. For example, the presence of IgM and IgA against EBV VCA antigens or IgA and IgG against early antigen D are indicators of EBV reactivation that were not assayed in our study [24].

Another limitation of this study is that we did not attempt to determine who was seropositive and who was seronegative. Even though we subtracted the background signal, it is possible that some of the signals we detected are due to cross-reactivity or nonspecific binding, particularly to the antigens that are whole pathogen lysate rather than specific recombinant proteins. In this exploratory study, we wanted to consider all the data for as many pathogens and antigens as possible and to look for pathogens that warrant further follow-up studies. If any pathogens had stood out as potential causative agents of ME/CFS, we would have been interested in following up with confirmatory ELISAs, which include positive and negative control reference serums to help determine seropositivity status, in addition to measuring the relative antibody levels. Such assays could be done in future work, particularly in studies focused on a smaller number of pathogens, such as EBV and/or *B. burgdorferi*.

CONCLUSIONS

While examining levels of antibodies to whole proteins and lysates would not be expected to identify a disease-causing pathogen specific to ME/CFS if the pathogen routinely affects large numbers of individuals, rare pathogens could be implicated if they are found to be more prevalent in the case group. Although some rare pathogens were probed in our study, none show significant differences between cases and controls after false discovery rate correction. To the best of our knowledge, this is the first time that antibody levels to many of the pathogens investigated here have been explored in ME/CFS patients, including tick-borne encephalitis virus, hepatitis E virus, and human metapneumovirus. We also probed the largest number of adenoviruses (14) and enteroviruses (20, in five different groups) of any study to date. While the primary conclusion from our study is the absence of differences between antibody levels of patients and controls, this type of exploratory analysis using high-throughput, multiplex technologies is important to characterize the humoral immune response of ME/CFS patients and to continue the search for a possible infectious agent that triggers ME/CFS. We also show a trend in male antibody levels suggesting immunosuppression as well as differences in antibody levels with age. The subtle serological alterations between healthy controls and ME/CFS subjects found here should be interpreted cautiously, but these findings do contribute to the growing body of evidence that the immune system of ME/CFS patients is dysregulated [28, 32]. We also recommend that future serological studies in ME/CFS patients should not combine males and females for analysis and that males should be studied in addition to females despite being a smaller subset of the patient population.

MATERIALS AND METHODS

ME/CFS Case Selection and Sample Acquisition

	ME/CFS	Controls	Mann–Whitney U-Test
Age	46.1 ± 10.5	42.1 ± 14.2	$p = 0.11$
Gender			
Female	47	29	NA
Male	12	15	NA
BMI (kg/m^2)	26.5 ± 5.7	27.5 ± 5.0	$p = 0.30$
Ethnicity			
Hispanic or Latino	9	6	NA
Not Hispanic or Latino	46	37	NA
Unknown	4	1	NA
Race			
American Indian or Alaska Native	0	1	NA
Asian	2	5	NA
Black or African American	0	3	NA
Native Hawaiian or other Pacific Islander	1	0	NA
White	51	32	NA
Unknown	5	3	NA
Onset of disease			
Gradual	44%	NA	NA
Sudden	56%	NA	NA
Illness Duration (years)	12.1 ± 9.6	NA	NA
Bell Score	34.6 ± 12.2	95.5 ± 8.5	$p < 0.001$
SF-36			
Physical function	38.6 ± 19.3	94.2 ± 9.3	$p < 0.001$
Role physical	16.1 ± 18.8	98.3 ± 4.5	$p < 0.001$
Pain	41.9 ± 22.0	83.9 ± 16.7	$p < 0.001$
General health	22.9 ± 11.6	81.2 ± 13.9	$p < 0.001$
Vitality	17.6 ± 14.0	70.3 ± 17.8	$p < 0.001$
PCS [a]	27.2 ± 7.2	56.1 ± 4.7	$p < 0.001$
Social function	26.3 ± 20.7	97.7 ± 11.5	$p < 0.001$
Role emotional	81.5 ± 24.8	97.0 ± 7.9	$p < 0.001$
Mental health	66.4 ± 18.8	83.9 ± 10.1	$p < 0.001$
MCS [a]	45.1 ± 9.5	55.3 ± 5.1	$p < 0.001$

Table 2.3. Study population characteristics. [a] PCS, physical component score; MCS, mental component score.

ME/CFS cases and healthy controls were identified by Geoffrey Moore, M.D. (Ithaca, NY, USA), John Chia, M.D. (Los Angeles, CA, USA), and Susan Levine, M.D. (Manhattan, NY, USA) between 15 October 2015 and 6 March 2020. A total of 59 ME/CFS cases and 44 healthy controls were included in this case–control cross-sectional study. Individuals were diagnosed with ME/CFS if they met the Canadian Consensus Criteria for ME/CFS [1] and controls were eligible if they were healthy, had not been diagnosed with depression, were sedentary, were between 18 and 70 years old, were non-smokers, were not pregnant or breast feeding, were not diabetic, and did not display a metabolic, cardiovascular, and/or other neuroimmune disease. Patients included in the study did not report the use of immune-modulating drugs. Peripheral blood from an antecubital vein was drawn into EDTA tubes. Once collected, blood tubes were put on ice and taken to labs for immediate separation of plasma, which was stored on the same day of collection at −80 °C until further use. Participants' age, sex, and age of onset of ME/CFS were recorded. The Bell Disability Scale [33] and Short Form-36 Health Survey [34] were administered to each participant on the day of blood sample collection. Written consent was obtained from all participants, and all protocols were approved by Weill Cornell Medical College, Protocol # 1708018518, Ithaca College IRB # 1017-12Dx2.

Augmenta Serological Testing

A panel of Luminex xMAP beads was constructed by coupling beads to recombinant proteins, inactivated viruses, and inactivated cell cultures (**Table Apx2.1**). Native antigens were inactivated by one or more standard methodologies (heat treatment, UV irradiation, chemical inactivation, gamma irradiation, detergent,

or electron beam irradiation) to render them safer for handling in BSL-2 conditions. Most antigens were received live from the ATCC. All antigens were buffer-exchanged into phosphate-buffered saline (PBS) with size exclusion chromatography prior to coupling. Concentrations were measured using the Pierce Rapid Gold BCA protein assay before and after buffer exchange.

Each antigen was assigned a unique Luminex bead region. The corresponding bead stock was resuspended and coupled to purified antigen via standard sulfo-NHS/EDC linking chemistry. Reactions were quenched, and the beads were washed and blocked against nonspecific binding with Surmodics StabilGuard. Up to 24 conjugations were performed in parallel using a Hamilton Liquid Handler (Hamilton Company, Reno, NV, USA). Conjugated beads were pooled into three separate panels for the assay of subject samples.

Three quality control measurements were run on every bead–antigen conjugation lot. First, the final bead concentration was determined using a BD AccuriC6 flow cytometer (BD, Franklin Lakes, NJ, USA) to compare the conjugated beads to bead standards of known size and concentration. Second, the NanoOrange Protein Quantitation assay was used to fluorometrically detect the presence of protein on coupled beads relative to uncoupled beads. Third, a full-scale Luminex assay was performed using intravenous immunoglobulin (IVIg) from a broad spectrum of donors to confirm positive signal detection (i.e., antibody binding to antigen-coupled beads above background).

For all three panels, the study samples were run in triplicate at 1:500, 1:1000, and 1:2000 dilutions. For ease of analysis, only data from the 1:1000 dilution was used.

Two replicates of CONSV3 control serum (Sigma, St. Louis, MO, USA) and three replicates of a single control plasma were used as technical controls in all plates, and three replicates of a secondary-only negative control (blank) were also included in all plates. All sample wells had bovine serum albumin (BSA) beads as a negative control and a bead conjugated to PE anti-human CD38/PE as a positive instrument control. The mixture was washed twice before the addition of a phycoerythrin (PE)-conjugated Goat Anti-Human IgM+IgG+IgA reporter antibody. Samples were washed twice and read on a Luminex 200 flow cytometer (Luminex, Austin, TX, USA) within 2 h of the final wash. The log2 difference in median fluorescence intensity (MFI) between a given antigen-coupled bead lot and its internal batch-specific negative control (BSA) was computed. Triplicates were averaged. Normalization was performed to compensate for technical variations between plates by centering the mean global intensity of a reference sample on each plate. MFI data were log2-transformed prior to statistical analyses. Each antigen's log2MFI value was calculated by subtracting the MFI value from a PBS negative control.

Statistical Analysis

All data were processed and analyzed using R version 3.5.2 (21 February 2019) via RStudio Version 1.4.1717 (RStudio, Boston, MA) and/or MetaboAnalyst version 5.0 (https://www.metaboanalyst.ca). The outlier amended dataset was created by first identifying outliers using the 1.5*IQR rule and then replacing outliers using the Bayesian PCA (BPCA) estimation method for outlier replacement. The Wilcoxon–Mann–Whitney U-test was used to determine the significance of differences ($p < 0.05$) in ME/CFS vs. control subjects across all sample population characteristic

measurements (**Table 2.1**) and for all individual pathogenic antigens (**Table Apx2.1**). For the 122 antigens, correction for multiple comparisons was done via the Benjamini–Hochberg method for false discovery rate (FDR) correction. We report for each antigen both the *p*-value ($\alpha = 0.05$) and q-value ($\alpha = 0.05$) to provide clarity about the level of statistical significance. Principal component analysis (PCA) was used to reduce the dimensionality of the anti-pathogen antibody data. The data correlation matrix was then calculated, and eigenvalue decomposition on the matrix was performed. Cluster tendency of the datasets was assessed using the Hopkins statistic (H) [35] by measuring the probability that a given data set is uniformly randomly distributed [36]. A H-value close to 1 indicates the data is highly clustered, and random data will result in values close to or below 0.5. PCA; cluster tendency was performed using the R packages ggplot2, factoextra, and clustertend. Fold change and volcano plot analyses were completed using MetaboAnalyst version 5.0 with a fold-change threshold of 1.01 and a *p*-value of 0.05.

REFERENCES

1. Carruthers BM, Jain AK, De Meirleir KL, Peterson DL, Klimas NG, Lerner AM, et al. Myalgic Encephalomyelitis/Chronic Fatigue Syndrome. J Chronic Fatigue Syndr. 2003;11(1):7-115.

2. Hyde BM, Goldstein J, Levine P, editors. The Clinical and Scientific Basis of Myalgic Encephalomyelitis/Chronic Fatigue Syndrome. Ottawa, Canada: Nightingale Research Foundation; 1992.

3. Sydenham T. The works of Thomas Sydenham, M. D., on acute and chronic diseases: with their histories and modes of cure. Philadelphia: Benjamin & Thomas Kite; 1809.

4. Manningham R. The Symptoms, Nature, Causes, and Cure of the Febricula, or Little Fever: Commonly Called the Nervous or Hysteric Fever; the Fever on the Spirits, Vapours, Hypo, or Spleen. London: printed for J. Robinson, at the Golden-Lion in Ludgate-fleet; 1750.

5. Gilliam AG. Epidemiological study of an epidemic, diagnosed as poliomyelitis, occurring among the personnel of the Los Angeles County General Hospital durring the summer of 1934.: Washington, Public Health Service, for sale by the Supt. of Docs., U.S. Govt. Print. Off.; 1938.

6. O'Neal AJ, Hanson MR. The enterovirus theory of disease etiology in Myalgic Encephalomyelitis/Chronic Fatigue Syndrome: a critical review. Front Med. 2021;8:688486.

7. Fisman D. Seasonality of viral infections: mechanisms and unknowns. Clin Microbiol Infect. 2012;18(10):946-54.

8. Parish JG. Early outbreaks of 'epidemic neuromyasthenia'. Postgrad Med J. 1978;54(637):711-7.

9. Chia JKS. The role of enterovirus in chronic fatigue syndrome. J Clin Pathol. 2005(11):1126.

10. Rasa S, Nora-Krukle Z, Henning N, Eliassen E, Shikova E, Harrer T, et al. Chronic viral infections in myalgic encephalomyelitis/chronic fatigue syndrome (ME/CFS). J Transl Med. 2018;16(1):268.

11. Hickie I, Davenport T, Wakefield D, Vollmer-Conna U, Cameron B, Vernon SD, et al. Post-infective and chronic fatigue syndromes precipitated by viral and non-viral pathogens: prospective cohort study. BMJ. 2006;333(7568):575.

12. Evengard B, Briese T, Lindh G, Lee S, Lipkin WI. Absence of evidence of Borna disease virus infection in Swedish patients with Chronic Fatigue Syndrome. J Neurovirol. 1999;5(5):495-9.

13. Nowotny N, Kolodziejek J. Demonstration of Borna disease virus nucleic acid in a patient with chronic fatigue syndrome. J Infect Dis. 2000;181(5):1860-2.

14. Sotzny F, Blanco J, Capelli E, Castro-Marrero J, Steiner S, Murovska M, et al. Myalgic Encephalomyelitis/Chronic Fatigue Syndrome – Evidence for an autoimmune disease. Autoimmunity Rev. 2018;17(6):601-9.

15. Brenu EW, Huth TK, Hardcastle SL, Fuller K, Kaur M, Johnston S, et al. Role of adaptive and innate immune cells in chronic fatigue syndrome/myalgic encephalomyelitis. Int Immunol. 2014;26(4):233-42.

16. Pickering JW, Martins TB, Schroder MC, Hill HR. Comparison of a Multiplex Flow Cytometric Assay with Enzyme-Linked Immunosorbent Assay for Quantitation of Antibodies to Tetanus, Diphtheria, and *Haemophilus influenzae* Type b. Clin Vaccine Immunol. 2002;9(4):872-6.

17. Graham H, Chandler DJ, Dunbar SA. The genesis and evolution of bead-based multiplexing. Methods. 2019;158:2-11.

18. Blomberg J, Rizwan M, Böhlin-Wiener A, Elfaitouri A, Julin P, Zachrisson O, et al. Antibodies to Human Herpesviruses in Myalgic Encephalomyelitis/Chronic Fatigue Syndrome Patients. Front Immunol. 2019;10:1946-.

19. Klein SL, Flanagan KL. Sex differences in immune responses. Nat Rev Immunol. 2016;16(10):626-38.

20. Valdez AR, Hancock EE, Adebayo S, Kiernicki DJ, Proskauer D, Attewell JR, et al. Estimating Prevalence, Demographics, and Costs of ME/CFS Using Large Scale Medical Claims Data and Machine Learning. Front Pediatr. 2019;6:412-.

21. Naviaux RK, Naviaux JC, Li K, Bright AT, Alaynick WA, Wang L, et al. Metabolic features of chronic fatigue syndrome. Proc Natl Acad Sci. 2016;113(37):E5472-80.

22. Anderson EJ, Weber SG. Rotavirus infection in adults. Lancet Infect Dis. 2004;4(2):91-9.

23. Ojobor CD, Olovo CV, Onah LO, Ike AC. Prevalence and associated factors to rotavirus infection in children less than 5 years in Enugu State, Nigeria. Virusdisease. 2020;31(3):1-7.

24. De Paschale M, Clerici P. Serological diagnosis of Epstein-Barr virus infection: Problems and solutions. World J Virol. 2012;1(1):31-43.

25. Loebel M, Eckey M, Sotzny F, Hahn E, Bauer S, Grabowski P, et al. Serological profiling of the EBV immune response in Chronic Fatigue Syndrome using a peptide microarray. PLoS One. 2017;12(6):e0179124.

26. Ory Fd, Guisasola ME, Sanz JC, García-Bermejo I. Evaluation of Four Commercial Systems for the Diagnosis of Epstein-Barr Virus Primary Infections. Clin Vaccine Immunol. 2011;18(3):444-8.

27. Domingues TD, Grabowska AD, Lee J-S, Ameijeiras-Alonso J, Westermeier F, Scheibenbogen C, et al. Herpesviruses Serology Distinguishes Different Subgroups of Patients From the United Kingdom Myalgic Encephalomyelitis/Chronic Fatigue Syndrome Biobank. Front Med. 2021;8.

28. Cliff JM, King EC, Lee J-S, Sepúlveda N, Wolf A-S, Kingdon C, et al. Cellular Immune Function in Myalgic Encephalomyelitis/Chronic Fatigue Syndrome (ME/CFS). Front Immunol. 2019;10.

29. Sepúlveda N, Carneiro J, Lacerda E, Nacul L. Myalgic Encephalomyelitis/Chronic Fatigue Syndrome as a Hyper-Regulated Immune System Driven by an Interplay Between Regulatory T Cells and Chronic Human Herpesvirus Infections. Front Immunol. 2019;10:2684.

30. Brouwer L, Moreni G, Wolthers KC, Pajkrt D. World-wide prevalence and genotype distribution of enteroviruses. Viruses. 2021;13(3).

31. Goldman L. Enteroviruses. In: Goldman LaS, A.I., editor. Goldman-Cecil Medicine. 26 ed. Philadelphia: Elsevier; 2020. p. 2664.

32. Mandarano AH, Maya J, Giloteaux L, Peterson DL, Maynard M, Gottschalk CG, et al. Myalgic encephalomyelitis/chronic fatigue syndrome patients exhibit altered T cell metabolism and cytokine associations. J Clin Invest. 2020;130(3):1491-505.

33. Bell DS. The Doctor's Guide to Chronic Fatigue Syndrome. Understanding, Treating, and Living with CFIDS. Bell DS, editor. Reading, Massachusetts: Addison-Wesley Publishing Company; 1994.

34. Ware JE, Jr., Sherbourne CD. The MOS 36-item short-form health survey (SF-36). I. Conceptual framework and item selection. Med Care. 1992;30(6):473-83.

35. Lawson RG, Jurs PC. New index for clustering tendency and its application to chemical problems. J Chem Inform Comput Sci. 1990;30(1):36-41.

36. Banerjee A, Dave RN, editors. Validating clusters using the Hopkins statistic. 2004 IEEE International Conference on Fuzzy Systems (IEEE Cat No04CH37542); 2004 25-29 July 2004.

CHAPTER 3

Enterovirus surveillance in the blood of Myalgic Encephalomyelitis/Chronic Fatigue Syndrome subjects via targeted RNA sequencing and *in vitro* biological amplification

ABSTRACT

The etiological basis of Myalgic Encephalomyelitis/Chronic Fatigue Syndrome (ME/CFS) remains unknown. The seasonality of ME/CFS epidemics, frequent historical spatiotemporal overlap with poliomyelitis epidemics, and symptom constellation similarity with chronic enterovirus-related clinical outcomes has fueled speculation about the link between chronic enteroviruses (EVs) and ME/CFS. The current body of literature focused on EVs' association with ME/CFS shows an increased prevalence of EV infections in ME/CFS cohorts throughout the majority of serological, tissue culture, immunochemical and molecular studies. Unfortunately, limitations of past investigations have resulted in unresolved questions about the role of chronic EV infection in ME/CFS. The aim of our study was to combine recently developed advanced RNA sequencing approaches with *in vitro* viral amplification to screen for EV transcripts at a sensitivity yet to be employed in the ME/CFS literature. We find that our EV-specific probe set allows efficient viral detection when as few as 10 copies are present in 1ml of blood. However, whether the technology is employed directly on patient samples or following attempts at *in vitro* biological amplification, EVs were undetected in both ME/CFS and healthy control samples despite all approaches that were pursued. While we could not detect EVs in blood, we cannot conclude whether or not chronic EV infection may be present in tissues and organs we

have not assayed. Our sensitive method will be useful for screening biopsy or cadaver samples from any individual suspected of having a chronic EV infection.

INTRODUCTION

The etiological basis of Myalgic Encephalomyelitis/Chronic Fatigue Syndrome (ME/CFS) remains unknown. Regular complaints of "flu-like" symptoms during disease initiation in addition to outbreaks of ME/CFS that have occurred implicate one or more unknown pathogenic agents. The seasonality of ME/CFS epidemics, frequent spatiotemporal overlap with poliomyelitis epidemics, and symptom constellation similarities to chronic neurotropic enterovirus-related clinical outcomes, has fueled widespread speculation of a possible link between chronic enterovirus (EV) infections and ME/CFS [1].

Human EVs are among the most common human pathogens globally, with members of this genus being the culprits of past epidemics, i.e. poliomyelitis, as well as many epidemics still occurring today. In the US, between 10 and 15 million non-polio EV infections occur annually with current leaders of EV-epidemics in the US including Coxsackievirus A16 (the most common cause of hand, foot, and mouth disease in the US), Coxsackievirus A6 (the most commonly reported EVs 2009-2013 in the US), Coxsackievirus A24 and EV70 (associated with conjunctivitis outbreaks), echovirus 13, 18, and 30 (associated with meningitis outbreaks in the US), EVA71 (associated with large numbers of global hand foot and mouth disease outbreaks) and EVD68 (associated with US outbreaks in 2014, 2016 and 2018 causing severe respiratory illness) [2].

Although EV infections typically resolve in a few weeks, chronic conditions following infection are known to occur in a subset of individuals leading to a multitude of clinical outcomes. Some examples include chronic viral cardiomyopathy, type 1 diabetes, post-polio syndrome and acute flaccid myelitis/paralysis [3-6]. The range of clinical outcomes and severity of chronic viral infection is due to the host immunologic susceptibility [7, 8], the EV serotype involved, the quasispecies composition of the infectious EV population [9], the cellular/tissue level tropism achieved by the virus, and the viral mutations underpinning its chronicity. Symptoms seen across the wide spectrum of EV-specific clinical outcomes, especially those caused by EVs with muscle and nervous system tropism, are mirrored in ME/CFS cases allowing one to postulate either a) involvement of an unknown serotype or strain of EV involved in ME/CFS b) a differential susceptibility existing only in ME/CFS patients that may be leading to an alternative but similar clinical outcome or c) both.

The association of EVs and ME/CFS is sufficiently strong to cause a number of ME/CFS investigators to explore this topic, as we have recently described in our review regarding the EV theory of disease etiology in ME/CFS [1]. Three of five EV-ME/CFS tissue culture studies report increased prevalence in ME/CFS subjects compared to controls [1]. Sixteen of twenty serological-based EV-ME/CFS studies found an increased prevalence in ME/CFS disease cohorts and four out of five immunochemical-based studies targeting VP1, and dsRNA targets report increased EV prevalence in the muscle, gastrointestinal, and brain tissue of ME/CFS cases [1]. Lastly, molecular approaches including RNA Blot, RT-PCR or RNAseq, were utilized in twenty independent studies with seventeen showing and increased prevalence in

ME/CFS cohorts [1]. A few prior studies were able to detect EVs by PCR in higher proportions in ME/CFS patients, though there also were negative reports (reviewed in [1]. The aim of our study is to combine recently developed targeted RNA sequencing (RNAseq) approaches with *in vitro* viral amplification to screen for EV RNAs in blood at a sensitivity yet to be employed in the study of ME/CFS.

Capture enrichment of EV transcript targets prior to sequencing was chosen to allow a comprehensive screen of both currently known and potential undiscovered EVs at an order of magnitude greater sensitivity than traditional RNAseq [10]. The technology involves the computational design of biotinylated nucleic acid probes that hybridize to complementary regions on target sequences, thereby allowing their positive selection. The ability of probes to hybridize to targets with sequence dissimilarities, due to the sheer size of the potential probe binding region (100nt), makes undiscovered EV detection possible because the entire probe length does not need to hybridize to a target for its positive selection. Probes are pulled down with streptavidin beads, reducing the amount of sequencing dedicated to extraneous nucleic acids present as background in the sample [10]. I used the Python package CATCH (Compact Aggregation of Targets for Comprehensive Hybridization) to design a probe set consisting of roughly 50,000 probes targeting over 3,000 EV complete genomic sequences. The probes are scaled in number dedicated to each EV species A-D according to genomic diversity within the species classification. This computational method was chosen to create our EV-specific probe set because the Python package is publicly available and was shown by the creators to increase sensitivity of viral detection by 10-fold when employing their V_{ALL} probe set consisting of 2 million

probes targeting all known viral genera [11]. *In vitro* co-culturing of patient samples with EV-susceptible cell cultures was pursued to allow biological amplification of low viral copy numbers before molecular detection. Super E-mix cells, containing both lung carcinoma cells (A549) and bovine green monkey kidney cells genetically modified to express the human decay accelerating factor (sBGMK) were used in the assay due to the combination of cells allowing culture of all known human EV serotypes [12].

RESULTS

Probe Design, Localization and Sensitivity

Figure 3.1. Probe localization, design parameters and targeted RNAseq sensitivity. (A) Coverage map indicating localization of probes across the CVB3 genome. Y-axis indicates coverage depth by number of reads. (B) Bubble plot indicating the chosen CATCH species-specific parameters across EV species A-D and ERCC experimental controls. Bubble size positively scales with the number of probes generated by CATCH to the respective EV species and ERCC group. (C) Graph showing the relationship between number of mapped reads and percent recovery of genomic sequence depending on EV71 dilution series concentration. Zero on the x-axis indicates negative control. Error bars indicate standard deviation.

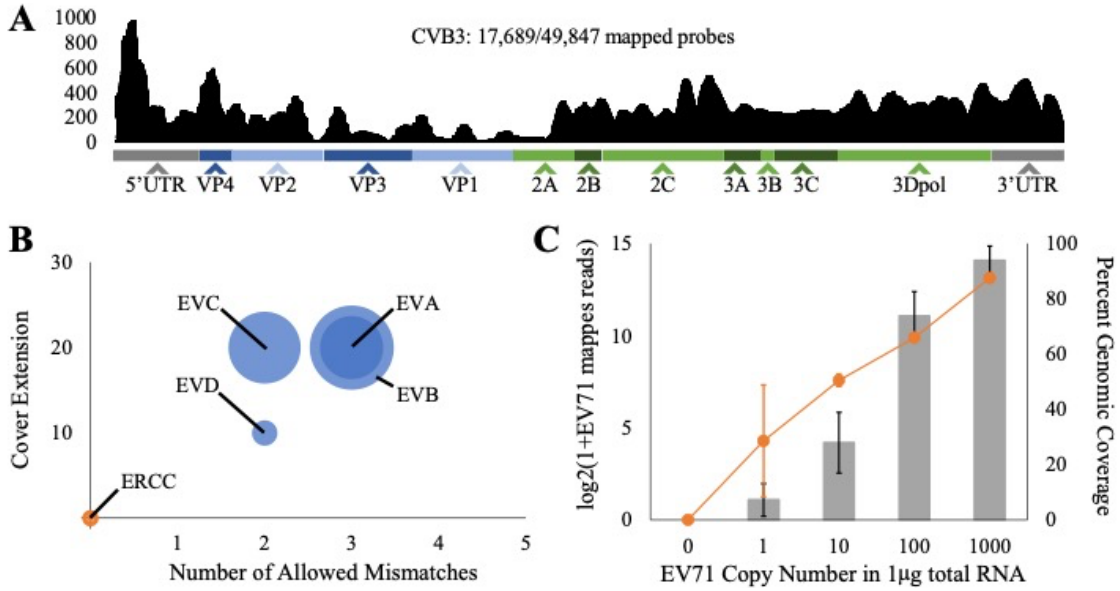

CATCH generated 49,847 probes targeting 3,410 EV complete genome sequences and 10 ERCC sequences. In-silico mapping of CATCH-designed probes shows variability in density of mapping across the genome. The variability in coverage depth is a product of the algorithms used within CATCH to optimize the scalability of probe design – most specifically, the use of the "set cover problem" to limit the number of designed probes. Genomic regions with highest variability across a genomic dataset are optimized to have the highest probe production directed against them, with fewer probes being generated to well conserved regions across the dataset. In total, 17,689 out of 49,847 probes mapped to CVB3 with most probes being localized towards the 5'UTR, P2 (2A-2C) and P3 (3A-3D) genomic regions of Coxsackievirus B3 (CVB3) (Figure 3.2A). This is not surprising as these regions represent locations where recombination events are common across EV species [13].

Within-species variability differs between EV species A-D leading to differential design parameters chosen by CATCH regarding the number of allowed mismatches and size of probe cover extension when limiting production to 50,000 probes. EV species A and B were each chosen to allow 3 mismatches with cover extensions of 20nt. EV species C probe sets were designed based on 2 mismatches with a cover extension of 20 and EV species D with 2 allowed mismatches and a cover extension of 10nt. ERCC directed probes were designed with zero mismatches and zero cover extension (Figure 3.2B).

To determine our assay's lower limit of detection (LOD), I used human heart total RNA and created a 1:10 dilution series ranging from 1 to 1,000 copies of EV71 in a 1μg background of total RNA. Almost complete genome recovery (90.1 $\pm$ 8.1%)

is obtained when assessing input levels of 1,000 EV71 copies in 1μg RNA. In terms of LOD, 10 EV71 copies/1μg was recovered at an average coverage of 24.0 $\pm$ 11.1% across triplicate dilution series tested. 1copy/1μg was detected in 2 of 3 triplicates with coverages of 7.2% and 14.6%.

PAXgene Whole Blood Targeted RNAseq

Figure 3.3. EV-RNAseq on PAXgene whole blood samples. Each sample was sequenced on a MiSeq platform (2x250bp) at a depth of ~ 2 million sequences/sample. Non-human, non-BGMK, non-ERCC indicate the reads remaining after alignment to each of these genomes/sequences.

	ME/CFS						Control	
	942	946	952	960	968	978	979	980
Non-human, non-BGMK, non-ERCC reads	141k	119k	144k	149k	127k	132k	134k	132k
EV-specific reads	0	0	0	0	0	0	0	0
ERCC								

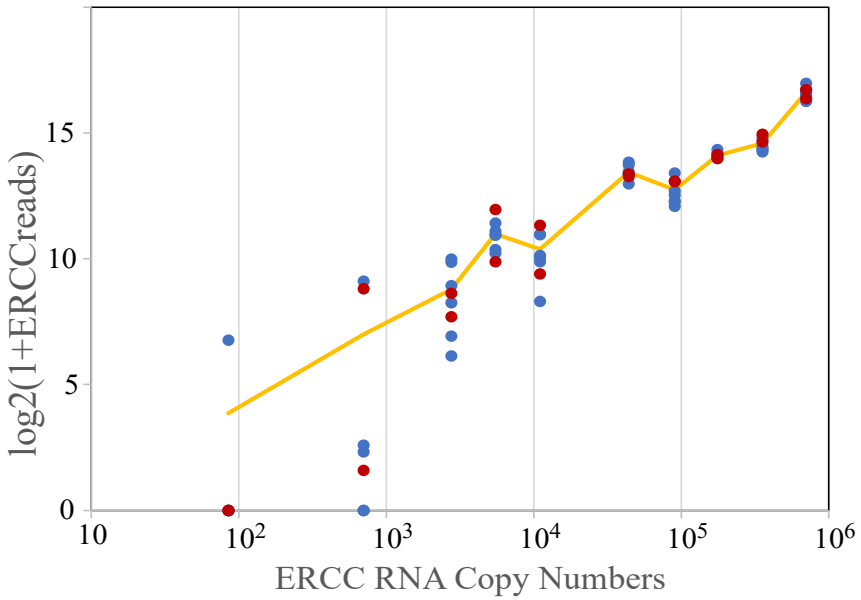

Although ERCC spike-in transcripts provide an internal standard due to their variation in concentration, their ability to be used as a standard scale to interpret EV

transcript recovery is only semi-quantitative. Each ERCC transcript varies in nucleotide length (521-2,022nt), leading to natural variations in the number of dedicated reads per transcript. Second, ERCC transcripts are overall smaller targets with the largest transcript targeted (ERCC00033) being more than 3.5x smaller than the average EV genome of 7500nt. These facts are highlighted when looking at how average ERCC recovery tracks with the EV71 dilution series (**Figure 3.1C, 3.4 and 3.5**). ERCC transcript recovery is nearly complete (5/8 samples) at 700 copies/250ng RNA and is complete at 2,750 copies/250ng RNA (8/8 samples) indicating reliable recovery starts between 700 and 2,750 ERCC transcripts/250ng total RNA when sequencing at a depth of ~2 million reads/sample (**Figure 3.2**). No EV-specific reads were detected for the 6 subject and 2 control samples interrogated.

In-vitro co-culture (PBMC + Extracellular Vesicles)

Figure 3.5. VP1 immunochemistry using the Quidel D^3 IFA Enterovirus Detection kit. (Top) Phase contrast images. (Bottom) Immunofluorescent images. Green, punctate fluorescent signal indicates antibody reaction with VP1 in infected cell cultures. (A) Negative control staining at 1000x using EV antigen control slides. (B) Positive control staining of Coxsackievirus B infected cultures at 1000x using EV antigen control slides. (C) Representative image showing negative staining in cultures inoculated with case and control samples. 100x magnification. (D) Same image as C but with oversaturation to show a lack of punctate signaling even after excitation is raised to levels higher than control slide imaging.

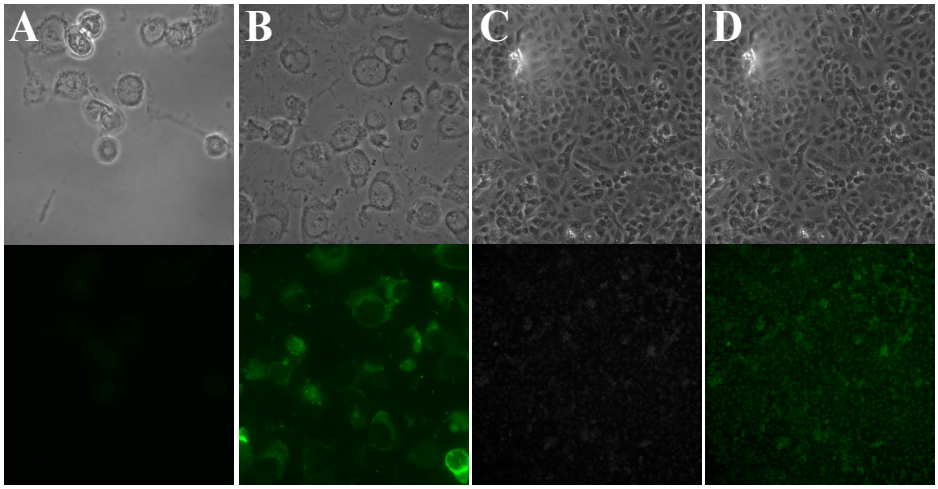

Initial *in vitro* co-culture experiments involved application of subject PBMC and plasma-derived extracellular vesicles to Super E-mix EV-susceptible cultures. Blood-derived PBMCs and extracellular vesicles were applied to cultures as they are both known sources of EVs in chronically infected individuals [14, 15]. Daily monitoring of cultures for CPE was negative throughout the course of study. Targeted RNAseq and immunochemical detection of EVs in culture both show negative results with zero EV-specific reads being detected and a lack of VP1 staining or CPE being present in culture (**Figure 3.3**). ERCC transcript recovery increased with 4/8 samples at showing reads mapped to ERCC 00083 (85 copies/250ng RNA). Near complete recovery of

	ME/CFS						Control	
	957	960*	968*	972	978*	981	954	979*
PBMCs	~1x10^6	~1x10^6	~1x10^6	~1x10^6	~1x10^6	~1x10^6	~1x10^6	~1x10^6
Plasma-derived extracellular vesicles	6ml	4ml	5ml	6ml	4ml	6ml	6ml	4ml
Non-human, non-BGMK, non-ERCC reads	133k	210k	191k	83k	141k	119k	163k	92k
EV-specific reads	0	0	0	0	0	0	0	0

ERCC

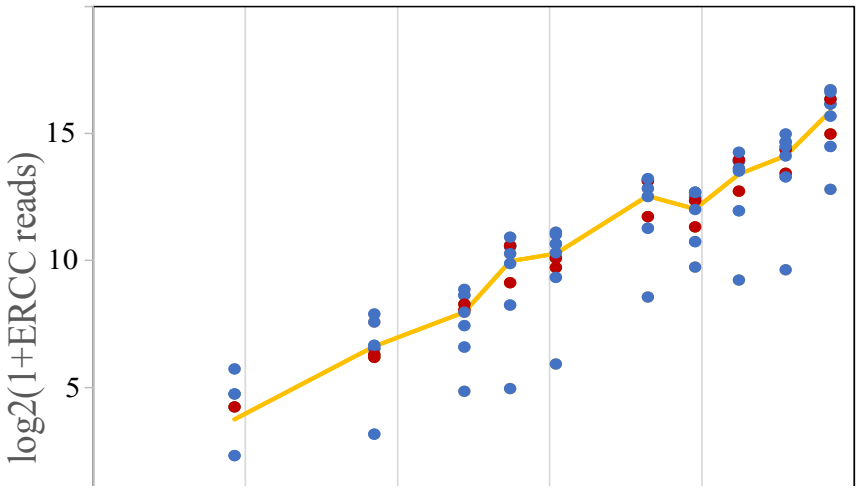

ERCC RNA Copy Numbers

Figure 3.6. EV-RNAseq to evaluate EV-susceptible cultures inoculated with subject PBMC and plasma-derived extracellular vesicles. Graph indicates number of ERCC mapped reads for a given ERCC transcript based on a 250ng background diluted according to ERCC usage recommendations. * Indicates subjects are repeats from PAXgene whole blood experiments (Figure 3.2). Each sample was sequenced on a MiSeq platform (2x250bp) at a depth of ~ 2 million sequences/sample.

ERCC 00123 (700 copies/250ng RNA) was achieved in 7/8 samples and complete recovery of ERCC 00147 (2,750 copies/250ng RNA) was achieved in 8/8 samples when sequencing at a depth of ~2 million reads/sample (**Figure 3.4**).

In-vitro co-culture (PBMC, Vesicles) assayed after 7 and 14 days of incubation

Based on the results from initial *in vitro* co-culture experiments (**Figure 3.4**), a second round of *in vitro* experiments was pursued with four experimental modifications. First, subject PBMC (**Figure 3.5**) and extracellular vesicle (**Figure**

Figure 3.8. EV-RNAseq to evaluate EV-susceptible cultures inoculated with subject PBMCs. Graphs indicates number of ERCC mapped reads for a given ERCC transcript based on a 250ng background diluted according to ERCC usage recommendations with an extra 10-fold dilution. Each sample was sequenced on a NextSeq platform (1x75bp) at a depth of ~ 20 million sequences/sample.

	ME/CFS		Control			ME/CFS		Control	
Week 1	707 4ml	807 4ml	760 4ml	795 4ml	Week 2	707	807	760	795
Non-human, non-BGMK, non-ERCC	880k	857k	851k	986k	Non-human, non-BGMK, non-ERCC	781k	676k	641k	733k
EV-specific ERCC	0	0	0	0	EV-specific	0	0	0	0

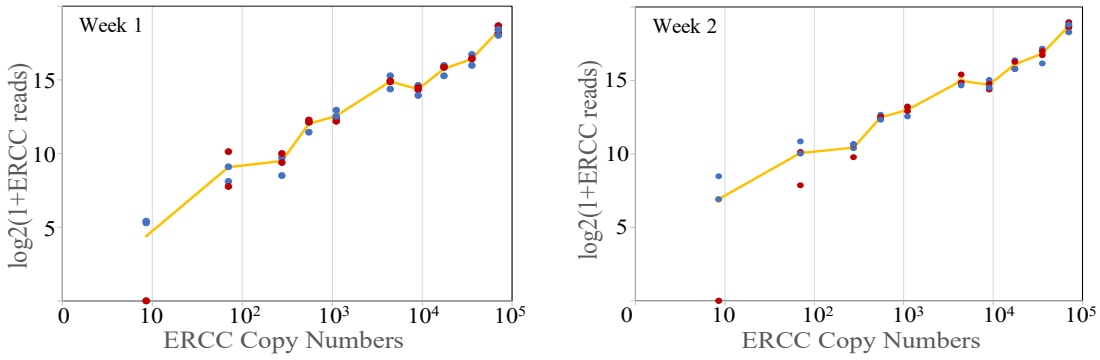

3.6) samples were applied independently to cultures to determine viral source in blood. Second, ICC and targeted RNAseq were performed on cultures at the end of week 1 and week 2 instead of week 2 alone (**Figures 3.5 and 3.6**). Third, the depth of sequences increased roughly 10-fold to ~20 million reads/sample. Fourth, ERCC spike-ins were diluted 10-fold to allow finer assessment of low copy number transcripts.

Figure 3.10. EV-RNAseq to evaluate EV-susceptible cultures inoculated with subject extracellular vesicles. Graphs indicates number of ERCC mapped reads for a given ERCC transcript based on a 250ng background diluted according to ERCC usage recommendations with an extra 10-fold dilution. Each sample was sequenced on a NextSeq platform (1x75bp) at a depth of ~ 20 million sequences/sample

	ME/CFS						Control	
Week 1: PBMC inoculation	707 ~1x10^6	807 ~1x10^6	834 ~1x10^6	883 ~1x10^6	902 ~1x10^6	925 ~1x10^6	760 ~1x10^6	795 ~1x10^6
Non-human, non-BGMK, non-ERCC reads	431k	326k	*	474k	412k	582k	496k	401k
EV-specific reads	0	0	*	0	0	0	0	0
Week 2: serial passage	707	807	834	883	902	925	760	795
Non-human, non-BGMK, non-ERCC reads	646k	455k	593k	630k	552k	498k	657k	576k
EV-specific reads	0	0	0	0	0	0	0	0

ERCC

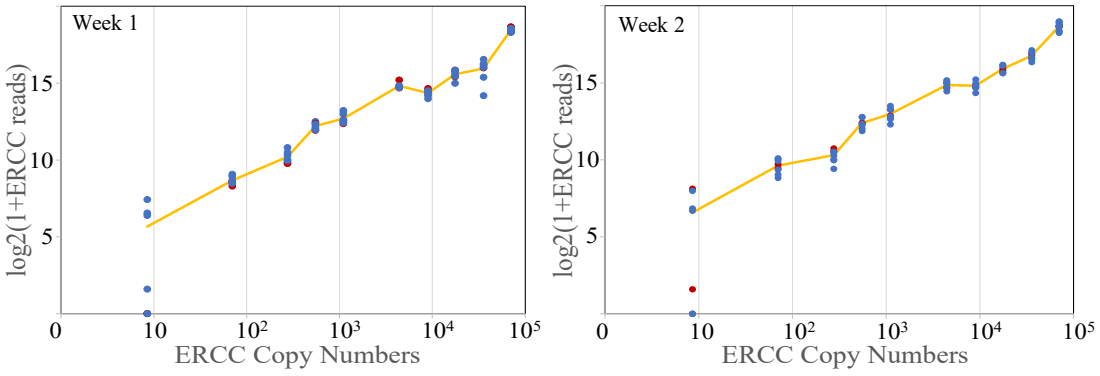

This round of co-culture experiments also shows no evidence of EV presence with zero EV-specific reads being detected and a lack of VP1 staining or CPE being present

in all cultures at both timepoints tested. Sensitivity of detection with increased sequencing depth could reliably detect ERCC00123 (70 copies/250ng) in all samples assayed with recovery of ERCC00083 (8.5 copies/250ng) being limited to 7/12 samples (**Figures 3.5 and 3.6**).

DISCUSSION

I used CATCH to design 49,847 probes targeting all known human EV complete genomic sequences downloaded from NCBI and ViPR databases as well as a subset of 10 ERCC spike-in transcripts. Recovery was achieved 2/3 EV71 positive control samples at 1 copy/1μg total RNA with complete recovery occurring at 10 copies/1μg. In a clinical context, this corresponds to a LOD at 10-25 copies/1ml blood based on the presence of 1-5μg RNA in 1ml of blood [16], although incomplete detection may sometimes take place in certain occasions at copy numbers lower than the LOD. This strategy therefore proves to be acutely sensitive, equal to RT-PCR, with the added benefit of being comprehensive in nature, allowing us to survey for all known, and potentially novel, human EV sequences at a sensitivity yet to be employed in the field of ME/CFS. This strategy, combined with the use of EV-susceptible cultures to perform in-vitro viral amplification is a promising strategy to employ in future ME/CFS, EV-related studies [14].

When comparing the sensitivity of our EV-specific probe set to the V_{ALL} probe set generated by the creators of CATCH, we find the EV-specific probe set to have a slightly increased sensitivity [11]. This is, however, not surprising when you consider how many fewer probes are dedicated to any one viral target in the V_{ALL} probe set. For example, V_{ALL} has roughly half (24,728) the number of probes dedicated to human

enteroviral targets due to increased cover extension and increased number of allowed mismatches [11]. Probes designed by the creators of VirCapSeqVERT are theoretically similar to those created by inventors of CATCH. Unfortunately, the sequences of the VirCapSeqVERT probe set are proprietary, making it impossible to make direct comparisons between probe sets. Nonetheless, our EV-specific probe set created in CATCH is more sensitive than VirCapSeqVERT, with nearly identical coverage and sequencing reads being gained at similar sequencing depths (10 million), but with an order of magnitude fewer EV transcripts spiked into our assay. For example, at 1 EV71 copy/1μg RNA we find two out of three triplicates show viral recovery with 30 and 73 of 10 million reads corresponding to genomic coverages of 7.2% and 14.6%, respectively. It was reported that VirCapSeqVERT can detect 10 EVD68 copies in a 1ml background of blood with an average of 34 out of 10 million reads at an average genomic coverage of 8.2% [17]. Because the dilution series used by Briese et al. (2015) was created in a 1ml background of blood, we could not make direct comparisons; each ml of blood could range anywhere from 1 to 5 μg in total RNA content [16].

While the targeted RNAseq was unable to detect EV genomic RNA in the blood of ME/CFS cases both before and after in-vitro attempts of viral amplification, a lack of EV detection does not prove a lack of chronic enteroviral infection. It is possible that an EV could persist within a tissue or organ and rarely be released into the blood. In the case of pathologies associated with chronic EV infections, the viruses are known to reside in a persistent state within tissue sites such as the central nervous system, muscle and even pancreas [3-6]. Many chronic enteroviral infections caused

by myotropic and neurotropic EVs invoke a symptom constellation profile consistent with ME/CFS [1]. The World Health Organization (WHO) guidelines on non-polio EV surveillance directs researchers to more appropriate preferred and alternative sample types based on clinical syndrome presentations [18]. In the case of ME/CFS, the WHO suggests EV surveillance should initially be focused on brain tissue and cerebrospinal fluid and secondarily to feces, throat swab, oropharyngeal swab, nasopharyngeal swab, and rectal swab [18]. In order to settle the question of chronic EV infection in ME/CFS, we need to use our integrated, comprehensive approach for sensitive EV detection on sample types such as brain, cerebrospinal fluid, muscle, and gastrointestinal tissues.

MATERIALS AND METHODS

Sample Selection

In total, 15 ME/CFS and 5 healthy control subjects were included in this case–control cross-sectional study. Samples were obtained at Ithaca College, where cases underwent 2-day cardiopulmonary exercise testing (CPET). Of these subjects, 8 (6 case/2 control) were used in PAXgene whole blood experiments and 16 (12 case/4 control) were used in in-vitro co-culture assays. Of the 16 subjects used in co-culture assays, 4 subjects (3 case/1 control) were carried forward from PAXgene whole blood experiments. Individuals were diagnosed with ME/CFS if they met the Canadian Consensus Criteria for ME/CFS [19] and controls were eligible if they were healthy as diagnosed by participating MDs. Cases included in the study did not report use of immune-modulating drugs. Peripheral blood from an antecubital vein was drawn into PAXgene Blood RNA tubes prior to day 2 CPET for 19 subjects and post day 1 CPET

for 1 subject (#707). Once collected, blood tubes were put on ice and taken to labs for immediate separation of plasma and PBMC isolation. Plasma samples were stored at −80 °C and PBMC samples were stored in liquid nitrogen until further use. Participants' age, sex, and age of onset of ME/CFS were prior to blood collection. Short Form-36 Health Surveys [20] were administered to 16/20 participants on the day of blood sample collection. No SF36 data was available for subjects 760, 795, 807, and 954.

Table 3.1. Study population characteristics.

	ME/CFS (n=15)	Controls (n=5)	Mann-Whitney U Test
Age	44.0 ± 11.7	49.4 ± 16.6	$p = 0.53$
Gender			
Female	11	2	NA
Male	4	3	NA
BMI (kg/m2)	24.8 ± 8.2	31.2 ± 5.8	$p = 0.12$
Onset of disease			
Gradual	57%	NA	NA
Sudden	43%	NA	NA
Illness Duration (years)	13.0 ± 11.8	NA	NA
SF-36			
Physical function	36.8 ± 25.2	97.5 ± 3.5	$p < 0.001$
Role physical	1.8 ± 6.7	87.5 ± 17.7	$p < 0.050$
Pain	41.0 ± 25.7	92.0 ± 11.3	$p < 0.010$
General health	14.3 ± 7.3	58.5 ± 9.2	$p < 0.050$
Vitality	8.6 ± 9.1	65.0 ± 35.4	$p = 0.131$
PCS	26.1 ± 11.7	55.6 ± 6.1	$p < 0.001$
Social function	10.7 ± 13.7	75.0 ± 35.4	$p < 0.115$
Role emotional	45.2 ± 50.0	66.7 ± 47.1	$p < 0.318$
Mental health	46.9 ± 25.7	66.0 ± 36.8	$p < 0.297$
MCSa	32.6 ± 13.5	43.0 ± 24.5	$p = 0.327$

Probe Design

Figure 3.12. Human EV-specific CATCH probe design parameters.

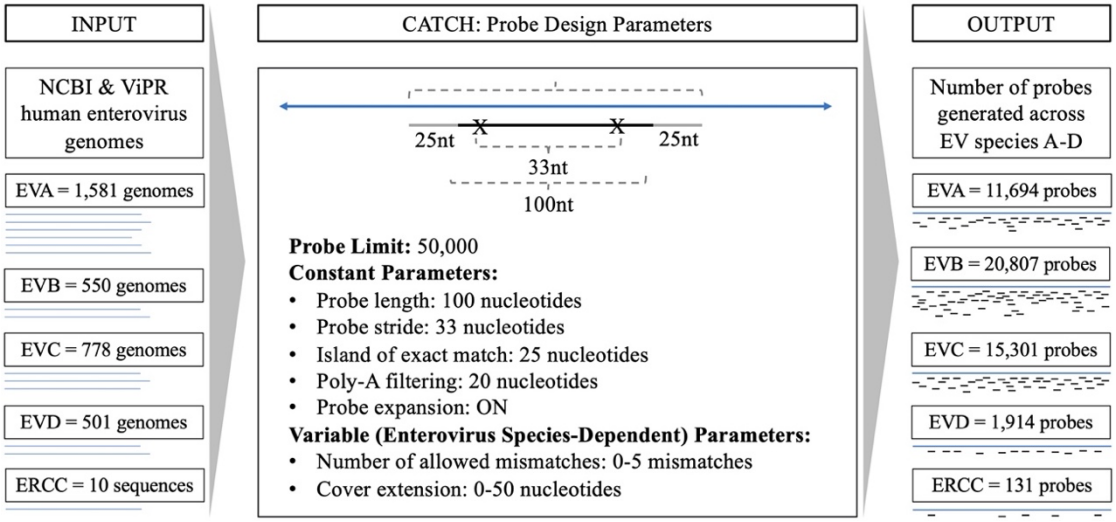

Probes were designed using CATCH (v1.2.0) with Python (v3.7). Constant parameters held throughout CATCH probe design are probe length = 100nt (nucleotides), probe stride = 33nt, island of exact match = 25nt, filtering of polyA sequences greater than or equal to 20nt in length and selection for probe sets to be expanded by converting "N" nucleotides to each of the 4 possible nucleotide substitutes "ATCG". Variables in probe design include the number of allowed mismatches and length of cover extension. Number of allowed mismatches and size of cover extension are chosen by CATCH based on the user chosen limit in probe design – in this case I limited CATCH to generate no more than 50,000 probes (**Figure 3.7**). Probes were designed using an input database of nonduplicate human enteroviral complete genomes across enteroviral species A-D downloaded from NCBI and ViPR (The Virus Pathogen Database and Analysis Resource, www.ViPRbrc.org) databases

accessed on March 7, 2019. In total, 3,410 genomes (EVA = 1581, EVB = 550, EVC = 778, EVD = 501, ERCC = 131) were used to generate a probe set containing 49,847 probes. Probes were generated to a common set of external RNA controls (ThermoFisher, Waltham, MA. CN: 4456740) developed by the External RNA Controls Consortium (ERCC) for use in monitoring library construction as well as providing an internal quantification standard due to variation in concentration between each ERCC transcript provided.

RNA isolation and sample preparation

Whole blood was collected in PAXgene Blood RNA tubes and stored at -20ºC to stabilize RNA prior to extraction. PBMCs were isolated from EDTA stored whole blood via centrifugation using SepMate tubes (STEMCELL Technologies, Vancouver, Canada) as previously described [21]. Extracellular vesicles were isolated from subject plasma using size exclusion chromatography with the qEV10/35nm columns (Izon Science, Christchurch, New Zealand) and concentrated using Amicon Ultra Centrifugal Filters (MilliporeSigma, Burlington, Massachusetts). RNA was extracted from PAXgene stored whole blood using the PAXgene Blood miRNA Kit (PreAnalytiX, Hombrechtikon, Switzerland) according to manufacture protocol. Individual PBMC samples and sample cultures isolated from *in vitro* co-culture experiments were processed for total RNA using the RNeasy Mini Kit (Qiagen, Valencia, CA). Human heart total RNA (Takara Bio, Mountain View, CA. PN: 636532) was utilized as background RNA during preparation of EV71 (ATCC® VR-1775DQ™) dilution series. All RNA isolates were quantified using Qubit RNA High

Sensitivity Quantitation Assay (ThermoFisher, Waltham, MA) and assessed for RNA integrity using the Fragment Analyzer (Agilent, Santa Clara, CA).

cDNA library construction and sequencing

Total RNA samples were submitted to the Cornell Transcriptional Regulation and Expression Facility for RNAseq including library prep with the NEBNext Ultra II Directional RNA Kit (New England Biolabs, Ipswich, MA) following rRNA depletion, sequencing, read preprocessing. In short, total RNA samples were first spiked with ERCC quality control RNA transcripts to monitor library construction and to use as internal sensitivity standards in CATCH experiments. Ribosomal RNA was removed by hybridization using the NEBNext rRNA Depletion Kit (New England Biolabs, Ipswich, MA). TruSeq-barcoded RNAseq libraries were generated with the NEBNext Ultra II RNA Library Prep Kit (New England Biolabs, Ipswich, MA). Each library was then quantified with a Qubit dsDNA High Sensitivity kit (ThermoFisher, Waltham, MA) and the size distribution was determined with a Fragment Analyzer (Agilent, Santa Clara, CA) prior to pooling.

Individual cDNA libraries were pooled to a total size of 1.5-4μg and then processed according to Twist Target Capture Enrichment Standard Hybridization Protocol [22]. Briefly, pooled cDNA libraries were dried using a vacuum concentrator. The CATCH designed EV-targeting probes synthesized by Twist were suspended in hybridization solution and then mixed with the reconstituted cDNA pool prepared in the presence of universal blockers. The hybridized cDNA targets were then bound to streptavidin beads via magnetic separation, put through several washes and then eluted directly prior to PCR amplification and subsequent purification. Each library was then

validated and quantified using an Agilent Bioanalyzer High Sensitivity DNA Kit and a Qubit dsDNA High Sensitivity Quantitation Assay. Library pools were then sequenced on either a MiSeq (2x250bp), NextSeq (1x75bp) or NovaSeq (2x150) platform based on desired sequencing depth. Total reads generated were reduced by eliminating any reads mapping to human (hg38) and *Chlorocebus sabaeus* (green monkey, chlSab2) - due to the use of buffalo green monkey cells during *in vitro* cell culture experiments. The database of 3,410 human EV reference genomes were indexed using Bowtie2. Non-human, non-monkey reads were then mapped to the EV genomes using the Bowtie2 read mapper. Location of mapped reads was verified with Samtools (v1.13) and visualized using Interactive Genome Viewer (IGV) (v2.6.2).

***In vitro* co-culture experiments**

PBMCs (4-6ml) and plasma-derived extracellular vesicles (~1x10^6) were applied, in triplicate, to a 24-well Super E-mix (Quidel – Diagnostic Hybrids, San Diego, CA) culture containing buffalo green monkey kidney cells genetically modified to express the Degradation Accelerating Factor (sBGMK) and human lung carcinoma (A549) cells. Cultures were prepared, inoculated, incubated, and screened according to manufacture recommendations. Briefly, cell cultures were immediately incubated upon arrival, monitored for proper morphology, and patient samples were applied once cultures were established at the appropriate confluence (70-80%). Plates were centrifuged (700xg) at room temperature (20-25ºC) for 1 hour and then incubated at 37ºC with a humidified 5% CO_2 atmosphere using Super E-Mix Refeed Medium (A defined medium with 0.1% FBS, NEAA, penicillin at 100 units/mL, and streptomycin at 100 µg/mL, sterile.). Cultures were monitored daily for cytopathic effect (CPE) via

microscopy. In-vitro experiments involving PBMCs in combination with patient matched plasma-derived extracellular vesicles were cultured for 7 days, serial passaged to a new 24-well plate, and again incubated for 7 days with daily CPE monitoring. Serial passaging (blind passage) was conducted as a subset of EVs are known to cause CPE in culture only after serial passaging [23]. Total RNA isolation for EV-RNAseq analysis as well as immunocytochemistry (ICC) of EV viral protein 1 (VP1) antigens did not occur until the end of week 2. Experiments involving inoculation with patient matched PBMC and extracellular vesicle samples were applied independently in culture and then similarly incubated for 1 week, serial passaged, and incubated a second week. This time, however, cultures were assessed via ICC and RNAseq at the end of both weeks 1 and 2. ICC was performed using the D3 IFA Enterovirus Kit (Diagnostic Hybrids, Athens, Ohio) according to manufacture recommendations with positive staining being verified using EV antigen control slides. The kit's utilization of a blend of FITC-conjugated EV VP1-specific monoclonal antibodies allows a comprehensive survey of human EV across species via immunofluorescence.

REFERENCES

1. O'Neal AJ, Hanson MR. The Enterovirus Theory of Disease Etiology in Myalgic Encephalomyelitis/Chronic Fatigue Syndrome: A Critical Review. Front Med (Lausanne). 2021;8:688486-.

2. Prevention CfDCa. Non-Polio Enteroviruses - Outbreak & Surveillance CDC [updated August 8, 2020. Available from: https://www.cdc.gov/non-polio-enterovirus/outbreaks-surveillance.html.

3. Bouin A, Gretteau PA, Wehbe M, Renois F, N'Guyen Y, Lévêque N, et al. Enterovirus Persistence in Cardiac Cells of Patients With Idiopathic Dilated Cardiomyopathy Is Linked to 5' Terminal Genomic RNA-Deleted Viral Populations With Viral-Encoded Proteinase Activities. Circulation. 2019;139(20):2326-38.

4. Richardson SJ, Morgan NG. Enteroviral infections in the pathogenesis of type 1 diabetes: new insights for therapeutic intervention. Curr Opin Pharmacol. 2018;43:11-9.

5. Baj A, Colombo M, Headley JL, McFarlane JR, Liethof M-a, Toniolo A. Post-poliomyelitis syndrome as a possible viral disease. International Journal of Infectious Diseases. 2015;35:107-16.

6. Helfferich J, Knoester M, Van Leer-Buter CC, Neuteboom RF, Meiners LC, Niesters HG, et al. Acute flaccid myelitis and enterovirus D68: lessons from the past and present. Eur J Pediatr. 2019;178(9):1305-15.

7. Garzo-Caldas N, Ruiz-Sainz E, Vila-Bedmar S, Llamas-Velasco S, Hernández-Lain A, Ruiz-Morales J, et al. Enteroviral T-cell encephalitis related to immunosuppressive therapy including rituximab. Neurology. 2017;89(4):408-9.

8. Anderson SM, Gold D, Olson G, Pisano J. Chronic aseptic meningitis caused by enterovirus in a humorally immunosuppressed adult patient presenting with sensorineural hearing loss: a case report. BMC Infectious Diseases. 2022;22(1):16.

9. Domingo E, Martin V, Perales C, Escarmis C. Coxsackieviruses and quasispecies theory: evolution of enteroviruses. Curr Top Microbiol Immunol. 2008;323:3-32.

10. Gaudin M, Desnues C. Hybrid Capture-Based Next Generation Sequencing and Its Application to Human Infectious Diseases. Frontiers in Microbiology. 2018;9.

11. Metsky HC, Siddle KJ, Gladden-Young A, Qu J, Yang DK, Brehio P, et al. Capturing sequence diversity in metagenomes with comprehensive and scalable probe design. Nat Biotechnol. 2019;37(2):160-8.

12. Hybrid D. D3 IFA Enterovirus Identification Kit Diagnostic Hybrids: Quidel; 2010 [updated 04/06/2010. Available from: https://www.quidel.com/cultures-fluorescent-tests/cell-cultures/continuous-cell-lines/super-e-mix-mixedcells.

13. Nikolaidis M, Mimouli K, Kyriakopoulou Z, Tsimpidis M, Tsakogiannis D, Markoulatos P, et al. Large-scale genomic analysis reveals recurrent patterns of intertypic recombination in human enteroviruses. Virology. 2019;526:72-80.

14. Genoni A, Canducci F, Rossi A, Broccolo F, Chumakov K, Bono G, et al. Revealing enterovirus infection in chronic human disorders: An integrated diagnostic approach. Sci Rep. 2017;7(1):5013-.

15. Netanyah E, Calafatti M, Arvastsson J, Cabrera-Rode E, Cilio CM, Sarmiento L. Extracellular Vesicles Released by Enterovirus-Infected EndoC-βH1 Cells Mediate Non-Lytic Viral Spread. Microorganisms. 2020;8(11):1753.

16. Qiagen. How much DNA and RNA can be expected from human blood cells? FAQ ID - 29502022.

17. Briese T, Kapoor A, Mishra N, Jain K, Kumar A, Jabado OJ, et al. Virome Capture Sequencing Enables Sensitive Viral Diagnosis and Comprehensive Virome Analysis. mBio. 2015;6(5):e01491-15.

18. Europe WHOROf. Enterovirus Surveillance Guidelines: Guidelines for Enterovirus Surveillance in Support of the Polio Eradication Initiative: World Health Organization, Regional Office for Europe.

19. Carruthers BM, Jain AK, De Meirleir KL, Peterson DL, Klimas NG, Lerner AM, et al. Myalgic Encephalomyelitis/Chronic Fatigue Syndrome. J Chronic Fatigue Syndr. 2003;11(1):7-115.

20. Ware JE, Jr., Sherbourne CD. The MOS 36-item short-form health survey (SF-36). I. Conceptual framework and item selection. Med Care. 1992;30(6):473-83.

21. Mandarano AH, Maya J, Giloteaux L, Peterson DL, Maynard M, Gottschalk CG, et al. Myalgic encephalomyelitis/chronic fatigue syndrome patients exhibit altered T cell metabolism and cytokine associations. J Clin Invest. 2020;130(3):1491-505.

22. Bioscience T. Twist target enrichment standard hybridization v1 protocol [updated February 2, 2022. DOC-001085 REV 4.0:[Available from: https://www.twistbioscience.com/resources/protocol/twist-target-enrichment-standard-hybridization-v1-protocol.

23. Smura T, Natri O, Ylipaasto P, Hellman M, Al-Hello H, Piemonti L, et al. Enterovirus strain and type-specific differences in growth kinetics and virus-induced cell destruction in human pancreatic duct epithelial HPDE cells. Virus research. 2015;210:188-97.

CHAPTER 4 Contribution to the Field, Limitations, and Future Directions

As all those involved in the field of ME/CFS know far too well, the disease has received subpar recognition from multiple government agencies resulting in inadequate appropriations of funds towards ME/CFS disease research. Between 2006 and 2016, the National Institutes of Health has allocated on average 5.4 million/year with an increase from 2017-2020 to roughly 15 million/year [1]. Unfortunately, this allocation is unable to fund large-scale human studies research in the era of costly multi-omics studies, which may serve as the best approach to untangling the molecular basis of this complicated disease. To give a comparison, disease areas with a fraction of the disease prevalence rate of ME/CFS, such as brain cancer (0.1%), liver cancer (0.1%), and colorectal cancer (0.5%), each receive funding between $135-476 million dollars annually [1]. While the history of ME/CFS disease research is disheartening, the unfortunate advent of COVID-19 is likely to indirectly increase funding towards ME/CFS research by using ME/CFS cohorts as comparative populations for viral-induced fatigue syndromes. In any case, the field of ME/CFS has increased its focus on viral triggers of ME/CFS giving increased relevance to the work I have completed throughout my tenure at Cornell. These investigations include 1) a critical review on enterovirus as disease initiators in ME/CFS 2) performing an analysis on global humoral immune profiles to 122 pathogenic antigens and 3) developing a targeted, comprehensive, and sensitive approach to survey for persistent chronic infections in ME/CFS cases.

The findings related to my review of the EV-ME/CFS literature highlighted two main facts. First, there is an increased prevalence of EV infections in most ME/CFS cohorts investigated. Second, the methodological approaches used in past investigations are limited in their sensitivity as well as comprehensiveness. My review represents the first publication to retrospectively perform in-silico PCR reactions using primers reported in past EV-ME/CFS studies. The results indicate no one primer set can amplify all 117 human EVs. The most comprehensive primer set utilized detects between 87% and 96% of human EVs depending on the stringency parameters chosen for in-silico PCR reactions [2]. This indicates RT-PCR studies have never truly screened for all known, and possibly novel, human EVs. Furthermore, the majority of primer sets used target the 5'UTR portion of the EV genome which suffers from significant deletions for chronic EVs with dramatically lower replication rates. This means there is a possibility for the primer binding site in chronic EVs infecting ME/CFS cases to be missing, causing a lack of EV detection via PCR. Both facts indicate RT-PCR based studies in ME/CFS have an appreciable likelihood for reporting false negatives. Nevertheless, the finding of most studies indicates increased EV prevalence in ME/CFS cases despite suboptimal sensitivity and comprehensiveness in detection supporting the continued investigation on the relationship between human EVs and ME/CFS.

Immunological differences in ME/CFS patients have often been reported with little understanding be gained about the underlying cause. Our study is the first of its kind to investigate ME/CFS humoral immune profiles by surveying subject levels of antibody that recognize an extremely broad array of 122 pathogenic antigens (107

pathogens). Serological testing of ME/CFS and control plasma samples on a broad pathogenic antigen panel allows us to find out whether there are differences in historical exposure to pathogens between cases and controls. Antibody levels to the antigens surveyed in this study do not implicate any one of the pathogens in ME/CFS nor do they rule out common pathogens that frequently infect the US population. Our analysis does, however, reveal sex-based differences in humoral immune profiles both within the ME/CFS cohort and when compared to trends seen in the healthy control cohort. Although understanding of the biological basis surrounding these sex-based humoral immune differences is outside the scope of our research approach, the findings still add to the growing body of literature supporting immune dysfunction in ME/CFS cases. Future studies should take into consideration multiple limitations surrounding our serological investigation.

First, the detection antibody used in our assay is unable to distinguish between antibody classes let alone subclasses. In this regard, we recommend that future studies investigate multiple Ig classes and subclasses independently. If a pathogen that commonly infects a large proportion of the population (such as EVs or herpesviruses) is involved in ME/CFS disease etiology, it is likely that that the differential humoral immune response to that pathogen could be highly nuanced and is simply not detected in our assay. For example, the presence of IgM and IgA against EBV VCA antigens or IgA and IgG against early antigen D are indicators of EBV reactivation that were not screened on our study [3].

Second, there was an unequal representation of pathogen classes screened by our assay leading to biases in the focus of the pathogen panel. 49/122 antigens

screened in our assay belong to the Picoranviridae family of viruses indicating an unequal representation of antigens across the 7 viral classification groups as well as bacterial and protozoan clades surveyed by our assay. Considering the focus of my thesis was directed at EVs as causative agents in ME/CFS, the biased nature of the panel was quite relevant to my work. However, this bias creates limitations when surveying other viral, bacterial or protozoan causative agents in ME/CFS and also presents problems in EV serotype implication as there is a high degree of cross reactivity in antibody responses amongst non-polio human EVs [4]. The lack of distinction between Ig classes and subclasses, even with a large focus on EV antigens, represents a challenge in gaining granularity to the nuances that may be associated with EV infections. A recent study by Puri et al. did assess both IgA and IgG classes related to EV infection in fibromyalgia with no correlation being identified [5]. Although Ig classes are distinguishable in this study, the study is limited in cohort size, number of antigens tested, and is similarly limited in the ability to understand nuances related to Ig subclasses.

Third, subjects being seropositive vs seronegative was not previously determined before or after screening. This is an important consideration as results gained in this assay are merely relative comparisons between case and control cohorts. The MFIs associated with any one antigen were not compared to clinical diagnostic platforms. In short, when case or control is elevated relative to the comparative cohort, we are unable to distinguish if the increased antibody levels in any one cohort is clinically relevant. Therefore, just because case or control is said to be increased or decreased relative to the comparative cohort does not mean the increase or decrease is

clinically relevant. In this regard, we suggest potential causative agents with significant differences in relative levels should be assayed with confirmatory ELISAs/ diagnostic platforms which are able to reveal clinical relevance.

Fourth, study design in terms of disease cohort selection was intended to appropriately represent the ME/CFS population at large, with ~70/30: female/male ratio within the patient and control cohorts. Once sex-based humoral immune differences were realized in the dataset at hand, statistical power limitations arose comparing male and female datasets due to a large difference in their relative sizes. In short, comparing 47 case females to 29 control females has a much higher statistical backing than comparing 12 case males to 15 control males. In this regard, it is no surprise that many more antigens were found to be significantly different between male cohorts (42 antigens) as compared to female cohorts (4 antigens). Future studies aimed at understanding global, sex-specific differences in humoral immune response should use male and female cohorts of similar sizes to allow increased strength in statistical comparisons.

Lastly, the assay in question is unable to determine if subjects were exposed to particular variants of a given pathogenic strain. Strain specificity is only differentiated if underlying mutations lead to changes in surface antigens recognized by antibodies. The possibility remains that ME/CFS cases may arise from an uncommon variant of one or more enteroviruses or another type of virus and/or uncommon reaction to a common endemic virus. We therefore recommend genomic strategies, such as RT-PCR or RNAseq, should be performed to reveal possible strain-specific differences in chronic infection.

The crux of my thesis work centers around the development of a targeted RNA sequencing strategy to survey for chronic EV infections with low copy numbers existing in ME/CFS patients. My primary research contribution to the field represents the first targeted RNA sequencing strategy solely dedicated at identifying chronic EV infections in ME/CFS whole blood, PBMC, blood-derived extracellular vesicles, and brain tissue samples. Our findings indicate a sensitivity of detection around 1-10 EV copies in a 1ug background of RNA when sequencing at a depth of ~20 million reads per sample. Despite this extreme sensitivity, results do not indicate presence of EV genomic material in all tissue samples surveyed. A lack of EV detection indicates either a) EVs are not present in the patient samples interrogated or b) chronic EV infections do exist in ME/CFS cases, but the extremely low level of viral copies evades our identification strategy by falling below our limit of detection.

Surveying blood as a source for enterovirus genomic material in subjects with chronic enteroviral infections requires active shedding to detect. If the virus is persisting in areas such as the CNS or muscle, theoretical detection is minimized. In the case of surveying brain tissue, we have looked only at multiple brain locations within just one subject. With a potential of 78 million sufferers, conclusions drawn from one investigation are insufficient. This argument is especially strengthened when one considers that 3 prior published brain studies did find evidence of brain EV infection [6-8]. A lack of EV detection in our study could be attributed to multiple sample storage and/or processing limitations. For instance, brain samples interrogated were not stored in an RNA preserving buffer leading to the possibility to viral genome degradation in samples assayed. Furthermore, it is possible brain tissue samples went

through multiple freeze/thaw cycles increasing the possibility for viral genome degradation. These points are substantiated by findings of poor RNA quality scores (RQN < 4) via bioanalyzer QC analysis.

In conclusion, I believe the investigation of EVs in ME/CFS should move to focusing on additional brain sample specimens as well as other likely tissue samples based on ME/CFS pathophysiology including cerebrospinal fluid and muscle tissue samples. The EV-specific targeted RNA sequencing strategy developed in our lab has proven to be both sensitive and comprehensive allowing the detection of all known, and possible novel, human EVs at a sensitivity yet to be seen in the EV-ME/CFS literature. This method should be applied in future studies both within and outside the context of ME/CFS. For instance, looking for low level coronavirus infections in patients exhibiting long COVID.

REFERENCES

1. RePORT N. Estimates of Funding for Various Research, Condition, and Disease Categories. NIH Research Portfolio Online Reportils Tools: NIH; 2022.

2. O'Neal AJ, Hanson MR. The enterovirus theory of disease etiology in Myalgic Encephalomyelitis/Chronic Fatigue Syndrome: a critical review. Front Med. 2021;8:688486.

3. De Paschale M, Clerici P. Serological diagnosis of Epstein-Barr virus infection: Problems and solutions. World J Virol. 2012;1(1):31-43.

4. Rosenfeld AB, Shen EQL, Melendez M, Mishra N, Lipkin WI, Racaniello VR. Cross-Reactive Antibody Responses against Nonpoliovirus Enteroviruses. mBio. 2022;13(1):e0366021.

5. Puri BK, Lee GS, Schwarzbach A. Human enteroviral infection in fibromyalgia: a case-control blinded study. Revista da Associacao Medica Brasileira (1992). Brazil: Associação Médica Brasileira; 2022.

6. McGarry F, Gow J, Behan PO. Enterovirus in the Chronic Fatigue Syndrome. Ann Intern Med. 1994;120(11):972-3.

7. Richardson J. Viral isolation from brain in Myalgic Encephalomyelitis. J Chroic Fatigue Syndr. 2001;9(3-4):15-9.

8. John Chia DW, Andrew Chia, Rabiha El-Habbal, editor Chronic enterovirus infection in. a patient with myalgic encephalomyelitis/chronic fatigue syndrome (ME/CFS) - clinical, virologic and pathological analysis. 19th International Picornavirus Meeting; 2016; les-Diablerets, Switzerland.

APPENDIX 1

Supplemental tables listing enterovirus-related ME/CFS studies and results of in-silico PCR amplification experiments

Table Apx1.1. Complete list of Enterovirus-related ME/CFS studies consulted in preparation of this review. Publications are grouped by tissue type interrogated and methodological approach is given. (% ME/CFS +) indicates percentage of the given ME/CFS patients who were enterovirus positive. (% Controls +) indicates percentage of the given controls who were enterovirus positive. (EV ME/CFS > EV Controls) indicates if the ME/CFS cohort was found to have a statistically significant higher prevalence of enterovirus infections compared to controls.

	Publication	Method	% ME/CFS +	% Controls +	EV ME/CFS > EV Control
Blood	S.G.B. Innes (1970)	Serological Testing - CVB Neutralization Test	50% (n=4)	N/A	+
	B.D. Keighley, E.J. Bell (1983)	Serological Testing - CVB Neutralization Test	80% (n=20)	N/A	+
	K.G. Fegan et al. (1983)	Serological Testing - CVB Neutralization Test	82% (n=22)	N/A	+
	B.D. Calder, P.J. Warnock (1984)	Serological Testing - CVB Neutralization Test	47% (n=81)	N/A	+
	B.D. Calder et al. (1984)	Serological Testing - CVB Neutralization Test	46% (n=140)	25% (n=100)	+
	E.J. Bell, R.A. McCartney (1984)	Serological Testing - CVB Neutralization Test	41% (n=52)	4% (n=950)	+
	I.E. Salit (1985)	Serological Testing - CVB Neutralization Test	8% (n=50)	N/A	+
	Behan et al. (1987)	Serological Testing - CVB Neutralization Test	70% (n=50)	N/A	+
		Serological Testing - CVB IgM ELISA	12% (n=50)	N/A	+
	G.E. Yousef et al. (1988)	Serological Testing - VP1 Antigen Test	51% (n=87)	0% (n=30)	+
		Serological Testing - CVB IgM ELISA	74% (n=87)	0% (n=30)	+
	E.J. Bell et al. (1988)	Serological Testing - CVB Neutralization Test	12.5% (n=247)	4% (n=950)	+
		Serological Testing - CVB IgM ELISA	37% (n=290)	9% (n=500)	+
	D. Halpin, S. Wessely (1989)	Serological Testing - VP1 Antigen Test	30% (n=30)	12% (n=43)	+
	P.M.J. Wilson et al. (1989)	Serological Testing - CVB Neutralization Test	44% (n=39)	N/A	+
		Serological Testing - CVB IgM ELISA	46% (n=39)	N/A	+
	E.G. Dowsett et al. (1990)	Serological Testing - CVB Neutralization Test	50% (n=205)	N/A	+
		Serological Testing - CVB IgM ELISA	31% (n=124)	N/A	+
	N.A. Miller et al. (1991)	Serological Testing - CVB IgM ELISA	24.4% (n=217)	22.6% (n=217)	-
		Serological Testing - IgG micrometabolic inhibition method	56.2% (n=217)	55.3% (n=217)	-
	J.W. Gow et al. (1991)	Serological Testing - CVB Neutralization Test	20% (n=60)	15% (n=41)	+

	A.L. Landay et al. (1991)	Serological Testing - Indirect Immunofluorescence CVB4	90% (n=63)	65% (n=40)	+
	J.W. Gow et al. (1991)	PCR - periphreal blood leukocytes	16% (n=20)	16% (n=20)	-
	C.M. Swanink et al. (1994)	Serological Testing - VP1 Antigen Test	67% (n=24)	77% (n=22)	-
		Serological Testing - Complement Fixation Test (geometric mean (median) titer)	51.3 (32)	53.6 (32)	-
		Serological Testing - CVB IgG ELISA	21% (n=24)	23% (n=22)	-
		Serological Testing - CVB IgM ELISA	21% (n=24)	18% (n=22)	-
		Serological Testing - CVB IgA ELISA	8% (n=24)	14% (n=22)	-
	G.B. Clements et al. (1995)	nested PCR	41% (n=88)	2% (n=126)	+
	C. Nairn et al. (1995)	Serological Testing – CVB Neutralization Test	34% (n=100)	41% (n=100)	-
		nested PCR	42% (n=100)	9% (n=100)	+
	D.N. Galbraith et al. (1995)	nested PCR	18% (n=238)	2% (n=130)	+
	D. Buchwald (1996)	Serological Testing – CVB Neutralization Test	20% (n=508)	N/A	+
	G. Lindh et al. (1997)	Serological Testing - echo30, CVB5 and echo9 IgG ELISA	0% (n=7)	N/A	-
	D.N. Galbraith et al. (1997)	nested PCR + sequencing of PCR product	100% (n=8)	N/A	+
	Jerome Bouquet (2017)	RNAseq	0% (n=25)	0% (n=25)	-
	Jerome Bouquet (2019)	RNAseq after CPET	0% (n=14)	9% (n=11)	-
Muscle Tissue	L.C. Archard et al. (1988)	Northern Blot	21% (n=96)	0% (n=4)	+
	L. Cunningham et al. (1990)	Northern Blot	50% (n=8)	0% (n=152)	+
	J.W. Gow et al. (1991)	PCR	53% (n=60)	15% (n=41)	+
	L. Cunningham et al. (1991)	Northern Blot	24% (n=140)	0% (n=152)	+
	N.E. Bowles et al. (1993)	Northern Blot	26% (n=158)	1% (n=152)	+
	J.W. Gow et al. (1994)	PCR	26.4% (n=121)	19.8% in OND (n=101)	-
	F. McGarry et al. (1994)	PCR	100% (n=1)	N/A	+
	A. McArdlle et al. (1996)	PCR	0% (n=34)	0% (n=10)	-
	G. Lindh et al. (1997)	semi-nested PCR	0% (n=29)	N/A	-
	R.J. Lane et al. (2003)	nested PCR	20.8% (n=48)	0% (n=29)	+
	F. Douche-Aourik et al. (2003)	PCR	13% (n=30)	0% (n=29)	+
		VP1 immunohistochemistry	0% (n=30)	0% (n=29)	-
Throat Swabs	D.N. Galbraith et al. (1995)	nested PCR		17% (n=175)	N/A +

Stomach Tissue	J.K. Chia, A.Y. Chia (2008)	RT-PCR ELISA - based on Rotbart's Method	37% (n=24)	<1% (n=21)	+
		VP1 immunohistochemistry	82% (n=165)	20% (n=34)	+
	J.K. Chia et al. (2015)	mAb against dsRNA	ME/CFS w/ FD 64% (n=416)	FD alone 63% (n=66)	+
		VP1 immunohistochemistry	ME/CFS w/ FD 82% (n=416)	FD alone 83% (n=66)	+
Heart Tissue	F. McGarry et al. (1994)	PCR	100% (n=1)	N/A	+
CSF	S.G.B. Innes (1970)	H.Ep.II tissue culture, monkey kidney tissue culture	50% (n=4)	N/A	+
	G. Lindh et al. (1997)	Serological Testing - echo30, CVB5 and echo9 IgG ELISA	0% (n=7)	N/A	-
Brain Tissue	F. McGarry et al. (1994)	PCR	100% (n=1)	N/A	+
	J. Richardson (2011)	VP1 immunohistochemistry	100% (n=1)	N/A	+
	J.K. Chia et al. (2015)	VP1 western blot	100% (n=1)	N/A	+
		RT-PCR	100% (n=1)	N/A	+
Feces	S.G.B. Innes (1970)	monkey kidney tissue culture	25% (n=4)	N/A	+
	G.E. Yousef et al. (1988)	VERO and Hep-2 tissue culture	22% (n=76)	7% (n=30)	+
	C.M. Swanink et al. (1994)	nested PCR	4% (n=24)	0% (n=22)	-
		human fetal lung fibroblast and tertiary monkey kidney cell tissue culture	0% (n=24)	0% (n=22)	-
	G. Lindh et al. (1996)	green monkey kidney cells, RD cells and HeLa cells tissue culture	0% (n=12)	N/A	-
		electron microscopy	0% (n=12)	N/A	-

Table Apx1.2. Complete in-silico PCR results. Mismatches = 1. 0 allowed mismatches within 2 base pairs of the 3'end. ** indicates faulty primer reported in publication.

Primer/Probe			
Method 1 (Detect 44% of Human Enteroviruses)		EP1, EP4 and EP2	
EPI: 5'-CGGTACCTTTGTGCGCCTGT-3'	EVA (25)	8/25	
Probe EP2: 5'-TATTGAGCTAGTTGGTAGTCCTCCGG-3'	EVB (63)	44/63	
EP4: 5'-TTAGGATTAGCCGCATTCAG-3'	EVC (24)	0/24	
	EVD (5)	0/5	
	total	52/117	
Method 2 (Detect 73% of Human Enteroviruses)		EP1 and EP4	
EPI: 5'-CGGTACCTTTGTGCGCCTGT-3'	EVA (25)	16/25	
EP4: 5'-TTAGGATTAGCCGCATTCAG-3'	EVB (63)	59/63	
	EVC (24)	9/24	
	EVD (5)	1/5	
	total	85/117	
Method 3 (Detect 73% of Human Enteroviruses)		EP1 and EP4	P9 and P6
EPI: 5'-CGGTACCTTTGTGCGCCTGT-3'	EVA (25)	16/25	13/16
EP4: 5'-TTAGGATTAGCCGCATTCAG-3'	EVB (63)	59/63	37/59
	EVC (24)	9/24	0/9
	EVD (5)	1/5	0/1
	total	85/117	50/117
Method 4 (Detect 68%, 87% of Human Enteroviruses)		Primer 1, Primer 3 and Probe	Primer 2, Primer 3 and Probe
Primer 1: 5'-CAAGCACTTCTGTTTCCCCGG-3'	EVA (25)	21/25	24/25
Primer 2: 5'-TCCTCCGGCCCCTGAATGCG-3'	EVB (63)	44/63	58/63
Primer 3: 5'-ATTGTCACCATAAGCAGCCA-3'	EVC (24)	15/24	17/24
Probe 5'-AAACACGGACACCCAAAGTA-3'	EVD (5)	0/5	3/5
	total	80/117	102/117

Method 5 (Detect 18%, 0% of Human Enteroviruses)		OL252 and OL68	OL24 and OL253
OL252: 5'-GGCCCCTGAATGCGGCTAA-3'	EVA (25)	0/25	0/0
OL68: 5'-GGGACCTTCCACCACCANCC-3'	EVB (63)	20/63	0/20
OL24: 5'-CTACTTTGGGTGTCCG-3'	EVC (24)	0/24	0/0
OL253: 5'-GATACTYTGAGCNCCCAT-3' **	EVD (5)	1/5	0/0
	total	21/117	0/117
Method 6 (Detect 76% of Human Enteroviruses)		RNC2, NC1, E2 and Probe	
RT primer: RNC2 - 5'-CACCGGATGGCC-3'	EVA (25)	19/25	
NC1: 5'-CTCCGGCCCCTGAATGCG-3'	EVB (63)	53/63	
E2: 5'-ATTGTCACCATAAGCAGCCA-3'	EVC (24)	16/24	
probe S08: 5'-AAACACGGACACCCAAAGTA-3'	EVD (5)	1/5	
	total	89/117	
Method 7 (Detect 62%, 33% of Human Enteroviruses)		Primer 1 and Primer 4	Primer 2, Primer 3 and Probe
Primer 1: 5'-CAAGCACTTCTGTTTCCCCGG-3'	EVA (25)	18/25	12/18
Primer 4: 5'-CACCGGATGGCCAATCCA-3'	EVB (63)	40/63	26/40
Primer 2: 5-TCCTCCGGCCCCTGAATGCG-3'	EVC (24)	14/24	1/14
Primer 3: 5'-ATTGTCACCATAAGCAGCCA-3'	EVD (5)	0/5	0/0
Probe: 5'-TGTGTCGTAACGGGCAACTCTGCAGCGGAA-3'	total	72/117	39/117
Method 8 (Detect 56%, 56% of Human Enteroviruses)		Primer 1 and Primer 2	Primer 3 and Primer 4
Primer 1: 5’-AGTCCTCCGGCCCCTGAATGCGGCTA-3’	EVA (25)	10/25	10/10
Primer 2: 5’-ACTGGCTGCTTATGGTGACA-3’	EVB (63)	48/63	48/48
Primer 3: 5’-AGTCCTCCGGCCCCTGAATGCGGCTA-3’	EVC (24)	6/24	6/6
Primer 4: 5’-ACTACTTTGGGTGTCCGTGTT-3’	EVD (5)	1/5	1/1
	total	65/117	65/117

Table Apx1.3. Complete in-silico PCR results. Mismatches = 4. Mismatches allowed within 3'end. ** indicates faulty primer reported in publication. Supplementary Table 2. Complete in-silico PCR results. Mismatches = 4. Mismatches allowed within 3'end.

Primer/Probe			
Method 1 (Detect 79% of Human Enteroviruses)		EP1, EP4 and EP2	
EPI: 5'-CGGTACCTTTGTGCGCCTGT-3'	EVA (25)	18/25	
Probe EP2: 5'-TATTGAGCTAGTTGGTAGTCCTCCGG-3'	EVB (63)	62/63	
EP4: 5'-TTAGGATTAGCCGCATTCAG-3'	EVC (24)	11/24	
	EVD (5)	1/5	
	total	92/117	
Method 2 (Detect 96% of Human Enteroviruses)		EP1 and EP4	
EPI: 5'-CGGTACCTTTGTGCGCCTGT-3'	EVA (25)	23/25	
EP4: 5'-TTAGGATTAGCCGCATTCAG-3'	EVB (63)	63/63	
	EVC (24)	23/24	
	EVD (5)	3/5	
	total	112/117	
Method 3 (Detect 96%, 96% of Human Enteroviruses)		EP1 and EP4	P9 and P6
EPI: 5'-CGGTACCTTTGTGCGCCTGT-3'	EVA (25)	23/25	23/23
EP4: 5'-TTAGGATTAGCCGCATTCAG-3'	EVB (63)	63/63	63/63
	EVC (24)	23/24	23/23
	EVD (5)	3/5	3/3
	total	112/117	112/117
Method 4 (Detect 93%, 96% of Human Enteroviruses)		Primer 1, Primer 3 and Probe	Primer 2, Primer 3 and Probe
Primer 1: 5'-CAAGCACTTCTGTTTCCCCGG-3'	EVA (25)	23/25	24/25
Primer 2: 5'-TCCTCCGGCCCCTGAATGCG-3'	EVB (63)	61/63	61/63
Primer 3: 5'-ATTGTCACCATAAGCAGCCA-3'	EVC (24)	22/24	23/24
Probe 5'-AAACACGGACACCCAAAGTA-3'	EVD (5)	3/5	4/5

	total	109/117	112/117
Method 5 (Detect 95%, 3% of Human Enteroviruses)		OL252 and OL68	OL24 and OL253
OL252: 5'-GGCCCCTGAATGCGGCTAA-3'	EVA (25)	22/25	0/22
OL68: 5'-GGGACCTTCCACCACCANCC-3'	EVB (63)	63/63	0/63
OL24: 5'-CTACTTTGGGTGTCCG-3'	EVC (24)	23/24	2/23
OL253: 5'-GATACTYTGAGCNCCCAT-3' **	EVD (5)	3/5	1/3
	total	111/117	3/117
Method 6 (Detect 92% of Human Enteroviruses)		RNC2, NC1, E2 and Probe	
RT primer: RNC2 - 5'-CACCGGATGGCC-3'	EVA (25)	24/25	
NC1: 5'-CTCCGGCCCCTGAATGCG-3'	EVB (63)	61/63	
E2: 5'-ATTGTCACCATAAGCAGCCA-3'	EVC (24)	21/24	
probe S08: 5'-AAACACGGACACCCAAAGTA-3'	EVD (5)	2/5	
	total	108/117	
Method 7 (Detect 88%, 64% of Human Enteroviruses)		Primer 1 and Primer 4	Primer 2, Primer 3 and Probe
Primer 1: 5'-CAAGCACTTCTGTTTCCCCGG-3'	EVA (25)	22/25	15/22
Primer 4: 5'-CACCGGATGGCCAATCCA-3'	EVB (63)	60/63	59/60
Primer 2: 5-TCCTCCGGCCCCTGAATGCG-3'	EVC (24)	18/24	1/18
Primer 3: 5'-ATTGTCACCATAAGCAGCCA-3'	EVD (5)	3/5	0/3
Probe: 5'-TGTGTCGTAACGGGCAACTCTGCAGCGGAA-3'	total	103/117	75/117
Method 8 (Detect 94%, 94% of Human Enteroviruses)		Primer 1 and Primer 2	Primer 3 and Primer 4
Primer 1: 5’-AGTCCTCCGGCCCCTGAATGCGGCTA-3’	EVA (25)	24/25	24/24
Primer 2: 5’-ACTGGCTGCTTATGGTGACA-3’	EVB (63)	61/63	61/61
Primer 3: 5’-AGTCCTCCGGCCCCTGAATGCGGCTA-3’	EVC (24)	21/24	21/21
Primer 4: 5’-ACTACTTTGGGTGTCCGTGTT-3’	EVD (5)	4/5	4/4
	total	110/117	110/117

APPENDIX 2

Supplemental tables listing Augmenta full pathogen names, comparison of case vs control MFIs, complete list of antigens found as significant amongst cases, controls, males, and females

Table Apx2.1. List of Augmenta short names with their respective full pathogen names. Viral nomenclature distinctions are as follows: (Hex) a major coat protein of adenoviruses (ag) antigen - implied if not followed by lysate (Spike) protein on surface of coronavirus (HA) hemagglutinin (sAG) surface antigen (mosaic) mosaic protein (Env) envelope protein (Orf2) Hepatitis E Virus capsid protein (MCP) major capsid protein (c/b and c/b2) two different coupling reactions of these control/blocking peptides.

Augmenta Short Name	Full Pathogen Name
AdD36-lysate	Adenovirus D Type 36_Strain: 275_cell lysate_EBeam50kGyIrradiated
AdD37-lysate	Adenovirus D Type 37_Strain: GW (76-19026)_cell lysate_EBeam50kGyIrradiated
AdE4-lysate	Adenovirus E Type 4_Strain: RI-67_cell lysate_EBeam50kGyIrradiated
AdV11-lysate	Adenovirus B Type 11_Strain: Slobitski_cell lysate_EBeam50kGyIrradiated
AdV3-lysate	Adenovirus Type 3_Species B_infectious culture fluid_EBeam50kGyIrradiated
AdV40-Hex	Adenovirus Type 40 Hexon Protein_100 kDa, HEK293 derived
AdV41-lysate	Adenovirus Type 41_Species F Strain Tak_infectious culture fluid_EBeam50kGyIrradiated
AdV5-Hex	Adenovirus Type 5 Hexon Protein_100 kDa, HEK293 derived
AdV9-lysate	Adenovirus Type 9_Species D_infectious culture fluid_EBeam50kGyIrradiated
AdVA12-lysate	Adenovirus A Type 12_Strain: Huie (NIAID V-212-001-014)_cell lysate_EBeam50kGyIrradiated

AdVA31-lysate	Adenovirus A Type 31_Strain: 1315/63 (NIAID V-231-001-014)_cell lysate_EBeam50kGyIrradiated
AdVB3-lysate	Adenovirus B Type 3_Strain: G.B._cell lysate_EBeam50kGyIrradiated
AdVC2-lysate	Adenovirus C Type 2_Species C_infectious culture fluid_EBeam50kGyIrradiated
AdVC6-lysate	Adenovirus C Type 6_lysate - gamma inactivation
Astrovirus-lysate	Astrovirus Type 1_strain A88/2 lysate from host cells is inactivated by propiolactone treatment
BBurgdorferi-lysate	*Borrelia burgdorferi*_Strain B31 (Clone 5A1)_EBeam50kGyIrradiated and lysed
CDifficil-lysate	*Clostridium difficile* (Hall and O'Toole) Prevot_EBeam50kGyIrradiated and lysed
CDiphtheriae-lysate	*Corynebacterium diphtheriae* (Kruse) Lehmann and Neumann_EBeam50kGyIrradiated and lysed
CJejuni-lysate	*Campylobacter jejuni*_Strain INP21_EBeam50kGyIrradiated and lysed
CMV-lysate	CMV-G antigen_Strain: AD169_grown in human fibroblasts_UV inactivated
CTrachomatis-lysate	Chlamydia trachomatis Serovar A_Strain Har-13_cell lysate_mycoplasmapositive_EBeam50kGyIrradiated and lysed
CXADR	Human CXADR / CAR Protein, His Tag
CoxA16-ag	Coxsackie A16 (G10 Strain)_Heat inactivated antigen
CoxA2-lysate	Coxsackie B Virus A2_Strain: Fleetwood_cell lysate_EBeam50kGyIrradiated
CoxA24-lysate	Human coxsackievirus A24_Strain: DN-19_cell lysate_EBeam50kGyIrradiated
CoxA24-ag	Enterovirus C. Cox A24 Recomb
CoxA4-lysate	Coxsackievirus A4_Strain Highpoint_infectious culture fluid_EBeam50kGyIrradiated
CoxA6/A9-ag	Coxsackie B Virus A6/A9 (aka Echovirus)_Recombinant
CoxA9-lysate	Coxsackie B Virus A9_Strain: P.B. (Bozek)_cell lysate_EBeam50kGyIrradiated
CoxA9-ag	Coxsackie A9 (P.B. Bozek strain)_Heat inactivated antigen

CoxB1-lysate	Coxsackie B Virus B1_Strain: Conn.-5_GMK cells_EBeam50kGyIrradiated
CoxB1-lysate2	Coxsackie B Virus B1_Strain: Tucson VP1_recombinant protein_27kDa_Ecoli derived
CoxB2-lysate	Coxsackie B Virus B2_Strain: Ohio-1_cell lysate_EBeam50kGyIrradiated
CoxB3-VP1	Enterovirus CoxB3 VP1 Protein_Enterovirus CoxB3 recombinant VP1 protein, ~20-40kDa ,E.Coli derived
CoxB4-lysate	Coxsackie B Virus B4_Strain: J.V.B. (Benschoten)_cell lysate_EBeam50kGyIrradiated
CoxB5-lysate	Coxsackie B Virus B5_Strain: Faulkner_cell lysate_EBeam50kGyIrradiated
CoxB6-lysate	Coxsackie B Virus B6_cell lysate_beta-propiolactone and UV inactivation
EBV-EBNA1	Epstein-Barr Virus (HHV-4) EBNA1 Mosaic Recombinant, 44 kDa, E.Coli derived
EBV-gp125	Epstein Barr Virus gp125_affinity purified antigen using mAb specific to EBVgp125
EColi-lysate	Mach1 *E. coli* lysate
EEEV-E3E2	Eastern Equine Encephalitis Virus E3E2 Recombinant Protein [His]_50 kDa, Sf9 derived
EV68-lysate	Enterovirus D68_Strain Fermon_cell lysate_EBeam50kGyIrradiated
EV71-lysate	Enterovirus Species A Type 71_Strain USA/2018-23092_cell lysate_EBeam50kGyIrradiated
FluBVictoria-lysate	Influenza B Virus Victoria_B/Brisbane/33/2008 (Victoria Lineage)_EBeam50kGyIrradiated
FluBYamagata-lysate	Influenza B Virus Yamagata_B/New York/1061/2004 (Yamagata Lineage)_EBeam50kGyIrradiated
H1-HA	Influenza A/South Carolina/1/1918 (H1N1)_Recombinant H1 HA with His Tag
H1N1-lysate	Influenza A Virus (H1N1)_A/California/04/2009 (H1N1)pdm09 Cell Isolate (Produced in Eggs)_EBeam50kGyIrradiated
H2-HA	Influenza A/Japan/305/1957 (H2N2)_Recombinant H2 HA with His Tag

H3N2-lysate	Influenza A Virus (H3N2)_A/Wisconsin/15/2009 (H3N2)_EBeam50kGyIrradiated
H5-HA	Influenza A/Anhui/1/2005 (H5N1)_Recombinant H5 HA with His Tag
H5N1-lysate	A/H5N1 Influenza Vaccine_Inactivated Whole Virion (A/Vietnam/1203/2004)_Vero-Cell Derived_Adjuvanted
H7-HA	Influenza A/New York/107/2003 (H7N2)_Recombinant H7 HA with His Tag
H9-HA	Influenza A/Hong Kong/33982/2009 (H9N2)_Recombinant H9 HA1 domain with His Tag
HAV-lysate	Hepatitis A_Strain: HM175/18f_cell lysate_EBeam50kGyIrradiated
HAV-VP1	HAV VP1_Hepatitis A Virus VP1 Recombinant_48 kDa_E.Coli derived
HBV-Core	Hepatitis B Virus Core delta Recombinant_14kDa_E.Coli derived
HBVadr-sAg	Hepatitis B Surface Antigen, adr CHO Recombinant_recombinant protein_23kDa_CHO derived
HBVayw-sAg	Hepatitis B Surface Antigen ayw Recombinant_31kDa_E.Coli derived
HCV-207	Hepatitis C Virus Combined Recombinant (nucleocapsid, NS3 genotype 1b, NS4 genotype 1b and 1a, and NS5 genotype 1b and 1a immunodominant regions), 70 kDa, E.Coli derived
HCoV-229E-lysate	Human Coronavirus 229E Purified Viral lysate_Group1CoV_detergent and heat inactivated viral lysate
HCoV-HKU1-Spike	Human coronavirus HKU1 (isolate N5) (HCoV-HKU1) Spike Protein (S1+S2 ECD, His Tag)_recombinant protein_>66kDa_Sf9derived
HCoV-NL63-lysate	Human Coronavirus NL63 Purified Viral lysate_Group1CoV_heat inactivated viral lysate
HCoV-OC43-lysate	Human Coronavirus OC43 Purified Viral lysate_Group2CoV_detergent and heat inactivated viral lysate
HERVK-Env	HERV-K_Endogenous retrovirus K Envelope Human Recombinant, 51 kDa, E.Coli derived
HEV-Orf2	Hepatitis E (HEV), ORF2, C-terminal His-Tag_Recombinant HEV ORF2, 75 kDa, HEK293 derived

HHV-7-lysate	HHV-7_HHV7 JI Infected Sup-T1 Cells_EBeam50kGyIrradiated
HHV6a-lysate	HHV-6a_Strain GS_infectious culture fluid_EBeam50kGyIrradiated
HHV6b-lysate	HHV-6b_Strain: SF_cell lysate_EBeam50kGyIrradiated
HPIV1-lysate	Human Parainfluenza Virus Type 1_HPIV1/FRA/29221106/2009_EBeam50kGyIrradiated
HPIV1-lysate2	Human Parainfluenza Virus Type 1 lysate_detergent and heat inactivated
HPIV3-lysate	Human Parainfluenza Virus 3_NIH 47885_derived from NIAID catalog number V-323-002-020_EBeam50kGyIrradiated
HPIV4-lysate	Human Parainfluenza Virus Type 4A lysate_detergent and heat inactivated
HPV11-MCP	Human Papillomavirus 11 Major Capsid Protein, Recombinant 84 kDa, E.Coli derived
HPV16-MCP	Human Papillomavirus 16 Major Capsid Protein, Recombinant 78 kDa, E.Coli derived
HPV18-MCP	Human Papillomavirus 18 Major Capsid Protein, Recombinant 78 kDa, E.Coli derived
HPV6-MCP	Human Papillomavirus 6 Major Capsid Protein, Recombinant_82kDa_E.Coli derived
HPylori-lysate	*Helicobacter pylori*_Strain Hp CPY6081_EBeam50kGyIrradiated and lysed
HSV1-lysate	HSV-1 Antigen_lysate - chemical disruption inactivation
HSV2-lysate	HSV2_lysate - gamma inactivation
KPneumoniae-lysate	*Klebsiella pneumoniae*_Strain 1.53_EBeam50kGyIrradiated and lysed
KSHV-Mosaic	Kaposi's sarcoma-associated herpesvirus (KSHV, aka HHV-8)_Herpes Simplex Virus-8 Mosaic Recombinant, ~46 kDa, E.Coli derived
MGenitalium-lysate	*Mycoplasma genitalium*_Strain TW10-6G_EBeam50kGyIrradiated and lysed
MHominis-lysate	*Mycoplasma hominis*_Strain PG21_EBeam50kGyIrradiated and lysed

Measles-lysate	Measles virus, Edmonston strain, cultured in Vero cells_gamma inactivation
Mumps-lysate	Mumps virus lysate_Isolate1 cultured in Vero cells_detergent and heat inactivated
NGonorrea-lysate	*Neisseria gonorrhoeae*_EBeam50kGyIrradiated and lysed
NoroGI-Capsid	Norovirus Group-1_Norovirus Group-1 Capsid Recombinant, 50 kDa, E.Coli derived
NoroGII.4-Capsid	Norovirus GII.4 VP1 virus-like particles recombinant protein_VP1 from norovirus GII.4, 50 kDa, HEK293 derived
PVR	Human Poliovurs receptor Protein_Recombinant Human PVR (CD155 or Necl-5) protein, 45 kDa, HEK293 derived
ParechoA3-lysate	Parechovirus A Type 3_US/MO-KC/2012/006_EBeam50kGyIrradiated
ParvoB19-VP1	Parvovirus B19 VLP VP1_Parvovirus VLP VP1 Recombinant, ~84kDa, E.Coli derived
Polio-PV1VP1	Recombinant Poliomyelitis Virus 1 Viral Protein 1 (Sabin; POLV1-VP1), 30 kDa, E.Coli derived
Polio-PV1c/b	Polio, PV1_control/blocking peptide (no Zeba purification)
Polio-PV1c/b2	Polio, PV1_control/blocking peptide (with Zeba purification)
Polio-PV2c/b	Polio, PV2_control/blocking peptide (no Zeba purification)
Polio-PV2c/b2	Polio, PV3_control/blocking peptide (with Zeba purification)
Polio-PV3c/b	Polio, PV3_control/blocking peptide (no Zeba purification)
Powassan-NS1	Powassan virus NS1 recombinant antigen_Recombinant powassan virus non-structural protein 1, 50 kDa, HEK293 derived
RRV-SP	Ross River virus recombinant antigen_Recombinant Ross River structural polyprotein, 50 kDa, HEK293 derived
RSV-lysate	Respiratory Syncytial virus, long strain cultured in BSC-1 cells, gamma inactivated
Reovirus-lysate	Reovirus Seortype 3_Strain: Dearing_cell lysate_EBeam50kGyIrradiated

RhinoA15-lysate	Human rhinovirus A/15_Strain: 1734_cell lysate_EBeam50kGyIrradiated
RhinoA2-lysate	Rhinovirus A/A2_Strain: HGP_cell lysate_EBeam50kGyIrradiated
RhinoB14-lysate	Rhinovirus B/B14_Strain: 1059_cell lysate_EBeam50kGyIrradiated
Rotavirus-SA11	Rotavirus SA-11_lysate - UV inactivation
Rubella-C	Rubella Virus Capsid C Recombinant_E.Coli derived
Rubella-E2	Rubella Virus E2 Recombinant_E.Coli derived
SARS-S1	SARS-CoV Spike/S1 Protein (S1 Subunit His Tag)_SARS-CoV (isolate:WH20) recombinant protein_86kDa_Sf9 derived
SARS2-lysate	USA-WA1/2020 RAD SNT; SARS-Related Coronavirus 2, Isolate USA-WA1/2020, Gamma-Irradiated
SLEV-lysate	St. Louis Encephalitis Virus (SLEV)_Strain Parton_culture fluid_heat inactivated
SV40-lysate	Simian Virus 40_Strain Baylor (SVB2E-WT)_cell lysate_EBeam50kGyIrradiated
StaphAureus-lysate	*Staphylococcus aureus*_Strain HIP06854_EBeam50kGyIrradiated and lysed
StrepAgalactiae-lysate	*Streptococcus agalactiae*_Strain SGBS001_EBeam50kGyIrradiated and lysed
StrepPyogenes-lysate	*Streptococcus pyogenes*_Strain ABC020060016_EBeam50kGyIrradiated and lysed
StrepPyogenes-lysate2	*Streptococcus pyogenes*_Strain ABC020059514_EBeam50kGyIrradiated and lysed
StreptDysgalactiae-lysate	*Streptococcus dysgalactiae* subsp. dysgalactiae_EBeam50kGyIrradiated and lysed
TBEV-lysate	Tick-Borne Encephalitis Virus lysate (Strain Moscow B-4)_virons inactivated by beta propiolactone treatment
Trichomonas-lysate	*Trichomonas vaginalis*_Strain C-1:NIH_manufac inactivated by sonication and freeze/thaw
VACV-lysate	Vaccinia virus_Strain: NYC Dept Health-Wyeth_cell lysate_EBeam50kGyIrradiated
Vaccinia-lysate	Vaccinia Virus_Modified Vaccinia Ankara (MVA) Purified From BHK-21 Cells_EBeam50kGyIrradiated

hMPVA1-lysate	Human Metapneumovirus (hMPV) 16 Type A1 lysate_Strain:IA10-2003_detergent and heat inactivated
hMPVB1-lysate	Human Metapneumovirus (hMPV) 5 Type B1 lysate_Strain:Peru3-2003_detergent and heat inactivated

Table Apx2.2. Comparison of case vs. control median fluorescence intensity antibody levels for all 122 antigens surveyed. Values are indicated as the log2 MFI average after background subtraction ± standard deviation. (Red) lower antibody levels in controls. (Blue) lower antibody levels in cases. Pathogen antigens with significantly different antibody levels between cases and controls ($p< 0.05$, $q>0.05$) are highlighted in grey.

Pathogen	Patient Average	Control Average
AdD36-lysate	3.7 ± 1.1	3.8 ± 1.0
AdD37-lysate	3.9 ± 1.2	4.0 ± 1.1
AdE4-lysate	2.8 ± 1.0	2.8 ± 1.0
AdV11-lysate	0.2 ± 0.5	0.3 ± 0.4
AdV3-lysate	1.8 ± 0.8	1.9 ± 1.0
AdV40	9.0 ± 1.3	9.3 ± 0.8
AdV41-lysate	2.8 ± 0.8	2.9 ± 0.8
AdV5	8.5 ± 1.5	8.5 ± 1.2
AdV9-lysate	4.9 ± 1.4	5.0 ± 1.2
AdVA12-lysate	3.5 ± 1.1	3.5 ± 1.0
AdVA31-lysate	4.1 ± 1.2	4.2 ± 1.1
AdVB3-lysate	3.0 ± 1.0	2.9 ± 1.0
AdVC2-lysate	1.0 ± 0.5	1.1 ± 0.8
AdVC6-lysate	6.1 ± 1.6	5.9 ± 1.5
Astrovirus-lysate	2.0 ± 0.9	2.1 ± 0.7
BBurgdorferi-lysate	1.4 ± 0.8	1.6 ± 0.7
CDifficil-lysate	2.1 ± 1.0	2.0 ± 0.8
CDiphtheriae-lysate	1.2 ± 0.5	1.1 ± 0.4
CJejuni-lysate	3.9 ± 1.6	3.9 ± 1.9
CMV-lysate	3.4 ± 2.0	4.0 ± 1.9
CTrachomatis-lysate	1.2 ± 0.7	1.3 ± 0.7
CXADR	7.1 ± 0.2	7.0 ± 0.5
CoxA16	2.9 ± 0.8	2.9 ± 0.5
CoxA2-lysate	1.3 ± 0.6	1.5 ± 0.7
CoxA24-lysate	1.4 ± 0.8	1.6 ± 0.9
CoxA24	7.9 ± 1.3	7.7 ± 1.3
CoxA4-lysate	1.4 ± 0.7	1.6 ± 0.9
CoxA6/A9	7.8 ± 1.8	7.7 ± 1.1
CoxA9-lysate	1.9 ± 0.6	2.1 ± 0.9
CoxA9	4.1 ± 1.1	4.4 ± 0.8
CoxB1-lysate	1.8 ± 0.7	1.8 ± 0.7
CoxB1-lysate2	8.6 ± 1.5	8.6 ± 1.0

CoxB2-lysate	1.2 ± 0.6	1.4 ± 0.9
CoxB3-VP1	7.9 ± 1.3	7.8 ± 1.0
CoxB4-lysate	1.3 ± 0.6	1.4 ± 0.8
CoxB5-lysate	1.6 ± 0.7	1.8 ± 0.9
CoxB6-lysate	1.1 ± 0.4	1.1 ± 0.3
EBV-EBNA1	3.6 ± 1.3	4.0 ± 1.2
EBV-gp125	6.7 ± 1.4	6.4 ± 1.7
EColi-lysate	7.2 ± 1.0	7.3 ± 0.8
EEEV-E3E2	3.2 ± 1.1	3.3 ± 1.1
EV68-lysate	1.2 ± 0.8	1.4 ± 1.0
EV71-lysate	1.3 ± 0.6	1.4 ± 0.9
FluBVictoria-lysate	4.6 ± 1.2	4.8 ± 0.9
FluBYamagata-lysate	3.3 ± 0.7	3.5 ± 0.5
H1-HA	8.8 ± 0.9	9.0 ± 0.8
H1N1-lysate	4.8 ± 1.1	4.9 ± 1.0
H2-HA	7.1 ± 1.1	7.2 ± 1.7
H3N2-lysate	4.5 ± 1.0	4.4 ± 1.2
H5-HA	6.9 ± 1.1	6.9 ± 1.1
H5N1-lysate	3.3 ± 0.7	3.3 ± 0.6
H7-HA	6.7 ± 1.0	6.9 ± 1.0
H9-HA	5.9 ± 1.6	6.1 ± 1.8
HAV-lysate	1.5 ± 0.7	1.7 ± 0.8
HAV-VP1	4.5 ± 1.2	4.7 ± 1.1
HBV-Core	6.1 ± 0.9	6.0 ± 1.0
HBVadr-sAg	1.1 ± 1.3	1.6 ± 1.8
HBVayw-sAg	2.7 ± 0.8	2.8 ± 0.7
HCV-207	1.3 ± 0.4	1.3 ± 0.4
HCoV-229E-lysate	2.9 ± 0.8	2.9 ± 0.7
HCoV-HKU1-Spike	7.0 ± 0.8	7.3 ± 0.8
HCoV-NL63-lysate	2.5 ± 0.9	2.5 ± 0.8
HCoV-OC43-lysate	4.7 ± 0.8	4.9 ± 0.7
HERVK-Env	2.3 ± 0.6	2.3 ± 0.6
HEV-Orf2	3.6 ± 0.9	4.0 ± 1.0
HHV-7-lysate	1.4 ± 0.8	1.6 ± 1.1
HHV6a-lysate	1.5 ± 0.9	1.7 ± 1.1
HHV6b-lysate	0.6 ± 0.6	0.8 ± 0.7
HPIV1-lysate	7.2 ± 1.1	7.3 ± 0.9
HPIV1-lysate2	1.4 ± 0.5	1.5 ± 0.5
HPIV3-lysate	1.5 ± 0.6	1.7 ± 0.9

HPIV4-lysate	1.6 ± 0.3	1.7 ± 0.3
HPV11-MCP	3.9 ± 0.9	4.1 ± 0.8
HPV16-MCP	4.1 ± 0.7	4.2 ± 0.6
HPV18-MCP	4.3 ± 1.1	4.3 ± 0.9
HPV6-MCP	4.6 ± 0.9	4.7 ± 0.7
HPylori-lysate	4.8 ± 1.3	5.2 ± 1.7
HSV1-lysate	4.2 ± 2.4	4.7 ± 2.4
HSV2-lysate	2.4 ± 1.3	2.7 ± 1.4
KPneumoniae-lysate	4.4 ± 1.2	4.6 ± 1.5
KSHV-Mosaic	2.7 ± 0.9	2.7 ± 0.9
MGenitalium-lysate	1.3 ± 0.5	1.5 ± 0.6
MHominis-lysate	1.0 ± 0.5	1.0 ± 0.4
Measles-lysate	2.9 ± 1.0	3.0 ± 1.1
Mumps-lysate	4.1 ± 0.9	4.3 ± 0.8
NGonorrea-lysate	5.0 ± 1.6	5.0 ± 1.6
NoroGI-Capsid	4.0 ± 0.8	4.2 ± 0.6
NoroGII.4-Capsid	9.4 ± 2.1	9.0 ± 1.9
PVR	0.1 ± 0.3	0.1 ± 0.1
ParechoA3-lysate	1.2 ± 0.7	1.4 ± 1.0
ParvoB19-VP1	3.0 ± 0.9	3.0 ± 0.9
Polio-PV1VP1	2.4 ± 0.9	2.5 ± 0.8
Polio-PV1c/b	2.5 ± 0.8	2.4 ± 0.7
Polio-PV1c/b2	2.5 ± 0.9	2.5 ± 0.8
Polio-PV2c/b	2.5 ± 0.9	2.5 ± 0.7
Polio-PV2c/b2	2.9 ± 0.7	2.9 ± 0.7
Polio-PV3c/b	2.8 ± 0.8	2.8 ± 0.7
Powassan-NS1	0.8 ± 0.5	0.8 ± 0.4
RRV-SP	0.7 ± 0.3	0.8 ± 0.4
RSV-lysate	2.3 ± 0.8	2.4 ± 0.9
Reovirus-lysate	0.9 ± 0.5	1.0 ± 0.8
RhinoA15-lysate	2.6 ± 0.6	2.9 ± 0.8
RhinoA2-lysate	1.8 ± 0.6	1.9 ± 0.7
RhinoB14-lysate	2.3 ± 0.5	2.5 ± 0.7
Rotavirus-SA11	2.8 ± 0.5	2.7 ± 0.6
Rubella-C	4.1 ± 1.0	4.3 ± 0.8
Rubella-E2	5.4 ± 0.7	5.3 ± 0.4
SARS-S1	5.9 ± 1.2	6.1 ± 1.2
SARS2-lysate	1.6 ± 0.6	1.9 ± 0.9
SLEV-lysate	0.8 ± 0.6	1.0 ± 0.9

SV40-lysate	1.2 ± 0.7	1.4 ± 0.9
StaphAureus-lysate	5.9 ± 0.5	5.9 ± 0.9
StrepAgalactiae-lysate	2.7 ± 1.0	2.5 ± 1.0
StrepPyogenes-lysate	2.8 ± 0.8	3.1 ± 0.9
StrepPyogenes-lysate2	5.3 ± 1.8	6.2 ± 1.9
StreptDysgalactiae-lysate	2.7 ± 0.9	3.1 ± 0.9
TBEV-lysate	1.8 ± 0.5	2.0 ± 0.7
Trichomonas-lysate	1.0 ± 0.4	1.0 ± 0.4
VACV-lysate	0.7 ± 0.5	0.8 ± 0.8
Vaccinia-lysate	0.9 ± 0.6	1.0 ± 0.6
hMPVA1-lysate	9.1 ± 0.8	9.2 ± 0.6
hMPVB1-lysate	8.0 ± 0.8	8.2 ± 0.6

Table Apx2.3. Comparison of case vs. control median fluorescence intensity antibody levels for all 122 antigens surveyed - outliers removed. Values are indicated as the log2 MFI average after background subtraction ± standard deviation. Outliers greater than 1.5 times the interquartile range (IQR) were removed and replaced using BPCA estimation for each antigen. (Red) lower antibody levels in controls. (Blue) lower antibody levels in cases. Pathogen antigens with significantly different antibody levels between patients and controls ($p< 0.05$, q>0.05) are highlighted in grey.

Pathogen	Patient Average	Control Average
AdD36-lysate	3.8 ± 1.1	3.8 ± 1.0
AdD37-lysate	3.9 ± 1.1	4.0 ± 1.1
AdE4-lysate	2.7 ± 1.0	2.8 ± 1.0
AdV11-lysate	0.1 ± 0.3	0.2 ± 0.3
AdV3-lysate	1.7 ± 0.7	1.7 ± 0.6
AdV40	9.2 ± 0.7	9.3 ± 0.8
AdV41-lysate	2.8 ± 0.8	2.9 ± 0.8
AdV5	8.7 ± 0.9	8.7 ± 0.9
AdV9-lysate	4.9 ± 1.4	5.0 ± 1.2
AdVA12-lysate	3.5 ± 1.0	3.5 ± 1.0
AdVA31-lysate	4.2 ± 1.1	4.3 ± 1.0
AdVB3-lysate	3.0 ± 1.0	2.9 ± 1.0
AdVC2-lysate	0.9 ± 0.4	0.9 ± 0.4
AdVC6-lysate	6.4 ± 1.1	6.0 ± 1.3
Astrovirus-lysate	1.7 ± 0.3	2.0 ± 0.5
BBurgdorferi-lysate	1.4 ± 0.6	1.6 ± 0.7
CDifficil-lysate	1.9 ± 0.8	1.9± 0.7
CDiphtheriae-lysate	1.1 ± 0.5	1.1 ± 0.4
CJejuni-lysate	3.9 ± 1.6	3.9 ± 1.9
CMV-lysate	3.4 ± 2.0	4.0 ± 1.9
CTrachomatis-lysate	1.1 ± 0.5	1.2 ± 0.6
CXADR	7.1 ± 0.2	7.0 ± 0.1
CoxA16	2.8 ± 0.7	2.9 ± 0.5
CoxA2-lysate	1.3 ± 0.5	1.3 ± 0.4
CoxA24-lysate	1.3 ± 0.6	1.4 ± 0.5
CoxA24	7.9 ± 1.3	7.7 ± 1.3
CoxA4-lysate	1.3 ± 0.5	1.4 ± 0.5
CoxA6/A9	8.0 ± 1.2	7.7 ± 1.1
CoxA9-lysate	1.9 ± 0.5	2.0 ± 0.5
CoxA9	4.0 ± 0.9	4.4 ± 0.8
CoxB1-lysate	1.8 ± 0.6	1.7 ± 0.5

CoxB1-lysate2	8.7 ± 0.9	8.6 ± 0.8
CoxB2-lysate	1.1 ± 0.4	1.2 ± 0.5
CoxB3-VP1	8.0 ± 0.9	7.8 ± 1.0
CoxB4-lysate	1.2 ± 0.5	1.3 ± 0.5
CoxB5-lysate	1.5 ± 0.5	1.6 ± 0.5
CoxB6-lysate	1.0 ± 0.3	1.1 ± 0.3
EBV-EBNA1	3.6 ± 1.2	4.0 ± 1.2
EBV-gp125	7.0 ± 0.8	6.9 ± 0.8
EColi-lysate	7.4 ± 0.7	7.3 ± 0.8
EEEV-E3E2	3.1 ± 0.9	3.3 ± 0.8
EV68-lysate	1.2 ± 0.6	1.3 ± 0.6
EV71-lysate	1.2 ± 0.5	1.3 ± 0.5
FluBVictoria-lysate	4.6 ± 1	4.8 ± 0.9
FluBYamagata-lysate	3.3 ± 0.5	3.5 ± 0.5
H1-HA	8.9 ± 0.6	9.1 ± 0.6
H1N1-lysate	4.8 ± 1	4.9 ± 1.0
H2-HA	7.1 ± 1.6	7.2 ± 1.7
H3N2-lysate	4.5 ± 1.0	4.5 ± 1.0
H5-HA	7.0 ± 0.9	7.0 ± 0.8
H5N1-lysate	3.2 ± 0.5	3.2 ± 0.5
H7-HA	6.7 ± 1.0	6.9 ± 0.9
H9-HA	5.9 ± 1.4	6.1 ± 1.8
HAV-lysate	1.4 ± 0.5	1.5 ± 0.5
HAV-VP1	4.5 ± 1.0	4.7 ± 1.1
HBV-Core	6.1 ± 0.7	5.9 ± 0.8
HBVadr-sAg	0.8 ± 0.6	0.8 ± 0.6
HBVayw-sAg	2.6 ± 0.6	2.7 ± 0.6
HCV-207	1.3 ± 0.4	1.4 ± 0.4
HCoV-229E-lysate	2.8 ± 0.7	2.8± 0.5
HCoV-HKU1-Spike	7.1 ± 0.7	7.3 ± 0.8
HCoV-NL63-lysate	2.3 ± 0.6	2.4 ± 0.6
HCoV-OC43-lysate	4.8 ± 0.7	4.9 ± 0.6
HERVK-Env	2.2 ± 0.5	2.3 ± 0.5
HEV-Orf2	3.5 ± 0.8	3.8 ± 0.7
HHV-7-lysate	1.3 ± 0.7	1.4 ± 0.7
HHV6a-lysate	1.4 ± 0.8	1.5 ± 0.7
HHV6b-lysate	0.5 ± 0.4	0.6 ± 0.4
HPIV1-lysate	7.2 ± 1.1	7.3 ± 0.9
HPIV1-lysate2	1.4 ± 0.5	1.5 ± 0.5

HPIV3-lysate	1.5 ± 0.5	1.5 ± 0.5
HPIV4-lysate	1.6 ± 0.3	1.6 ± 0.2
HPV11-MCP	4.0 ± 0.8	4.1 ± 0.7
HPV16-MCP	4.2 ± 0.6	4.2 ± 0.6
HPV18-MCP	4.2 ± 1.0	4.3 ± 0.9
HPV6-MCP	4.6 ± 0.8	4.7 ± 0.7
HPylori-lysate	4.7 ± 1.0	5.0 ± 1.1
HSV1-lysate	4.2 ± 2.4	4.7 ± 2.4
HSV2-lysate	2.4 ± 1.3	2.7 ± 1.4
KPneumoniae-lysate	4.5 ± 1.1	4.7 ± 1.3
KSHV-Mosaic	2.5 ± 0.6	2.5 ± 0.6
MGenitalium-lysate	1.3 ± 0.5	1.4 ± 0.5
MHominis-lysate	1.0 ± 0.4	1.0 ± 0.4
Measles-lysate	2.9 ± 0.9	3.0 ± 1.1
Mumps-lysate	4.3 ± 0.7	4.4 ± 0.7
NGonorrea-lysate	5.0 ± 1.6	5.1 ± 1.5
NoroGI-Capsid	4.1 ± 0.7	4.2 ± 0.6
NoroGII.4-Capsid	9.9 ± 1.0	9.6 ± 1.1
PVR	0.1 ± 0.1	0.1 ± 0.1
ParechoA3-lysate	1.1 ± 0.6	1.2 ± 0.5
ParvoB19-VP1	3.0 ± 0.9	3.1 ± 0.8
Polio-PV1VP1	2.3 ± 0.6	2.4 ± 0.6
Polio-PV1c/b	2.4 ± 0.6	2.4 ± 0.6
Polio-PV1c/b2	2.4 ± 0.6	2.4 ± 0.6
Polio-PV2c/b	2.5 ± 0.7	2.5 ± 0.7
Polio-PV2c/b2	2.8 ± 0.5	2.8 ± 0.4
Polio-PV3c/b	2.7 ± 0.5	2.7 ± 0.5
Powassan-NS1	0.7 ± 0.3	0.8 ± 0.4
RRV-SP	0.7 ± 0.3	0.7 ± 0.3
RSV-lysate	2.2 ± 0.6	2.2 ± 0.5
Reovirus-lysate	0.8 ± 0.4	0.9 ± 0.4
RhinoA15-lysate	2.5 ± 0.5	2.7 ± 0.4
RhinoA2-lysate	1.7 ± 0.5	1.8 ± 0.4
RhinoB14-lysate	2.3 ± 0.4	2.4 ± 0.4
Rotavirus-SA11	2.8 ± 0.6	2.7 ± 0.6
Rubella-C	4.0 ± 0.9	4.3 ± 0.8
Rubella-E2	5.3 ± 0.6	5.3 ± 0.4
SARS-S1	5.9 ± 1.1	6.1 ± 1.2
SARS2-lysate	1.6 ± 0.5	1.7 ± 0.5

SLEV-lysate	0.8 ± 0.4	0.8 ± 0.4
SV40-lysate	1.2 ± 0.6	1.2 ± 0.5
StaphAureus-lysate	5.9 ± 0.5	5.9 ± 0.6
StrepAgalactiae-lysate	2.7 ± 1.0	2.5 ± 1.0
StrepPyogenes-lysate	2.8 ± 0.8	3.2 ± 0.7
StrepPyogenes-lysate2	5.3 ± 1.8	6.2 ± 1.9
StreptDysgalactiae-lysate	2.6 ± 0.7	3.1 ± 0.7
TBEV-lysate	1.7 ± 0.4	1.9 ± 0.5
Trichomonas-lysate	0.9 ± 0.3	1.0 ± 0.3
VACV-lysate	0.6 ± 0.4	0.6 ± 0.3
Vaccinia-lysate	0.8 ± 0.4	0.9 ± 0.4
hMPVA1-lysate	9.2 ± 0.6	9.2 ± 0.5
hMPVB1-lysate	8.2 ± 0.5	8.2 ± 0.5

Table Apx2.4. Complete list of antigens with significantly different antibody levels between ME/CFS and healthy control males. Values are given as log2 MFI averages ± standard deviations. n = number of antigens found to have a $p<0.05$.

Male (n = 42)			
Antigen	p-value	-log10(p)	q-value
BBurgdorferi-Lysate	0.000	3.985	0.013
EBV-EBNA1	0.002	2.641	0.124
RhinoA15-Lysate	0.005	2.277	0.124
Astrovirus-Lysate	0.005	2.268	0.124
HEV-Orf2	0.007	2.131	0.124
RhinoB14-Lysate	0.010	1.991	0.124
SARS2-Lysate	0.010	1.983	0.124
CoxB2-Lysate	0.012	1.922	0.124
CTrachomatis-Lysate	0.014	1.865	0.124
AdV40-Hex	0.014	1.863	0.124
EV71-Lysate	0.014	1.858	0.124
Rubella-E2	0.016	1.805	0.124
VACV-Lysate	0.016	1.805	0.124
CoxB5-Lysate	0.016	1.794	0.124
AdVA31-Lysate	0.019	1.731	0.124
CoxA9-ag	0.019	1.718	0.124
H1-HA	0.020	1.690	0.124
RhinoA2-Lysate	0.020	1.690	0.124
CoxB4-Lysate	0.021	1.669	0.124
Vaccinia-Lysate	0.022	1.661	0.124
AdV41-Lysate	0.023	1.634	0.124
CoxA9-Lysate	0.025	1.609	0.124
Rotavirus-SA11	0.025	1.608	0.124
Polio-PV1VP1	0.026	1.580	0.124
EEEV-E3E2	0.026	1.579	0.124
HHV6b-Lysate	0.026	1.579	0.124
HPIV1-Lysate2	0.028	1.551	0.125
StrepPyogenes-Lysate	0.030	1.525	0.125
Rubella-C	0.030	1.525	0.125
HPylori-Lysate	0.032	1.493	0.125
StrepAgalactiae Lysate	0.032	1.493	0.125
HCV-207	0.034	1.473	0.125
Powassan-NS1	0.034	1.472	0.125

HPIV4-Lysate	0.036	1.446	0.125
HPV11-MCP	0.036	1.445	0.125
CoxA4-Lysate	0.038	1.419	0.129
H1N1-Lysate	0.040	1.394	0.131
EV68-Lysate	0.041	1.383	0.131
Trichomonas-Lysate	0.043	1.369	0.131
HHV-7-Lysate	0.043	1.369	0.131
AdD37-Lysate	0.045	1.343	0.135
MGenitalium-Lysate	0.048	1.318	0.140

Table Apx2.5. Complete list of antigens found to be significantly between age groups overall (All) and within experimental subgroups (Case, Control and Female). Antigens shown are significant following false discovery rate correction. FC = fold change, *p* = *p*-value.

All: Over 50/Under 50				
Antigen	FC	log2(FC)	*p*.ajusted	-log10(*p*)
H2-HA	4.30	2.11	0.00	4.19
EBV-EBNA1	0.51	-0.97	0.00	3.52
SV40-Lysate	0.74	-0.44	0.00	3.52
SARS2-Lysate	0.88	-0.19	0.00	3.52
EV68-Lysate	0.75	-0.41	0.00	3.48
CoxB2-Lysate	0.78	-0.36	0.00	3.48
EV71-Lysate	0.78	-0.35	0.00	3.48
AdVC2-Lysate	0.81	-0.31	0.00	3.48
CoxA2-Lysate	0.81	-0.31	0.00	3.48
RhinoA15-Lysate	0.84	-0.25	0.00	3.48
CoxB5-Lysate	0.86	-0.22	0.00	3.42
HHV-7-Lysate	0.74	-0.43	0.00	3.20
HAV-Lysate	0.79	-0.34	0.00	3.13
ParechoA3-Lysate	0.78	-0.36	0.00	3.11
RhinoA2-Lysate	0.80	-0.32	0.00	3.11
CoxA4-Lysate	0.78	-0.36	0.00	3.03
HHV6a-Lysate	0.73	-0.45	0.00	2.97
CoxA9-Lysate	0.87	-0.21	0.00	2.96
Astrovirus-Lysate	0.77	-0.37	0.00	2.92
HHV6b-Lysate	0.80	-0.31	0.00	2.92
CoxA24-Lysate	0.78	-0.36	0.00	2.79
CoxA9-ag	0.51	-0.98	0.00	2.79
CoxB4-Lysate	0.79	-0.33	0.00	2.76
SLEV-Lysate	0.95	-0.07	0.00	2.52
HPIV4-Lysate	0.89	-0.17	0.00	2.40
VACV-Lysate	0.96	-0.05	0.00	2.37
SARS-S1	0.56	-0.84	0.00	2.33
HBVadr-sAg	0.35	-1.53	0.01	2.18
HPIV3-Lysate	0.82	-0.28	0.01	2.01
RhinoB14-Lysate	0.90	-0.16	0.01	1.85

AdV3-Lysate	0.80	-0.33	0.01	1.85
CoxB6-Lysate	0.89	-0.16	0.01	1.85
HBVayw-sAg	0.66	-0.60	0.02	1.80
CoxB1-Lysate	0.71	-0.49	0.02	1.70
Reovirus-Lysate	0.99	-0.01	0.02	1.65
CoxB1-Lysate2	0.75	-0.41	0.02	1.63
RSV-Lysate	0.83	-0.27	0.02	1.63
Polio-PV1VP1	0.59	-0.75	0.03	1.59
CoxA6/A9-ag	0.66	-0.60	0.04	1.39
CoxA16-ag	0.79	-0.34	0.05	1.32
HCoV-NL63-Lysate	0.62	-0.68	0.05	1.32

Case: Over 50/Under 50				
Antigen	FC	log2(FC)	*p*.ajusted	-log10(*p*)
H2-HA	3.80	1.92	0.01	2.18
SARS2-Lysate	0.64	-0.65	0.01	1.98
Astrovirus-Lysate	0.48	-1.07	0.02	1.76
CoxB5-Lysate	0.64	-0.64	0.02	1.76
RhinoA15-Lysate	0.70	-0.51	0.02	1.76
HPIV4-Lysate	0.83	-0.27	0.02	1.76
CoxA2-Lysate	0.71	-0.50	0.02	1.74
CoxA9-ag	0.38	-1.39	0.02	1.68
SARS-S1	0.51	-0.98	0.02	1.68
SV40-Lysate	0.61	-0.70	0.02	1.68
CoxB2-Lysate	0.66	-0.61	0.02	1.68
CoxA9-Lysate	0.66	-0.59	0.02	1.68
VACV-Lysate	0.76	-0.40	0.02	1.64
EBV-EBNA1	0.58	-0.77	0.02	1.63
EV68-Lysate	0.60	-0.74	0.02	1.63
EV71-Lysate	0.66	-0.61	0.02	1.63
HHV6b-Lysate	0.68	-0.57	0.02	1.63
AdVC2-Lysate	0.72	-0.48	0.03	1.60
ParechoA3-Lysate	0.62	-0.69	0.04	1.43
HHV6a-Lysate	0.54	-0.89	0.05	1.33
RhinoA2-Lysate	0.70	-0.51	0.05	1.33

Control: Over 50/Under 50				
Antigen	FC	log2(FC)	*p*.ajusted	-log10(*p*)

HBVadr-sAg	0.53	-0.90	0.04	1.37
Mumps-Lysate	1.72	0.78	0.04	1.37

Female: Over 50/Under 50

Antigen	FC	log2(FC)	*p*.ajusted	-log10(*p*)
H2-HA	4.44	2.15	0.00	2.95
EBV-EBNA1	0.50	-1.00	0.00	2.95
Astrovirus-Lysate	0.52	-0.95	0.00	2.95
SARS2-Lysate	0.75	-0.41	0.00	2.95
CoxA9-ag	0.42	-1.26	0.00	2.54
EV68-Lysate	0.73	-0.46	0.00	2.54
SV40-Lysate	0.73	-0.44	0.00	2.54
ParechoA3-Lysate	0.74	-0.43	0.00	2.54
CoxB5-Lysate	0.77	-0.38	0.00	2.54
CoxB2-Lysate	0.77	-0.38	0.00	2.54
HHV6b-Lysate	0.78	-0.36	0.00	2.54
RhinoA15-Lysate	0.78	-0.35	0.00	2.54
EV71-Lysate	0.78	-0.35	0.00	2.54
AdVC2-Lysate	0.79	-0.33	0.00	2.54
CoxA2-Lysate	0.80	-0.32	0.00	2.54
HPIV4-Lysate	0.86	-0.22	0.00	2.54
CoxA4-Lysate	0.74	-0.43	0.00	2.51
HHV-7-Lysate	0.72	-0.46	0.00	2.37
RhinoA2-Lysate	0.79	-0.34	0.00	2.37
HAV-Lysate	0.78	-0.36	0.01	2.28
CoxA9-Lysate	0.78	-0.36	0.01	2.28
HHV6a-Lysate	0.67	-0.58	0.01	2.23
CoxB4-Lysate	0.78	-0.35	0.01	2.16
CoxA24-Lysate	0.76	-0.39	0.01	2.14
SLEV-Lysate	0.82	-0.28	0.01	2.00
VACV-Lysate	0.85	-0.23	0.01	1.87
HBVayw-sAg	0.60	-0.73	0.02	1.69
CoxB1-Lysate2	0.71	-0.50	0.02	1.62
CoxA16-ag	0.74	-0.44	0.03	1.57
HPIV3-Lysate	0.82	-0.29	0.03	1.55
CoxA6/A9-ag	0.64	-0.64	0.04	1.37
CoxB6-Lysate	0.89	-0.17	0.04	1.37

APPENDIX 3

Cytokine profiling of extracellular vesicles isolated from plasma in myalgic encephalomyelitis/chronic fatigue syndrome: a pilot study[3]

As discussed in Giloteaux L. *et al.* [1], immune-profiling of ME/CFS plasma-derived extracellular vesicles were surveyed for differences in cytokine cargos between cases and age, sex, and BMI matched healthy controls. Circulating extracellular vesicles and their cytokine cargos were investigated due to 1.) prior evidence for differences in ME/CFS circulating extracellular vesicles [2-4] 2.) prior demonstration of ME/CFS-specific immune system dysregulation via the assessment of blood-derived cytokines [5] and 3.) the potential for extracellular vesicles to be used as ME/CFS specific biomarkers as demonstrated in other disease contexts such as autoimmune diseases [6], cancer and Parkinson's disease [7]. In short, we found a significant increase in extracellular vesicles ranging from 30-130nm in ME/CFS cases compared to controls. Furthermore, cytokine-cytokine correlations in plasma revealed a significantly higher number of interactions in ME/CFS cases along with 13 inverse correlations that were mainly driven by the Interferon gamma-induced Protein 10 (IP-10), whereas in the plasma of controls, no inverse relationships were found across any of the cytokines. Network analysis in EVs from controls showed 2.5 times more

[3] Data in this appendix was included in "Cytokine profiling of extracellular vesicles isolated from plasma in myalgic encephalomyelitis/chronic fatigue syndrome: a pilot study" by Ludovic Giloteaux, Adam O'Neal, Jesús Castro-Marrero, Susan M. Levine, and Maureen R. Hanson. *J Transl Med.* © The Authors, 2020; 18(1):387. Extracellular vesicle isolation via ExoQuick was done in collaboration with and under the supervision of L. Giloteaux. All other experiment shown here (Nanoparticle Tracking Analysis, Transmission Electron Microscopy and Western Blot Analysis) were performed by me.

significant inter-cytokine interactions than in the ME/CFS group, and both groups presented a unique negative association.

I isolated extracellular vesicles via ExoQuick™ precipitation and then quantified vesicle size using Nanoparticle Track Analysis (**Figure Apx3.1**).

Figure Apx3.1. Sizing and quantification of Extracellular Vesicles. Size in nm (a), total concentration (b), 30–130 nm concentration (c) and > 130 nm concentration (d) of particles per ml of plasma in ME/CFS subjects and healthy controls (CTRL) as determined by Nanoparticle Tracking Analysis. Yellow dot represents the mean.

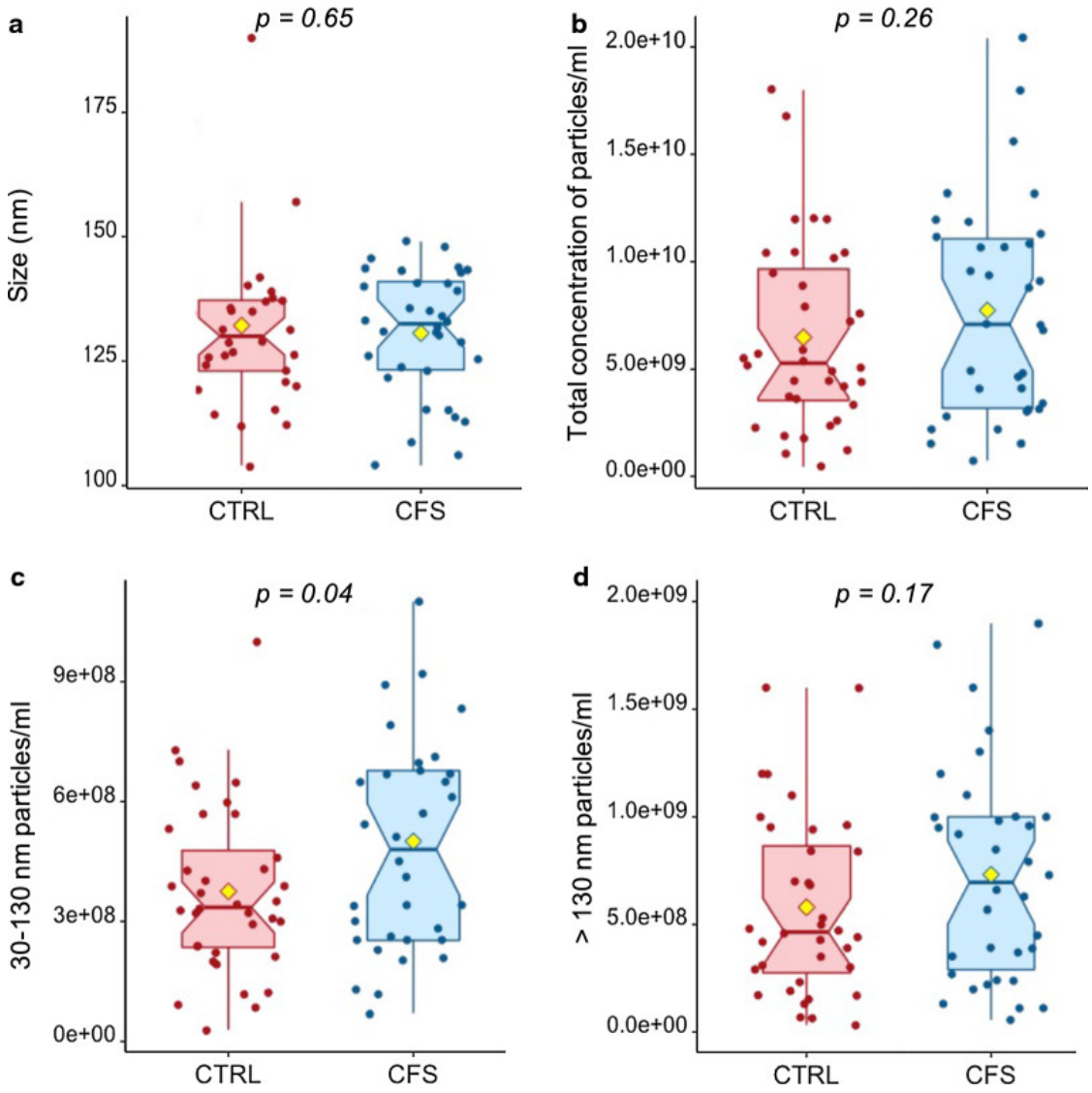

In accordance with the International Society for Extracellular Vesicles: minimal information for studies of extracellular vesicle 2018 guidelines (MISEV 2018), I characterized case and control extracellular vesicles via immunoblot analysis with at least three positive extracellular vesicle protein markers, Nanoparticle Tracking Analysis (NTA), and Transmission Electron Microscopy (TEM) (**Figure Apx3.2**) [8].

Figure Apx3.2. Characterization of Extracellular Vesicles. (a) Morphology of isolated EVs from ME/CFS was confirmed by transmission electron microscopy (a representative image is shown; scale bars: 200 nm and 500 nm) and (b) Western blot analysis of isolated EVs from healthy controls (CTRL) and ME/CFS subjects as representative samples. Thirty μg of protein was loaded in each lane and probed with specific antibodies to EV protein markers. Cytochrome C (mitochondrial marker) was used as negative control for EV and positive for PBMCs.

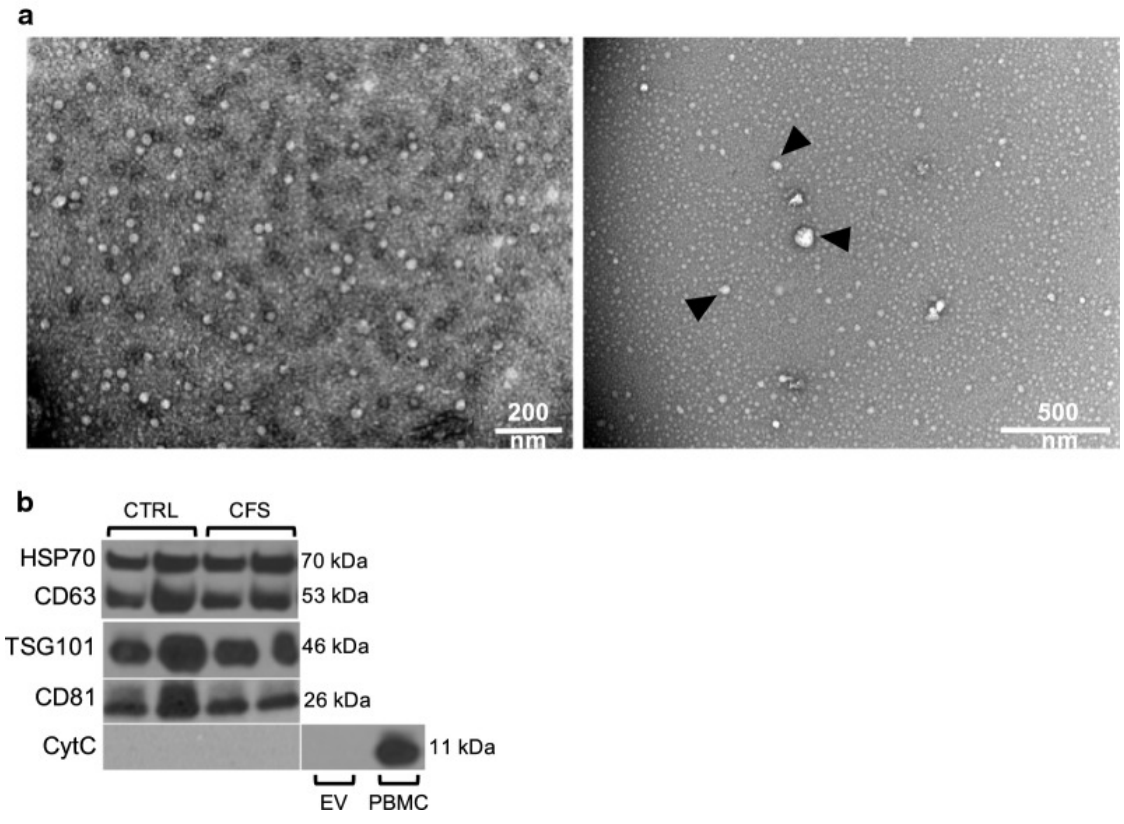

MATERIALS AND METHODS

Extracellular vesicle isolation and characterization

Total extracellular vesicles (EVs) were isolated from 750µl of plasma by precipitation using the ExoQuick™ reagent (System Biosciences, Palo Alto, CA, USA). Plasma samples from each subject were thawed on ice and centrifuged at 3000×g for 15 min at room temperature to remove cells and debris. The supernatant was transferred to a new tube, and thrombin (611 U/ml) (System Bioscience, Palo Alto, CA, USA) was added and samples were incubated for 5 min at room temperature to remove fibrinogen, centrifuged at 10,000×g for 5 min, and the supernatant was collected. The samples were then incubated with ExoQuick™ for 60 min at 4 °C. The ExoQuick™/serum-like samples were then centrifuged at 12,000×g for 5 min, and the resulting pellet was resuspended in 250ul of sterile phosphate buffered saline 1X, pH 7.4. To prevent aggregation and cryodamage, 25 mM of trehalose was added to the isolated EV fraction [9]. Samples were aliquoted for total protein determination, Western blot analysis, Nanoparticle Tracking Analysis (NTA), Transmission Electron Microscopy (TEM), and measurement (quantification) of cytokines/chemokines and growth factors.

Protein quantification and western blot analysis

Total protein quantification from EV isolates was performed using the PierceTM BCA Protein Assay kit (ThermoFisher Scientific) according to manufacturer's instructions. The assay is a detergent-compatible formulation based on bicinchoninic acid for the colorimetric detection (A562 nm) and quantitation of total protein.

Purified EVs were assayed for Western blot analysis (WB). WB is used to validate the presence or absence of EV protein markers in purified samples based on the availability of specific antibodies CD63, CD81, HSP70 and TSG101 (System Biosciences, LLC, Palo Alto, CA, USA). Protein samples were prepared by adding 100 µl ice-cold RIPA buffer containing protease/phosphatase inhibitors to 100 µl extracted EV samples resuspended in the appropriate buffer. EV lysates were adjusted to the same protein content (150 µg), denatured for 10 min in 2X Laemmli buffer, resolved by 8–10% SDS-PAGE, and then proteins were transferred to PVDF membranes (Amersham, GE Healthcare, USA). Membranes were blocked in 5% non-fat dry milk using TBS containing 0.1% Tween-20 and then incubated with various primary polyclonal antibodies (anti-CD63, anti-CD81, anti-HSP70, anti-TSG101; dilution 1/500; Santa Cruz Biotech, CA, USA) and cytochrome C antibody as a negative control for overnight at 4 °C, washed with 1X TBS-T and then incubated with secondary conjugated antibody for 1 h at room temperature. X-ray films were exposed in a darkroom and films were developed and visualized using and infrared Odyssey machine (LI-COR Biosciences).

Extracellular vesicle isolation and characterization

Extracellular vesicles' concentration and size distribution were assayed in samples using a NanoSight NS300 (Malvern). Samples were thawed and diluted to 1:2000 in PBS 1X and 1 ml was injected through the laser chamber (NanoSight Technology, London, UK). The NanoSight NS300 uses a source light to illuminate nanoscale particles (30–800 nm) as point scatters moving under Brownian motion. Three recordings of 60-second digital videos of each sample were acquired and analyzed by

the NanoSight NTA 2.3 software to determine the size and the concentration of nanoparticles. Results were averaged together.

Transmission electron microscopy

EV suspensions were visualized under a 120 kV field emission transmission electron microscope (FEI T12 Spirit TEM/STEM) at the Cornell Center for Materials Research in Ithaca, NY. Isolated EV suspensions were thawed and diluted at either 1:100, 1:500, 1:1000 or 1:2000 in 2% PFA overnight at 4 °C before proceeding with negative staining. Samples were applied to copper 300-mesh Formvar coated carbon stabilized grids and were allowed to adsorb to the grid for 20 min. Grids were then washed in PBS 1X and transferred to a 1% glutaraldehyde solution for one min post-fixation. Samples were then washed 8 times by floating on distilled water for 2 min. Negative staining was then achieved through placing the grids on a drop of 2% Aqueous Uranyl Acetate for 10 min followed by air drying and storage in an EM grid box.

REFERENCES

1. Giloteaux L, O'Neal A, Castro-Marrero J, Levine SM, Hanson MR. Cytokine profiling of extracellular vesicles isolated from plasma in myalgic encephalomyelitis/chronic fatigue syndrome: a pilot study. J Transl Med. 2020;18(1):387.

2. Almenar-Pérez E, Sarría L, Nathanson L, Oltra E. Assessing diagnostic value of microRNAs from peripheral blood mononuclear cells and extracellular vesicles in Myalgic Encephalomyelitis/Chronic Fatigue Syndrome. Scientific reports. 2020;10(1):2064-.

3. Castro-Marrero J, Serrano-Pertierra E, Oliveira-Rodríguez M, Zaragozá MC, Martínez-Martínez A, Blanco-López MDC, et al. Circulating extracellular vesicles as potential biomarkers in chronic fatigue syndrome/myalgic encephalomyelitis: an exploratory pilot study. Journal of extracellular vesicles. 2018;7(1):1453730-.

4. Eguchi A, Fukuda S, Kuratsune H, Nojima J, Nakatomi Y, Watanabe Y, et al. Identification of actin network proteins, talin-1 and filamin-A, in circulating

extracellular vesicles as blood biomarkers for human myalgic encephalomyelitis/chronic fatigue syndrome. Brain, behavior, and immunity. 2020;84:106-14.

5. Corbitt M, Eaton-Fitch N, Staines D, Cabanas H, Marshall-Gradisnik S. A systematic review of cytokines in chronic fatigue syndrome/myalgic encephalomyelitis/systemic exertion intolerance disease (CFS/ME/SEID). BMC Neurology. 2019;19(1):207.

6. Xu K, Liu Q, Wu K, Liu L, Zhao M, Yang H, et al. Extracellular vesicles as potential biomarkers and therapeutic approaches in autoimmune diseases. Journal of Translational Medicine. 2020;18(1):432.

7. Ciferri MC, Quarto R, Tasso R. Extracellular Vesicles as Biomarkers and Therapeutic Tools: From Pre-Clinical to Clinical Applications. Biology (Basel). 2021;10(5):359.

8. Théry C, Witwer KW, Aikawa E, Alcaraz MJ, Anderson JD, Andriantsitohaina R, et al. Minimal information for studies of extracellular vesicles 2018 (MISEV2018): a position statement of the International Society for Extracellular Vesicles and update of the MISEV2014 guidelines. Journal of Extracellular Vesicles. 2018;7(1):1535750.

9. Bosch S, de Beaurepaire L, Allard M, Mosser M, Heichette C, Chrétien D, et al. Trehalose prevents aggregation of exosomes and cryodamage. Sci Rep. 2016;6:36162.

APPENDIX 4

CATCH Method. Example Coronaviridae probe design.[4]

CATCH resources on GitHub: https://github.com/broadinstitute/catch

Step 1. Download all viral genomic sequences from relevant databases.

Using both NCBI and ViPR databases creates the most complete list possible.

All data from VIPR except severe acute respiratory syndrome-related coronaviruses:

Result (1 file): *CoA.fa* (fasta file containing 520 sequences)

SARS and SARS-CoV2 sequences retrieved from NCBI (https://www.ncbi.nlm.nih.gov/datasets/coronavirus/genomes/, https://www.ncbi.nlm.nih.gov/genome/browse#!/overview/coronaviridae):

Result (3 files): *GCF_000864885.1_ViralProj15500_genomic.fna*

GCF_009858895.2_ASM985889v3_genomic.fna

genomic.fna

Step 2. Concatenate separate NCBI fasta files and remove potential duplicate genomes using seqkit v2.0.0

In the case of VIPR downloaded sequences, internal filter was used to automatically remove duplicates)

In the case of NCBI downloaded sequences, the following script was utilized to concatenate fasta files:

[4] Coronaviridae capture probe production was performed by Hannah Smith with my guidance and supervision.

`cat genomic.fna GCF_000864885.1_ViralProj15500_genomic.fna GCF_009858895.2_ASM985889v3_genomic.fna`

Once concatenated, duplicates are removed using the following script:

`seqkit rmdup -s < CoB_raw.fa > CoB.fa`

Notes: genomic.fna contained GCF_000864885.1_ViralProj15500_genomic.fna and GCF_009858895.2_ASM985889v3_genomic.fna sequences as well as 75574 duplicates. Total CoB sequences = 366064.

Step 3. Design probes using CATCH

Although one could choose to specify the number of mismatches and cover extension, these parameters can also be chosen by CATCH based on a restriction set around the number of probes. In this case you have to ask CATCH to run multiple iterations using a range of mismatches from 0 to 5 and a range of cover extensions from 0 to 50. In order to do this, the script needs to be coded to repeat under each parameter (echo).

```
`echo -n "" > commands.txt; INPUTDIR=/workdir/hjs99;
OUTPUTDIR=/workdir/hjs99; for d in CoA CoB; \
do for m in 0 1 2 3 4 5; do for e in 0 10 20 30 40 50; do echo "design.py
$INPUTDIR/${d}.fa -pl 100 -ps 50 -m ${m} -e ${e} \
--island-of-exact-match 25 --filter-polya 20 4 --expand-n 2 -o
$OUTPUTDIR/${d}.m${m}.e${e}.fa \
--write-analysis-to-tsv $OUTPUTDIR/${d}.m${m}.e${e}.tsv --verbose --limit-
target-genomes-randomly-with-replacement 50 \
&> $OUTPUTDIR/${d}.m${m}.e${e}.txt" >> commands.txt; done; done; done`
```

To speed up the length of time CATCH takes to determine optimal probes, you can run the job in parallel so more computer bandwith is used at once. Script below:

```
parallel --jobs 20 --no-notice --progress < commands.txt
```

The items highlighted in the echo script above (red) should be changed by the researcher to fit their setting. See below for an explanation regarding each of these user selected parameters.

INPUTDIR = Input directory. This is the location in which your fasta files (CoA and CoB in this example) exist. For simplicity, you could just set this as your desktop.

OUTPUTDIR = Output directory. This is the location in which any files generated by CATCH will be written to.

for d in ____ = this is where you would designate the file names in your input directory (in this example we have CoA and CoB).

do for m in ___ = this code sets the range of allowed mismatches to query. In this scenario we are asking the program to run iterations from 0 to 5 mismatches at intervals of 1 mismatch.

do for e in ___ = this code sets the range of allowed cover extensions to query. In this scenario we are asking the program to run iterations from 0 to 50 nucleotide cover extensions at 10 nucleotide intervals.

-pl = probe length. In this case we selected a length of 100 nucleotides.

-ps = probe stride. In this case we selected a probe stride of 50 nucleotides.

-island of exact match = requires there to be an exact match of length __ between a portion of the probe and the target sequence. If 2 mismatches are allowed, they may not be within __ distance of one another. In this case, we set the length to be 25

nucleotides. This means every probe will have a region of at least 25 nucleotides that is perfectly complementary to the target sequence with zero theoretical mismatches allowed in this region.

filter polyA = requires CATCH to not generate probes targeting regions of poly adenylation. In this case, we requested CATCH to not generate probes to regions with a polyA tail 20 nucleotides or greater.

limit target genomes randomly with replacement = requires CATCH to limit the number of target genomes within a dataset in a randomized fashion. This script was added in to simply the workflow during explanation. In reality, this should only be used if there is high sequence similarity between genomes and the user is limited on the number of probes to be generated. As a reminder, CoA contains 520 sequences in total and we limited the number of probes to be generated based off of 50/520 sequences. If the user is not hindered by cost or scale in creating their desired probe set, this script should not be utilized and only utilized to scale with probe production.

A complete list of possible arguments to enter in the design.py script can be generated using the following script:

```
design.py –help
```

Files generated with this script include a .txt, .tsv and .fa file for each of the iterations. The .fa files generated will ultimately be the files sequences are pulled from to synthesize probes. The .txt file shows an output of how the software was performing during probe creation. Lastly, the .tsv file for each iteration shows: a) number of bases covered for each genome b) fraction of bases covered for each genome c) fraction of bases covered over unambiguous for each genome d) average

coverage/depth for each genome and e) the average coverage/depth over unambiguous for each genome. An example .tsv file for CoA at 0 mismatches and 0 cover extension is shown below:

Table Apx4.1. tsv file showing number of bases covered, fraction of bases covered, fraction of bases covered over unambiguous, average coverage/depth over unambiguous.

CoA.fa, Genome (#1-50)	Num bases covered	Frac bases covered	Frac bases covered over unambig	Average coverage/depth	Average coverage/depth over unambig
0	30589	1.00	1.00	1.61	1.61
1	30031	1.00	1.00	1.67	1.67
2	31029	1.00	1.00	1.19	1.19
3	30096	1.00	1.00	1.65	1.65
4	30040	1.00	1.00	1.65	1.65
5	30699	1.00	1.00	1.57	1.57
6	29566	1.00	1.00	1.66	1.66
7	30573	1.00	1.00	1.63	1.63
8	27055	0.99	0.99	1.23	1.23
9	30022	1.00	1.00	1.66	1.66
10	27523	1.00	1.00	1.57	1.57
11	27413	1.00	1.00	1.56	1.56
12	30713	1.00	1.00	1.71	1.71
13	29896	1.00	1.00	1.65	1.65
14	30108	1.00	1.00	1.69	1.69
15	30716	1.00	1.00	1.68	1.68
16	30111	1.00	1.00	1.69	1.69
17	30116	1.00	1.00	1.67	1.67
18	30069	1.00	1.00	1.66	1.66
19	29594	0.99	1.00	1.18	1.19
20	20540	0.75	0.98	1.11	1.45
21	27398	1.00	1.00	1.52	1.53
22	30119	1.00	1.00	1.61	1.61
23	29547	0.99	1.00	1.14	1.15
24	27516	1.00	1.00	1.55	1.55
25	30713	1.00	1.00	1.70	1.70
26	30029	1.00	1.00	1.62	1.62

27	29609	0.99	1.00	1.18	1.19
28	30581	1.00	1.00	1.67	1.67
29	30597	1.00	1.00	1.61	1.61
30	30678	1.00	1.00	1.65	1.65
31	29995	1.00	1.00	1.66	1.66
32	30713	1.00	1.00	1.67	1.67
33	29981	1.00	1.00	1.65	1.65
34	30076	1.00	1.00	1.68	1.68
35	30668	1.00	1.00	1.64	1.64
36	30036	1.00	1.00	1.62	1.62
37	25400	1.00	1.00	1.00	1.00
38	30589	1.00	1.00	1.61	1.61
39	30119	1.00	1.00	1.68	1.68
40	27487	1.00	1.00	1.56	1.56
41	30581	1.00	1.00	1.64	1.64
42	30065	1.00	1.00	1.64	1.64
43	29774	1.00	1.00	1.66	1.66
44	29896	1.00	1.00	1.64	1.64
45	27237	1.00	1.00	1.24	1.24
46	29784	1.00	1.00	1.24	1.24
47	30118	1.00	1.00	1.62	1.62
48	30713	1.00	1.00	1.70	1.70
49	30714	1.00	1.00	1.66	1.66

Use of "--limit-target-genomes-randomly-with-replacement 50" in the above script is the reason why only a subsample (50) of the 520 sequences in CoA.fa are shown as target genomes. Please read the above section for a thorough explanation of how "-limit target genomes randomly with replacement" performs.

Step 4. Create tab-separated values (.tsv) file outputting number of probes created under each iteration.

As CATCH performs probe design under each iteration (mismatches 0-5 and cover extension 0-50), 36 total possibilities are produced for each initial dataset (CoA and Cob). The parameters selecting 0 mismatches and 0 cover extension produce the

greatest number of probes while selecting 5 mismatches with a cover extension of 50 would create the fewest number of probes. Probe set design through synthesizing manufactures such as TWIST requires the researcher to select the number of probes they would like produced. Before selecting our limit on the number of probes, we first ask CATCH to count the number of probes generated under each of the 72 (36x2) iterations and output this in a tab-separated values (.tsv) file used by spreadsheet applications to view the number of probes generated under each iteration. The script used to run this step is listed below:

```
`echo -e "dataset\tmismatches\tcover_extension\tnum_probes" > num-probes.tsv;
INPUTDIR=/workdir/hjs99/; OUTPUTDIR=/workdir/hjs99/; \
for d in CoA CoB; do for m in 0 1 2 3 4 5; do for e in 0 10 20 30 40 50; \
do num_probes=$(grep '>' $OUTPUTDIR/${d}.m${m}.e${e}.fa | wc -l); echo -e
"${d}\t${m}\t${e}\t${num_probes}" >> num-probes.tsv; \
done; done; done`
```

Once again, the items highlighted in the echo script above (red) should be changed by the researcher to fit their setting. See below for an explanation regarding each of these user selected parameters.

INPUTDIR = This should be equal to the output directory related to Step 3 as the files created in Step 3 are being analyzed for the number of probes generated.

OUTPUTDIR = This is where the .tsv file will be generated and stored. For ease, it can be written to the same location as the INPUTDIR.

do for m in __ = This script should match whatever was chosen by the user for "d for m in __" in step 3.

do for e in __ = This script should match whatever was chosen by the user for "d for e in __" in step 3.

An example .tsv output file showing the number of probes generated (num-probes.tsv) under each iteration for each dataset is shown below:

Table Apx4.2. .tsv output file showing the number of mismatches, size of cover extension for each dataset with the number of probes under each parameter combination (mismatches + cover extension) given.

Dataset	Mismatches	Cover extension	Number probes
CoA	0	0	4550
CoA	0	10	3563
CoA	0	20	3061
CoA	0	30	2397
CoA	0	40	2214
CoA	0	50	1298
CoA	1	0	2000
CoA	1	10	2173
CoA	1	20	2334
CoA	1	30	1790
CoA	1	40	1774
CoA	1	50	1157
CoA	2	0	1796
CoA	2	10	2027
CoA	2	20	1980
CoA	2	30	1731
CoA	2	40	1467
CoA	2	50	667
CoA	3	0	1753
CoA	3	10	1659
CoA	3	20	2034
CoA	3	30	1467
CoA	3	40	1722
CoA	3	50	857
CoA	4	0	1570
CoA	4	10	2352
CoA	4	20	1982

CoA	4	30	1576
CoA	4	40	1464
CoA	4	50	844
CoA	5	0	1640
CoA	5	10	1964
CoA	5	20	2366
CoA	5	30	1731
CoA	5	40	1541
CoA	5	50	757
CoB	0	0	1216
CoB	0	10	719
CoB	0	20	671
CoB	0	30	0
CoB	0	40	482
CoB	0	50	368
CoB	1	0	452
CoB	1	10	468
CoB	1	20	434
CoB	1	30	0
CoB	1	40	331
CoB	1	50	285
CoB	2	0	389
CoB	2	10	435
CoB	2	20	423
CoB	2	30	336
CoB	2	40	318
CoB	2	50	284
CoB	3	0	435
CoB	3	10	432
CoB	3	20	434
CoB	3	30	343
CoB	3	40	362
CoB	3	50	287
CoB	4	0	408
CoB	4	10	479
CoB	4	20	412
CoB	4	30	331
CoB	4	40	319
CoB	4	50	261

CoB	5	0	418
CoB	5	10	422
CoB	5	20	432
CoB	5	30	336
CoB	5	40	319
CoB	5	50	201

Step 5. Identify optimal parameters based on the number of desired probes in the total probe set.

In respect to creating a CoA and CoB targeting probe set, CoA with m=0 and e=0 requires 4550 probes and Cob with m=0 and e=0 requires 1216 probes for a combined total of 5766 probes. If for some reason we were limited to only producing 4000 probes, we would want to determine which iteration for CoA and which iteration for CoB is best to combine to stay at or as close to 4000 probes. While this may be easy enough to assume when only working with two sequence datasets (CoA and CoB), it would be hard to determine when creating datasets to many sequence datasets. To determine the best combination of iterations that allows one to stay us to stay under 5000 probes, the following script should be executed:

`OUTPUTDIR=/workdir/hjs99/; for i in $(seq 1 10); do pool.py num-probes.tsv 4000 \

$OUTPUTDIR/params-run${i}.tsv \ --round-params 1 10 --loss-coeffs 1 0.01 &> $OUTPUTDIR/params-run${i}.txt; done`

Once again, the items highlighted in the echo script above (red) should be changed by the researcher to fit their setting. See below for an explanation regarding each of these user selected parameters.

OUTPUTDIR = The directory where the num-probes.tsv file currently exists. This will similarly be the location where the .txt and, .tsv output files generated by this script will be read to.

4000 = Requires CATCH to determine the best combination of probe parameters for each dataset based on a specified total probe number limitation. In this case, we selected 4000 probes.

--round-params = Requires CATCH to perform the analysis a total of 10 times with each analysis theoretically producing a different loss coefficient (see below for explanation of loss coefficient).

--loss-coeffs = User sets the range of possible loss coefficients from 1 to 0.01. Although this should not be changed, an explanation of loss coefficients in this context is still required. Each time CATCH performs this analysis, it queries the coverage of target genomes based on the probe parameters selected. For instance, if CATCH selects CoA (m=0 and e=10) and CoB (m=1 and e=20) we could have a total of 3997 probes. However, we could also imagine picking CoA (m=0 and e=10) and CoB (m=2 and e=10) for a total of 3998 probes. The question is then, which combination is the best? Which combination provides the greatest coverage of target genomes. To answer this, the above script would be utilized and the combination producing the lowest cost efficient is produced. By running the analysis, a total of 10 times, each iteration will produce its own loess coefficient based on the probe parameters it has selected to stay at or as close to 4000 probes as possible. We then mine through each of the 10 analyses output files and pick the combination with the lowest loss coefficient as the probe sets we would like to generate for our target capture experiments.

Once we have defined the best combination, we take their respective fasta files, read to our output work directory, and these will be the probes sequences submitted for probe synthesis. In practicality, a total of 5776 probes is well beneath limitations of probe set design by relevant manufacturers and this portion of the script would not need to be run. We would simply select CoA (m=0 and e=0) as well as CoB (m=0 and e=0).

APPENDIX 5

Target capture enrichment protocol using Twist synthesized probes.

A panel of our custom EV-specific probe set was synthesized by Twist Biosciences. Total RNA, extracted from subject samples was submitted to Cornell's TREx facility for cDNA library construction (see Chapter 3, Materials and Methods, cDNA library construction and sequencing). cDNA libraries were then enriched using the Twist Custom Panel Hybridization Capture of DNA Libraries according to the manufacture protocol (Steps 4-7) that can be found at the url below. PCR cycle number was set to 15. https://www.twistbioscience.com/resources/protocol/twist-target-enrichment-standard-hybridization-v1-protocol